Improving Usability of Weather Radar Data in Environmental Sciences: Potentials, Challenges, Uncertainties and Applications

Von der Naturwissenschaftlichen Fakultät der Gottfried Wilhelm Leibniz Universität Hannover

zur Erlangung des Grades

Doktorin der Naturwissenschaften (Dr. rer. nat.)

genehmigte Dissertation

von

Jennifer Kreklow, M. Sc.

2020

Referent: Prof. Dr. rer. nat. Gerald Kuhnt

Korreferent: Prof. Dr. rer. nat. Benjamin Burkhard

Gutachterliche Stellungnahme: Dr. rer. nat. Björn Tetzlaff

Tag der Promotion: 08.10.2020

Summary

Precipitation is a crucial driver for many environmental processes and exhibits a high spatiotemporal variability. The traditional, widely-used point-scale measurements by rain gauges are not able to detect the spatial rainfall distribution in a comprehensive way. Throughout the last decades, weather radars have emerged as a new measurement technique that is capable of providing areal precipitation information with high spatial and temporal resolution and put precipitation monitoring on a new level. However, radar is an indirect remote sensing technique. Rain rates and distributions are inferred from measured reflectivities, which are subject to a series of potential error sources. In the last years, several operational national radar data archives exceeded a time series length of ten years and several new radar climatology datasets have been derived, which provide largely consistent, well-documented radar quantitative precipitation estimate (QPE) products and open up new climatological application fields for radar data. However, beside uncertainties regarding data quality and precipitation quantification, several technical barriers exist that can prevent potential users from working with radar data. Challenges include for instance different proprietary data formats, the processing of large data volumes and a scarcity of easy-to-use and free-of-charge software, additional effort for data quality evaluation and difficulties concerning data georeferencing.

This thesis provides a contribution to improve the usability of radar-based QPE products, to raise awareness on their potentials and uncertainties and to bridge the gap between the radar community and other scientific disciplines which are still rather reluctant to use these highly resolved data.

First, a GIS-compatible Python package was developed to facilitate weather radar data processing. The package uses an efficient workflow based on widely used tools and data structures to automate raw data processing and data clipping for the operational German radar-based and gauge-adjusted QPE called RADOLAN ("RADar OnLine Aneichung") and the reanalysed radar climatology dataset named RADKLIM. Moreover, the package provides functions for temporal aggregation, heavy rainfall detection and data exchange with ArcGIS. The Python package was published as an Open Source Software called *radproc.* It was used as a basis for all subsequent analyses conducted in this study and has already been applied successfully by several scientific working groups and students conducting heavy rainfall analysis and data aggregation tasks.

Second, this study explored the development, uncertainties and potentials of the hourly RADOLAN and RADKLIM QPE products in comparison to ground-truth rain gauge data. Results revealed that both QPE products tend to underestimate total precipitation sums and particularly high intensity rainfall. However, the analyses also showed significant improvements throughout the RADOLAN time series as well as major advances through the climatologic reanalysis regarding the correction of typical radar artefacts, orographic and winter precipitation and range-dependent attenuation. The applicability of the evaluation results was underpinned by the publication of a rainfall inter-comparison geodataset for the RADOLAN, RADKLIM and rain gauge datasets. The intercomparison dataset is a collection of precipitation statistics and several parameters that can potentially influence radar data quality. It allows for a straightforward comparison and analysis of the different precipitation datasets and can support a user's decision on which dataset is best suited for the given application and study area. The data processing workflow for the derivation of the intercomparison dataset is described in detail and can serve as a guideline for individual data processing tasks and as a case study for the application of the *radproc* library.

Finally, in a case study on radar composite data application for rainfall erosivity estimation, RADKLIM data with a 5-minute temporal resolution were used alongside rain gauge data to compare different erosivity estimation methods used in erosion control practice. The aim was to assess the impacts of methodology, climate change and input data resolution, quality and spatial extent on the R-factor of

the Universal Soil Loss Equation (USLE). Moreover, correction factors proposed in other studies were tested with regard to their ability to compensate for different temporal resolutions of rainfall input data and the underestimation of precipitation by radar data. The results clearly showed that R-factors have increased significantly due to climate change and that current R-factor maps need to be updated by using more recent and spatially distributed rainfall data. The radar climatology data showed a high potential to improve rainfall erosivity estimations, but also a certain bias in the spatial distribution of the R-factor due to the rather short time series and a few radar artefacts. The application of correction factors to compensate for the underestimation of the radar led to an improvement of the results, but a possible overcorrection could not be excluded, which indicated a need for further research on data correction approaches.

This thesis concludes with a discussion of the role of open source software, open data and of the implementation of the FAIR (Findable, Accessible, Interoperable, Re-usable) principles for the German radar QPE products in order to improve data usability. Finally, practical recommendations on how to approach the assessment of QPE quality in a specific study area are provided and potential future research developments are pointed out.

Zusammenfassung

Niederschlag ist ein wesentlicher Antrieb vieler Umweltprozesse und weist eine hohe räumliche und zeitliche Variabilität auf. Die traditionellen, weit verbreiteten punktuellen Messungen mit Ombrometern sind nicht in der Lage, die räumliche Niederschlagsverteilung flächendeckend zu erfassen. Im Laufe der letzten Jahrzehnte hat sich mit dem Wetterradar eine neue Messtechnik etabliert, die in der Lage ist, flächenhafte Niederschlagsinformationen mit hoher räumlicher und zeitlicher Auflösung zu erfassen und die Niederschlagsüberwachung auf ein neues Niveau zu heben. Radar ist jedoch eine indirekte Fernerkundungstechnik. Niederschlagsraten und -verteilungen werden aus gemessenen Reflektivitäten abgeleitet, die einer Reihe von potenziellen Fehlerquellen unterliegen. In den letzten Jahren überschritten mehrere nationale Radardatenarchive eine Zeitreihenlänge von zehn Jahren. Es wurden mehrere neue Radarklimatologie-Datensätze abgeleitet, die weitgehend konsistente, gut dokumentierte Radarprodukte zur quantitativen Niederschlagsschätzung liefern und neue klimatologische Anwendungsfelder für Radardaten eröffnen. Neben Unsicherheiten bezüglich der Datenqualität und der Niederschlagsquantifizierung gibt es jedoch eine Vielzahl technischer Barrieren, die potenzielle Nutzer von der Verwendung der Radardaten abhalten können. Zu den Herausforderungen gehören beispielsweise unterschiedliche proprietäre Datenformate, die Verarbeitung großer Datenmengen, ein Mangel an einfach zu bedienender und kostenloser Software, zusätzlicher Aufwand für die Bewertung der Datenqualität und Schwierigkeiten bei der Georeferenzierung der Daten.

Diese Dissertation liefert einen Beitrag zur Verbesserung der Nutzbarkeit radarbasierter quantitativer Niederschlagsschätzungen, zur Sensibilisierung für deren Potenziale und Unsicherheiten und zur Überbrückung der Kluft zwischen der Radar-Community und anderen wissenschaftlichen Disziplinen, die der Nutzung der Daten immer noch eher zögerlich gegenüberstehen.

Zunächst wurde eine GIS-kompatible Python-Bibliothek entwickelt, um die Verarbeitung von Wetterradardaten zu erleichtern. Die Bibliothek verwendet einen effizienten Workflow, der auf weit verbreiteten Werkzeugen und Datenstrukturen basiert, um die Rohdatenverarbeitung und das Zuschneiden der Daten zu automatisieren. Alle Routinen wurden für die operationellen deutschen RADOLAN-Kompositprodukte ("RADar OnLine Aneichung") und den reanalysierten Radarklimatologie-Datensatz (RADKLIM) umgesetzt. Darüber hinaus bietet das Paket Funktionen für die zeitliche Datenaggregation, die Identifikation und Zählung von Starkregen sowie den Datenaustausch mit ArcGIS. Das Python-Paket wurde als Open-Source-Software namens *radproc* veröffentlicht. *Radproc* bildet die methodische Grundlage für alle nachfolgenden Analysen dieser Studie und wurde zudem bereits erfolgreich von mehreren wissenschaftlichen Arbeitsgruppen und Studenten zur Analyse von Starkregen und zeitlichen Aggregierung von Radardaten eingesetzt.

Des Weiteren wurden in dieser Arbeit die Entwicklung, Unsicherheiten und Potentiale der stündlichen RADOLAN- und RADKLIM-Kompositprodukte im Vergleich zu Ombrometerdaten analysiert. Die Ergebnisse haben gezeigt, dass beide Radarprodukte die Gesamtniederschlagssummen und inbesondere Niederschläge hoher Intensität tendenziell unterschätzen. Die Analysen zeigten jedoch auch signifikante Verbesserungen im Verlauf der RADOLAN-Zeitreihe sowie deutliche Qualitätsverbesserungen durch die klimatologische Reanalyse, insbesondere im Hinblick auf die Korrektur typischer Radarartefakte, orographischer und winterlicher Niederschläge sowie der entfernungsabhängigen Abschwächung des Radarsignals. Die Anwendbarkeit der Auswertungsergebnisse wurde durch die Veröffentlichung eines Geodatensatzes zum Niederschlagsvergleich für die RADOLAN-, RADKLIM- und Ombrometer-Datensätze untermauert. Der Vergleichsdatensatz ist eine Sammlung von Niederschlagsstatistiken sowie verschiedener Parameter, die die Qualität der Radardaten potenziell beeinflussen können. Er ermöglicht einen einfachen Vergleich und eine Analyse der verschiedenen Niederschlagsdatensätze und kann die Entscheidung

von Anwendern unterstützen, welcher Niederschlagsdatensatz für die jeweilige Anwendung und das jeweilige Untersuchungsgebiet am besten geeignet ist. Der Workflow für die Ableitung des Vergleichsdatensatzes wurde ausführlich beschrieben und kann als Leitfaden für individuelle Datenverarbeitungsaufgaben und als Fallstudie für die Anwendung der *radproc*-Bibliothek dienen.

Darüber hinaus wurde eine Fallstudie zur Anwendung von Radar-Komposits für die Abschätzung der Erosivität des Niederschlags durchgeführt. Dazu wurden RADKLIM-Daten und Ombrometerdaten mit einer zeitlichen Auflösung von 5 Minuten verwendet, um verschiedene Methoden zur Abschätzung der Niederschlagserosivität zu vergleichen, die in der Erosionsschutzpraxis Anwendung finden. Ziel war es, die Auswirkungen der Methodik und des Klimawandels sowie der Auflösung, Qualität und der räumlichen Ausdehnung der Eingabedaten auf den R-Faktor der Allgemeinen Bodenabtragsgleichung zu bewerten. Darüber hinaus wurden von anderen Studien vorgeschlagene Korrekturfaktoren im Hinblick auf ihre Fähigkeit getestet, unterschiedliche zeitliche Auflösungen von Niederschlagsdaten und die Unterschätzung des Niederschlags durch Radardaten zu kompensieren. Die Ergebnisse haben deutlich gezeigt, dass die R-Faktoren aufgrund des Klimawandels erheblich zugenommen haben und dass die aktuellen R-Faktor-Karten unter Verwendung neuerer, flächendeckender und räumlich höher aufgelöster Niederschlagsdaten aktualisiert werden müssen. Die Radarklimatologiedaten zeigten ein hohes Potenzial zur Verbesserung der Abschätzung der Niederschlagserosivität, aber aufgrund der vergleichsweise kurzen Zeitreihe und einiger Radarartefakte auch gewisse Unsicherheiten in der räumlichen Verteilung des R-Faktors. Die Anwendung von Korrekturfaktoren zur Kompensation der Unterschätzung des Radars führte zu einer Verbesserung der Ergebnisse, allerdings konnte eine mögliche Überkorrektur nicht ausgeschlossen werden, wodurch weiterer Forschungsbedarf bezüglich der Datenkorrektur aufgezeigt wurde.

Diese Arbeit schließt mit einer Diskussion der Rolle von Open-Source-Software, frei verfügbarer Daten und der Umsetzung der FAIR-Prinzipien (Findable, Accessible, Interoperable, Re-usable) für die deutschen Radar-Produkte zur Verbesserung der Nutzbarkeit von Radarniederschlagsdaten. Abschließend werden praktische Empfehlungen zur Vorgehensweise bei der Bewertung der Qualität radarbasierter quantitativer Niederschlagsschätzungen in einem bestimmten Untersuchungsgebiet gegeben und mögliche zukünftige Forschungsentwicklungen aufgezeigt.

Schlagworte: Niederschlag, Wetterradar, Radarklimatologie, Open-Source-Software, Bodenerosion, Erosivität, Starkregen, RADOLAN, RADKLIM

Contents

List of Figures

List of Abbreviations

BB	Bright Band
CC	Clausius-Clapeyron
DWD	Deutscher Wetterdienst (German Weather Service)
DOI	Digital Object Identifier
ECV	Essential Climate Variable
ES	Ecosystem Services
FAIR	Findable, Accessible, Interoperable, Re-usable
GDI-DE	Geodateninfrastruktur Deutschland (Geodata infrastructure Germany)
GIS	Geographic Information System
INSPIRE	Infrastructure for Spatial Information in Europe
InVEST	Integrated Valuation of Ecosystem Services and Tradeoffs
MAES	Mapping and Assessment of Ecosystems and their Services
NASA	National Aeronautics and Space Administration
OPERA	Operational Program on the Exchange of Weather Radar Information
OSS	Open Source Software
QPE	Quantitative Precipitation Estimate
Radar	Radio Detection and Ranging
RADKLIM	"RADarKLIMatologie" (German radar climatology dataset)
RADOLAN	"RADar OnLine Aneichung" (German operational radar dataset)
TRMM	Tropical Rainfall Measuring Mission
USLE	Universal Soil Loss Equation
UTM	Universal Transverse Mercator
WMS	Web Map Service

1

Introduction

1 Introduction

1.1 Motivation and Objectives

Precipitation is an Essential Climate Variable (ECV) and a major component of the hydrological and energy cycles in the environment. As one of the main sources for water supply, it plays an important role for the biosphere and is a driver for many environmental processes. However, precipitation may also be the cause for natural hazards such as heavy rainfall-induced flash floods or floodings, landslides and soil erosion, but also for droughts if rainfall fails to occur.

The occurrence of **floods** and **droughts** has enormous **impacts on society and the environment**. Consequently, the spatiotemporal distribution of precipitation and the expected increase of rainfall-related weather extremes are important issues for many scientific disciplines including meteorology, hydrology, geography, biology, ecology, ecosystem services research and social sciences, but also for stakeholders and decision makers in water management, agriculture, forestry, environmental and urban planning institutions, civil protection, insurance business and policy and decision making.

Due to a warming climate, **heavy rainfall events are expected to increase in terms of frequency and intensity** (IPCC 2013; Asadieh and Krakauer 2015; Field *et al.* 2015). They can induce flash floods that may cause high material damages and even casualties and that are hard to predict. Flash-flood-inducing heavy rainfall events are often caused by small-scale convective cells in the atmosphere with high spatial variabilities of the rain rates. Precipitation monitoring has always been essential for many applications such as water management, agriculture and weather forecasting. However, in order to identify changes and adapt to these changes, to ensure water supply and to mitigate weather extremes, precipitation measurements of high spatial and temporal resolution are crucial.

In the past, precipitation was measured by **rain gauge recorders** that collect the hydrometeors and continuously record the amount of water using a float and a plotter drum. Approximately since the beginning of the 2000s, the recorders have been replaced more and more by **automated rain gauges**, which are based on the recorder's general layout, but provide continuous digital rainfall measurements and recordings. Still, these point-scale measurements are not able to detect the spatial rainfall distribution in a comprehensive way.

Throughout the last decades, **weather radars** have emerged as a new measurement technique that is capable of providing areal precipitation observations with high spatial and temporal resolution. The comprehensive rainfall detection put precipitation monitoring on a new level and opened up new applications in the fields of meteorology and hydrology (Seo *et al.* 2010). However, it is an indirect remote sensing technique which suffers from various uncertainties regarding quantitative precipitation estimations. Several potential error sources have to be considered and their effects have to be corrected (Seo and Krajewski 2010; Villarini and Krajewski 2010). The radar community has put much effort into the development of error correction and gauge adjustment algorithms (Germann *et al.* 2006; Goudenhoofdt and Delobbe 2009; Seo and Krajewski 2010; Villarini and Krajewski 2010; Hazenberg *et al.* 2011). Nonetheless, all radar-based quantitative precipitation estimates (QPEs) may be subject to some systematic or random biases, which have to be evaluated and taken into account when using the data. Until recently, working with radar data required significant individual data correction and processing effort and, thus, considerable methodological knowledge to obtain reliable radar-based QPEs (Jessen *et al.* 2005; Krajewski *et al.* 2011). Consequently, radar rainfall data have received growing attention, but operational usage was largely limited to the radar community for a long time (Einfalt *et al.* 2004).

Throughout the last decade, the understanding of application requirements of radar data and their limits have improved and QPEs have become more mature. Along with advances in radar and computer

hardware, this lead to an increase of radar QPE applications, particularly in urban hydrology (Thorndahl *et al.* 2017). However, despite the undisputed potential for various applications across different scientific disciplines, **weather radar data** have still **not been used as extensively as one could expect** (Berne and Krajewski 2013).

In the last years, several operational national radar data archives exceeded a time series length of ten years and many new climatological correction algorithms were developed. Several **new radar climatology datasets** have been derived, which provide largely consistent, well-documented radar QPE products and open up new climatological application fields for radar data (Overeem *et al.* 2009; Wright *et al.* 2014; Fairman *et al.* 2015; Marra and Morin 2015; Keupp *et al.* 2017; Winterrath, T. *et al.* 2017).

Despite these achievements and recent enhancements in radar QPE quality, several **challenges** remain on the way to increase **radar data utilisation** beyond the radar community. For potential users, challenges include for instance different proprietary data formats, the processing of large data volumes and a scarcity of easy-to-use and free-of-charge software, a lack of knowledge on typical radar-related errors, additional effort for data quality evaluation and difficulties concerning data georeferencing (Berne and Krajewski 2013; Heistermann *et al.* 2013).

The overall objective of this thesis is to develop and test tools to **facilitate the use of radar-based QPE products** and to raise awareness on their **potentials and uncertainties**. For this purpose, this study provides different methodologic and scientific contributions that aim to reduce the necessary effort for radar data processing and evaluation. At the same time, our understanding of radar error structure and its impacts in space and time will be improved. Firstly, a workflow for automated raw data processing and subsequent analysis was developed and implemented into an open source software. Secondly, developments, potentials and uncertainties of the new radar-based QPE climatology dataset were analysed and evaluated. The applicability of the evaluation results was underpinned by the publication of a rainfall inter-comparison geodataset for three different precipitation datasets, which enables the user to straightforwardly assess data quality for his or her study area and analysis period. Finally, in a case study on the estimation of rainfall erosivity from radar QPEs, the advantages and uncertainties as well as correction approaches to compensate for radar errors were analysed. All contributions were implemented for the nationwide weather radar QPE products in Germany which are provided by the German Weather Service (Deutscher Wetterdienst, DWD) and presented in detail in the Chapters 2 to 5.

In the introductory part of this thesis, an overview of the observed and expected changes in precipitation against the background of climate change is given as a meteorological motivation on the increasing necessity of highly resolved precipitation data. Next, background knowledge is provided on the operating principles, uncertainties, potentials and challenges of weather radar-based QPEs. Finally the detailed goals and research questions and the outline of the thesis, including four individual scientific articles, are presented.

1.2 Precipitation and Climate Change

The troposphere has warmed globally since the mid-20th century and this trend is expected to continue and likely increase, mainly depending on the atmospheric concentrations of greenhouse gases (IPCC 2013). Due to a warming climate, **precipitation events are expected to become more intense** in many regions of the world (Frei *et al.* 1998; Min *et al.* 2011; Donat *et al.* 2013; Madsen *et al.* 2014; Abraham *et al.* 2015; Asadieh and Krakauer 2015). This intensification is mainly attributed to the fact that warmer air can retain more moisture. According to the **Clausius-Clapeyron (CC)** relation, the water-holding capacity of the atmosphere increases by about 7% per degree of warming (Trenberth *et al.*

2003). Several studies have indeed found evidence that precipitation rates actually increase with temperature approximately at the CC rate. Particularly for short-duration convective thunderstorms, even exceedances of this rate have been observed, which is referred to as **super-CC scaling** (Lenderink and van Meijgaard 2008; Berg *et al.* 2013; Lenderink *et al.* 2017; Lengfeld *et al.* 2018; Förster and Thiele 2019). However, the spatiotemporal variability of observed and modelled trends is very high with both positive and negative directions.

In Europe, the frequency and intensity of heavy precipitation events tend to increase at the majority of weather stations (Field *et al.* 2015). Frei *et al.* (2006) expect the increase in frequency to be particularly pronounced in winter and north of about 45°N, while Fiener *et al.* (2013) observed an increase of erosive heavy rainfall events in frequency and magnitude in Central Europe during summer. Moreover, temperature and, thus, **pressure gradients between the polar and tropical latitudes** will change. It is expected that, particularly in winter, the lower-tropospheric meridional temperature gradient will decrease, whereas the meridional temperature gradient in the upper troposphere will increase between approximately 30° and 40° north and south. The latter comes along with a rise in the height of the tropopause as well as a strengthening and a poleward shift of the tropospheric zonal jets (Lorenz and DeWeaver 2007). The effects of these changes on the intensity, tracks and passage speed of extratropical cyclones, which have a major impact on the spatiotemporal precipitation distribution in the midlatitudes, are still highly uncertain (Catto *et al.* 2019).

Several scenarios predict that precipitation increases in most of Europe during winter and decreases in summer. The latter may be attributed to more stable anticyclones over the northeastern Atlantic, which block summer storms and lead them northward (Giorgi *et al.* 2004). In return, more stable atmospheric conditions and lower pressure gradients in the lower troposphere may result in a lower pace of extratropical cyclones. On the one hand, thunderstorms may tend to stay longer in the same area, which would cause higher precipitation amounts and heavy rainfall events of longer durations. On the other hand, the blocking by anticyclones may cause longer dry periods, which would lead to more short-term droughts (Field *et al.* 2015). Accordingly, for many regions in Europe, the **number of wet days** is expected to decrease, whereas the **intensity** and the **return levels of daily precipitation events** are expected to increase (Semmler and Jacob 2004). As a consequence, cloud cover and soil water content will decrease significantly (Giorgi *et al.* 2004). This combination of increasingly intense heavy rainfall and the reduced water infiltration capacity of dry soils is expected to amplify the risk of floodings (Kyselý and Beranová 2009).

1.3 Radar-Based Quantitative Precipitation Estimates

1.3.1 Operating Principle of Weather Radars

Radar is the abbreviation for "**Radio Detection and Ranging**". It is a collective term for various procedures for radio detection and ranging of reflective objects. Depending on the area of application of the radar, reflecting objects can be aircraft, ships, precipitation, objects in the landscape such as mountains, buildings, vegetation, wind energy plants or power lines, as well as icebergs, birds, people, aircrafts, space probes or even planets (Skolnik 2008).

Although there are many different types of radar systems, the basic design and operating principle are always similar: a stationary radar usually consists of a radar dish with a transmitter unit and an antenna, a radome as weather protection and a building that houses the radar computer and electronics (Sene 2010). The transmitter uses a magnetron to generate **electromagnetic energy pulses** of a constant length and frequency in a specified cycle. The antenna bundles these and radiates them in the desired direction at the speed of light. When the radiated energy hits a reflecting object, the object scatters the energy in different directions and reflects a part back towards the antenna. After

the energy pulse has been emitted, a duplexer converts the operating mode of the antenna, which now serves as a receiver for the reflected radar echoes. The distance between the radar and the reflector can be calculated from the transit time between the transmission of the pulse and the arrival of the echo. In addition, the strength of the received signal provides information about the properties of the reflecting object (Skolnik 2008).

When used as weather radar, the radar pulses are directed towards clouds and precipitation, and the **strength of the echo** depends on the **number, size distribution and phase of the hydrometeors** contained therein. The wavelength emitted by the radar systems is selected based on the size distribution of the hydrometeors. It is generally assumed that the observed hydrometeors are Rayleigh scatterers. Since their diameter is ten times smaller than the wavelength, the wavelength must be at least 3 cm, for example, to be able to detect water droplets with a size of 3 mm. Therefore, the wavelengths used in weather radar systems are usually between 3 cm (X-band) and 10 cm (S-band), with 5 cm (C-band) being the most commonly used wavelength (Löwe 2008). When choosing a wavelength, it must also be taken into account that electromagnetic pulses with a shorter wavelength have a shorter range due to increased attenuation of the signal in the atmosphere, but at the same time a smaller, less expensive dish is required (Sene 2010).

Weather radar systems can provide a wide variety of products for a wide range of applications, using three different atmospheric scanning methods: The "Vertical Scan Mode" allows a vertical profile of the distribution of hydrometeors in the lowest 20 km of the atmosphere. The second option is the "Volume Scan Mode" for the three-dimensional, holistic recording of the air space and the third option is the area-wide recording of the lowest altitude level, where precipitation occurs almost exclusively, with the "Base Scan Mode" (Löwe 2008). In most operational radars, the scanning strategy consists of a volume scan with several azimuthal sweeps or elevations scans, which means that the antenna rotates at a fixed elevation angle before the elevation angle is increased for each subsequent sweep (see. Figure 1) (Holleman *et al.* 2006).
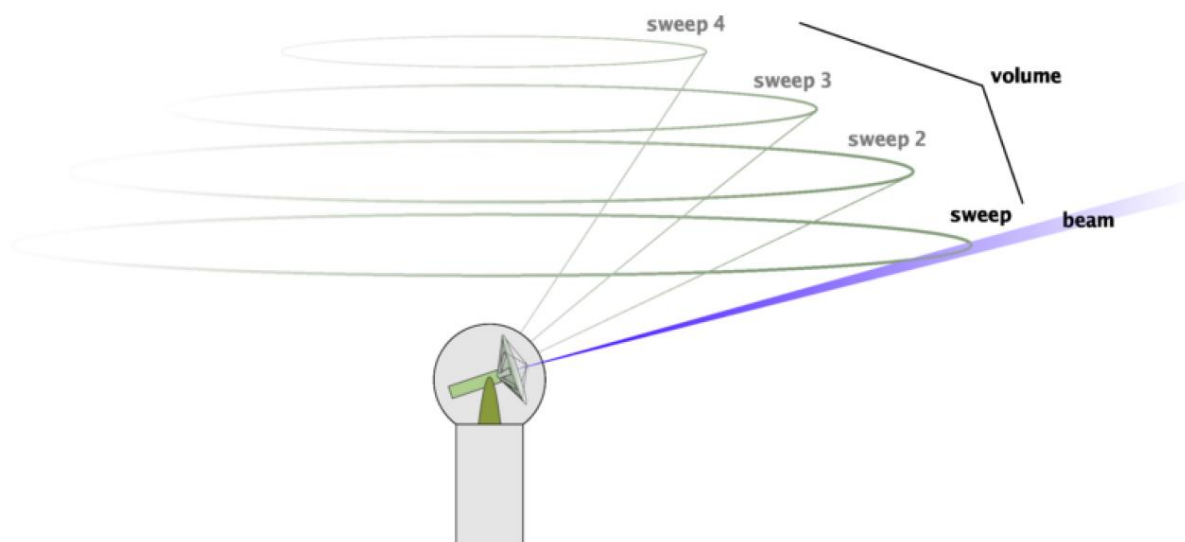
Figure 1: A typical scanning strategy of an operational weather radar (Holleman *et al.* 2006, p. 30).

Moreover, many operational weather radars are capable of providing information on the direction of movement and speed of rainfall cells by using the **Doppler technology**. This is based on the Doppler effect, which describes the frequency shift of an electromagnetic pulse with a varying distance between radar and backscatterer (Berne and Krajewski 2013). Thus the frequency increases as the reflector approaches the radar and decreases as the reflector moves away (Shelton 2008).

In recent years, a new type of weather radar has increasingly been established in operational weather radar networks. This so-called **polarimetric** or **dual polarisation radar** can collect further information about the shape and size of hydrometeors. Classical radars have a single polarisation, i.e. they transmit and receive a usually horizontally-oriented energy pulse. Polarimetric radar systems transmit and receive both horizontally and vertically polarised signals. By calculating the difference between the two signals, the shape of the hydrometeor can be inferred. This differential reflectivity is primarily used to distinguish different types of hydrometeors and, in particular, to identify hail. Hail tumbles when falling and does not change its shape, while falling drops of water larger than 1 mm flatten. As a result, the horizontal and vertical reflectivity of hailstones are approximately equal, so that the difference is very small or can even be slightly negative. In the case of flattened raindrops, on the other hand, the main axis is almost horizontal, so that the horizontal reflectivity is significantly higher than the vertical reflectivity and the difference is positive (Keeler and Serafin 2008; Cifelli and Chandrasekar 2010). In addition, polarimetric radar offers new possibilities for correcting interference and attenuation effects, as well as for improved rain rate estimations and estimations on the space-time distribution of the drop size distribution (Berne and Krajewski 2013).

For operational applications and a coverage of large areas, the reflectivity data from the individual radar stations must be merged into a common image, the so-called radar composite. Finally, the determination of the amount of precipitation is basically carried out in two steps: First, the power reflected by hydrometeors, the reflectivity, is determined and then the intensity of the precipitation is estimated. The conversion from reflectivity to rain rates is done by using an empirical relationship, the **Z-R relationship**:

$$ Z = a \cdot R^b \;\leftrightarrow\; R = \left(\frac{Z}{a}\right)^{\frac{1}{b}} = \left(\frac{10^{\frac{dBZ}{10}}}{a}\right)^{\frac{1}{b}} \tag{1} $$

where R is the rain rate [mm h^{-1}] and a and b are constants (Keeler and Serafin 2008). However, the determination of a and b is problematic. The constants depend on the formation of precipitation (convective, stratiform, orographic), the type of hydrometeors (rain, snow, hail, sleet), the location and the season and can vary greatly depending on the resulting drop size distribution.

1.3.2 Potentials

The main advantage of weather radars is their capability to provide **comprehensive spatially distributed precipitation information**. The spatial resolution of the radar data depends on the radar hardware, whereby the wavelength determines the radial resolution and the design and size of the antenna determine the azimuthal horizontal resolution (Thorndahl *et al.* 2017). For operational C-band radars as they are used, for example, in the German radar network, the former is usually about 1 km and the latter is 1°. After merging the local radar station data to a nationwide composite, the German QPE composites have a spatial resolution of approximately 1 km * 1 km. This corresponds to a total of approximately 392,000 pixels for the whole area of Germany. In order to illustrate this high degree of spatial resolution and coverage in comparison to the operational point-scale rain gauge network operated by the German Weather Service (DWD), Winterrath *et al.* (2017) presented a remarkable sample calculation: The German rain gauge network comprises approximately 4401 stations, each of them with an opening of 200 cm^2. This covers approximately 0.000000025 % of the total area of Germany. Consequently, each station represents an area of 81.2 km^2 on average and the mean distance between stations amounts to about 9 km. Considering the large spatial heterogeneity of rainfall and the average size of a convective rainfall cell, which amounts only to a few kilometres, it

becomes obvious how much information on the spatial rainfall distribution cannot be detected even by a dense network of rain gauges. By correlating this calculation example to a global scale, Kidd *et al.* (2017) concluded that only about 0.000000000593 % of the Earth's surface is covered by operational rain gauges. When visualising these numbers based on a 105 * 68 m soccer field, the total area measured globally by currently available rain gauges is equivalent to less than half of the field, whereby the German gauge network fits completely into the inner goal area.

The **temporal resolution** of radar data is determined by the scanning strategy, in other words, by the rotation speed and the number of azimuthal elevations that are scanned. A full volume scan can last several minutes and the highest available temporal resolution for operational weather radars is usually 5 minutes. X-band radars are capable of providing precipitation information with a temporal resolution of 1 minute and spatial resolutions of up to 100 m, but have a smaller range in return (Thorndahl *et al.* 2017).

Consequently, in contrast to rain gauges, which measure the actual precipitation at a specific location, weather radars provide comprehensive spatially distributed precipitation observations with high temporal resolution. This higher level of detail allows not only spatially much more differentiated estimates of precipitation amounts or the tracking of storm paths, but also the detection of small-scale, mostly convective precipitation or thunderstorm cells, which are often not registered by the precipitation recorders as they pass by.

Furthermore, weather radar observations provide **additional information** such as vertical reflectivity profiles and dual-frequency information from which information on the atmospheric conditions and hydrometeor type, size and shape can be inferred.

As another promising approach for spatially distributed precipitation information as well as other metadata on atmospheric conditions, **satellite-based observations** should be mentioned. The first weather satellites were tested in 1959 and the early 1960s and the first consistent global measurements have been provided by the weather satellites of the Nimbus series launched by the National Aeronautics and Space Administration (NASA) since 1964. The first dedicated precipitation observation satellite was launched in 1997 within the Tropical Rainfall Measuring Mission (TRMM), so the time series are of a similar length compared to many operational radar networks. Satellite observations are also indirect remote sensing measurements, which are prone to errors and uncertainties. Their major advantage is a global spatial coverage, whereas gauge and radar networks are not equally distributed and radar is not at all established in many countries. However, satellite observations are currently still limited to spatial resolutions of approximately 4 km * 4 km or 0.1° * 0.1° to 1° * 1° every 15 to 30 minutes (Kidd and Levizzani 2011; Ramsauer *et al.* 2018). Consequently, especially for near real-time applications and applications that require high quality and high resolution rainfall information, for instance for heavy rainfall analysis, weather radars provide precipitation data of significantly higher spatial and temporal resolution. However, both datasets are complementary since they can serve as valuable references for data quality evaluation and inter-comparisons.

In regard to the length of the available time series, rain gauges obviously still provide the most long-term data. However, due to instrumentation changes and improvements as well as changes in the number and positioning of stations, these datasets also suffer from inconsistencies. Both the radar and satellite archives now exceed the length of half of a climate reference period and, thus, have become relevant for climatological and statistical applications**.** In order to **leverage the full potential of these datasets as soon as they reach the length of an actual climatological time series, challenges in data application** (i. e. data processing, knowledge about error structure and correction factors/algorithms for bias correction, models that can deal with the new error structure and input data resolution) **should be addressed now**.

1.3.3 Uncertainties

As described in Section 1.3.1, precipitation observation using weather radar is an indirect measurement approach. Rain rates and distributions are inferred from measured reflectivities, which are subject to a series of potential error sources. This introductory Section provides an overview of the most common uncertainties that radar QPE users should be aware of in order to correctly interpret their results. For a more exhaustive treatment of all error sources, their interrelations and correction approaches, please refer to Krajewski and Smith (2002) and Villarini & Krajewski (2010) and the references therein, as these issues are beyond the scope of this study.

Rain rate estimation: The mathematical-physical relationship between reflected energy and precipitation, which varies depending on location and weather conditions, must be applied for the conversion from radar echoes to rain rates. The key meteorological property of precipitation for the interpretation of reflectivity is the **drop size distribution**. Since this distribution is never exactly assessed, all conversions with **Z-R relationships** are always actually precipitation estimates (Krajewski and Smith 2002). Moreover, the **precipitation phase** plays an important role because rain, snow, melting snow, hail and graupel, all have different reflection properties. A particular source of uncertainty is the melting layer, which is also referred to as the **Bright Band (BB)**. Snowflakes have a greater diameter and lower reflectivity than raindrops. If these relatively large melting hydrometeors are coated by a film of water, which has a higher conductivity than ice, the return signal increases significantly and precipitation can be overestimated. In contrast, snowfall and hail are often underestimated due to their low reflectivity and uncertainties in the selection of the appropriate Z-R-relation (Einfalt and Michaelides 2008; Hazenberg *et al.* 2011).

Gauge adjustment: In addition, the derivation of QPEs requires adjustment and comparison to ground observations by rain gauge measurements. The latter need to be thoroughly checked and be of high quality to avoid random or systematic bias from gauge measuring and sampling errors due to missing data, clogging of the gauge or local wind effects (Villarini *et al.* 2008; Thorndahl *et al.* 2017).

However, the conversion of the received radar echoes into rain rates is by far not the only source of uncertainty in precipitation estimation with weather radars. The received echoes themselves are often already subject to errors. Figure 1 gives an overview of the most important error sources that can distort radar echoes.
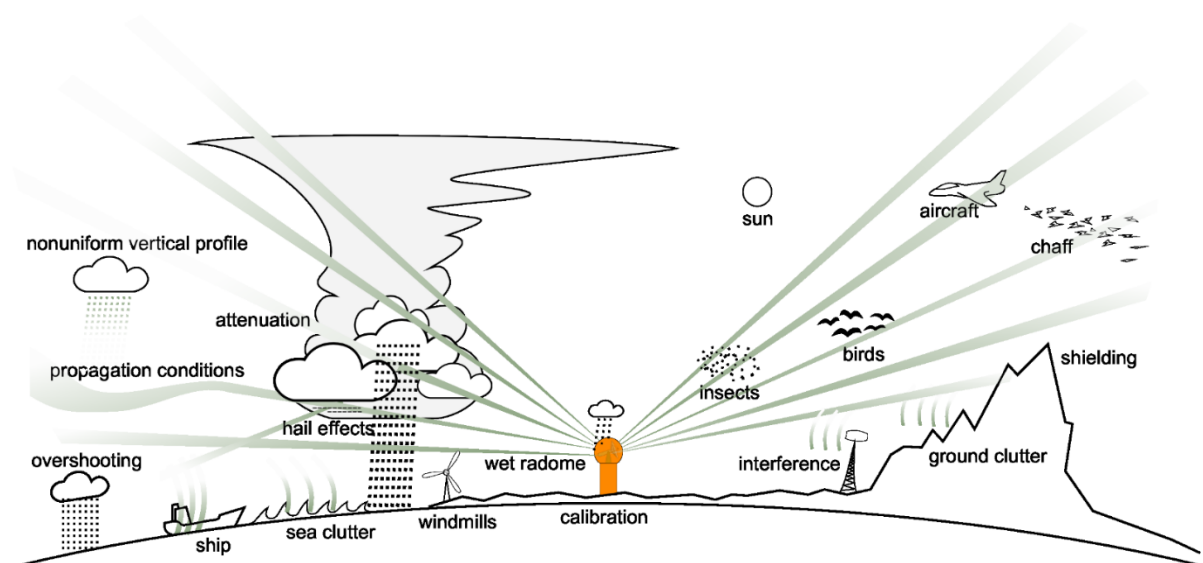
Figure 2: Phenomena affecting weather radar data quality (Holleman *et al.* 2006, p. 29).

Non-precipitation echoes: The radar beam detects also various non-meteorological objects that disturb the signal, such as mountains, buildings, wind energy plants or trees. These echoes are called **Ground Clutter** and can be reduced with intelligent radar siting, a good scanning strategy with appropriate elevation angles of the radar beam, visibility analyses using Digital Elevation Models, static clutter maps and Doppler techniques. Return signals from moving objects such as aircrafts, insects or birds are more difficult to detect, but also have a lower impact on rainfall amounts on a climatological time scale. Ground Clutter may also be caused by **anomalous beam propagation**. Different temperature and pressure gradients in the atmosphere may cause a refraction downwards and return signals from the Earth's surface at rather long range from the radar (Einfalt and Michaelides 2008; Sene 2010).

Shielding: The radar beam may be blocked in whole or in part by nearby mountains, high buildings or trees, which leads to a shielding of the sector behind the obstacle. The so-called negative spoke is a typical linear radar artefact that results from beam blockage (Einfalt and Michaelides 2008).

Signal attenuation: During heavy rainfall or the winter season, the radome of a radar may be covered by a thin film of water or by snow and ice, which causes strong attenuation of the radar beam. Moreover, heavy precipitation events and hail can cause a strong underestimation of precipitation intensity due to path-integrated attenuation of the radar signal (Bronstert *et al.* 2018).

Range degradation: One of the biggest problems in radar-based QPE is the underestimation of rainfall at a far range from the radar, which can be caused by overshooting of precipitation systems, broadening of the radar beam, but also signal attenuation. Due to the Earth's curvature, the height of the radar beam increases at farther ranges from the radar. Moreover, in areas with complex terrains, the elevation angle of the radar may need to be higher in order to avoid Ground Clutter from mountains. Both effects may cause the radar beam to scan the atmospheric layers above the cloud level, which leads to an underestimation of the actual precipitation. This **overshooting** is of particular importance for orographic precipitation as well as during winter or in cold climates, where snow and rainfall events are primarily of rather shallow and stratiform character. At a far range from the radar, the beam broadens, sample volume increases and, thus, the radar beam is often only partially filled. This **partial beam filling** causes small but intense rainfall to be averaged out and leads to underestimations (Villarini and Krajewski 2010).

Further errors may be caused by **non-uniformly vertically distributed precipitation** and **subcloud evaporation**, **electromagnetic interference** by other radars or microwave links, **radar miscalibration**, **precipitation drift**, **projection issues** and **QPE composite creation** (Villarini and Krajewski 2010).

1.3.4 Challenges

The use of radar data poses a series of challenges, which has prevented the data from being used more widely. In 2013, Berne & Krajewski published a review of radar data usage in hydrology and summarised the challenges for the current decade.

As indicated in the previous Section, the most obvious challenge is raised by the manifold uncertainties concerning the quality and interpretation of the indirect radar measurements. In the end, radar-based precipitation products will always be estimates with some inherent bias. This **radar error structure and its distribution in space and time** need to be properly characterised in order to assess the uncertainties associated with each individual QPE product (see Chapter 4). With regard to many potential applications related to water resources management, flood regulation and climate change, three main challenges concerning the reduction and evaluation of uncertainties can be identified.

First, particular emphasis needs to be put on the improvement of **precipitation estimation in mountainous regions** as they are affected by many of the sources of error mentioned above.

Second, the **quantitative estimation of snowfall** is still a major issue. Advances in polarimetric radar finally allow for a better distinction of different types of hydrometeors and will hopefully help reduce this uncertainty.

Third, the **quantification of heavy and extreme rainfall** is very important for flood regulation, erosion control, studies of climate change and many more, but subject to significant uncertainties due to attenuation of the radar beam. Using rain gauge data to adjust heavy rainfall measurements is difficult due to the lack of information on the spatial distribution. Satellite-based measurements could provide additional data for improving the quantification of heavy rainfall, although this is very challenging. For example, information on cloud-top texture derived from visible sensors and cloud-top temperatures measured by infrared sensors can provide information on the size, type, height and temperature of clouds. Since larger, taller clouds with a cold top are associated with heavy rainfall (Kidd and Levizzani 2011), this information could help to identify and characterise extreme events and to estimate the precipitable water loads of such thunderstorm cells. Moreover, recent advances in stochastic spatiotemporal rainfall modelling could help to improve extreme rainfall estimates by generating ensembles of intensity-duration-frequency curves at radar subpixel scale (Thorndahl *et al.* 2017; Peleg *et al.* 2018).

As radar data time series are becoming longer and climatological applications are therefore being established, a very important challenge from a user's perspective is **data management and processing**. Radar datasets are significantly larger than rain gauge datasets due to their high spatial resolution (Berne and Krajewski 2013). The processing of such large datasets requires not only an efficient workflow, but also an automation which requires either programming skills or a dedicated software. However, the availability of such software as well as the data processing are hampered by several different proprietary formats used for data provision (Hänsel *et al.* 2018). Despite efforts such as the OPERA programme (Operational Program on the Exchange of Weather Radar Information) (Michelson *et al.* 2014) to establish a common data exchange format, many national meteorological authorities still use their own custom formats, which require individual processing software (see Chapter 2). Furthermore, uncommon and custom projections and spatial references used for radar data may hamper data usability due to spatial distortions and challenges concerning the intersection of radar data with other geodata (see Chapter 3 and 4).

Besides the outlined challenges regarding data quality and processing, additional efforts are necessary on the **application level** in order to increase the usability of radar data. Especially for hydrological modelling, but also for other applications such as the modelling of soil erosion (see Chapter 5) and landslides or the provision of water-related ecosystem services (e.g. flood regulation, cooling capacity, soil water cycling), precipitation is a key input parameter.

Due to the point-scale resolution of historical precipitation data, many of the available **hydrological models** do either not provide the possibility to input highly resolved gridded data or are hard to **calibrate** for the use of such high resolution inputs. For example, (Reed *et al.* 2004) compared 12 distributed rainfall-runoff-models against a lumped model which does not support high resolution input data and found that the lumped model outperformed most of the distributed models. Here, technical and scientific developments as well as new calibration approaches to account for the higher resolution and the different error structure of radar data are necessary (Berne and Krajewski 2013). Moreover, an evaluation of **uncertainty propagation** is required in order to interpret results correctly, improve the models and select the best-suited QPE product for the respective application (Heistermann and Kneis 2011; Thorndahl *et al.* 2017).

Furthermore, many models in environmental sciences require either **temporally aggregated rainfall data or individual indices** derived from the original data instead of temporally highly resolved raw data. For example, the InVest (Integrated Valuation of Ecosystem Services and Tradeoffs) suite of models, which is widely used in **ecosystem services (ES) research**, contains several models requiring rainfall information (e. g. urban flood risk mitigation, annual and seasonal water yield, nutrient and sediment delivery) (Sharp *et al.* 2020). The required input precipitation file can be one single grid of arbitrary spatial resolution, which has to be generated with an additional preprocessing routine. Particularly for Mapping and Assessment of Ecosystems and their Services (MAES), which is characterised by a holistic, interdisciplinary analysis and spatially explicit mapping of ecosystems, many input datasets from strongly varying disciplines (environmental sciences, social sciences, economy) are required (Burkhard and Maes 2017). The generated maps are useful to identify and evaluate synergies and trade-offs between different ES and between ES and biodiversity and can thus support decision makers in policy and regional planning (BISE 2020). Problems regarding data acquisition for ES modelling include varying availability, spatial resolution and overall data quality. Due to the large diversity of required data, model users might have less profound expertise on individual measuring techniques and datasets compared to researchers in the respective dedicated disciplines such as hydrology. Thus, freely available and easy-to-use software solutions for data preprocessing, the publication of ready-to-use aggregated (geo)datasets and studies that summarise developments and uncertainties of individual datasets could improve the usability of any new dataset.

Such contributions to the scientific landscape can also help to **interpret and evaluate published results and proposed changes to modelling approaches based on weather radar data**. For **modelling soil erosion** by water, the Universal Soil Loss Equation (USLE) is widely used (Wischmeier and Smith 1978). Rainfall data are required to estimate rainfall erosivity, which is implemented into USLE as the R-factor (see Chapter 5). In 2019, Auerswald *et al.* (2019) proposed a new R-factor map for Germany derived from weather radar composites. Their methodology comprised several deviations from the methodology widely used in practice (Schwertmann *et al.* 1990; Deutsches Institut für Normung 2017). Changes include smoothing algorithms and modified thresholds for determining erosive rainfall, but also correction factors to compensate for differences in the measuring method compared to rain gauges as well as for systematic radar errors such as the underestimation of heavy rainfall intensity, which is crucial for estimating rainfall erosivity (Fischer *et al.* 2018; Auerswald *et al.* 2019). The new R-factor shows on average 66% higher values than the map by Sauerborn (1994), which is still widely used in Germany (Auerswald *et al.* 2019). As such a large increase of the R-factor will have a significant impact on modelling results and subsequent decision making for soil erosion control, there is scepticism in the soil erosion community in regard to the new R-factor map. Due to changes in input data quality and resolution, but also climate and methodology, the respective impact of the radar QPE uncertainties and the other aspects on the results remains unclear. Comparative studies analysing the impacts and interrelations of respective influencing factors may help to interpret results and either increase the confidence in new propositions or raise the awareness of their weaknesses (see Chapter 5).

1.4 Research Questions and Outline of the Thesis

This study provides **a contribution to improve the usability of weather radar composite data and bridge the gap between the radar community and other scientific disciplines** which are still rather reluctant to use these highly resolved data. Despite their large potential outlined above, weather radar data are not as widely used as one would expect, particularly beyond the fields of hydrology and meteorology. According to many of the challenges described in the previous Section, this reluctance is due to QPE uncertainties, a lack of knowledge about available QPE products and their quality as well as the high effort for data processing and the scarcity of dedicated software.

Placing a focus on user challenges for radar QPE usage, this thesis addresses the following main research questions:

- How can the barrier to weather radar data usage be reduced and what role can open source software and open data have in this case?

- Which developments, potentials and uncertainties have to be considered when using operational radar-based QPEs and reanalysed radar climatology QPEs in comparison to rain gauge data?

- How do the German reanalysed radar climatology QPEs perform in a case study on rainfall erosivity and to what extent can correction factors compensate for systematic radar errors?

The objectives and research questions are addressed in four successive chapters, whereby each chapter corresponds to an article published in or submitted to a peer-reviewed international journal (see List of Publications, p. 108).

Chapter 2 has a strong methodological focus on radar data processing and analysis workflows and on software availability. First, it provides an extensive review of existing software for the processing of German weather radar composites and an overview of the software availability in other countries. The review puts an emphasis on the role of open source software because, especially in research, there is often a need to develop new algorithms or analysis techniques for which existing source code needs to be manipulated or a new code needs to be written.

Second, Chapter 2 presents the Python package *radproc* as primary methodological contribution of this thesis to facilitate weather radar data processing in Germany and beyond. *Radproc* is a GIS-compatible open source software, which uses an efficient workflow based on widely used tools and data structures to automate raw data processing and data clipping. Moreover, the package provides functions for temporal aggregation, heavy rainfall detection and data exchange with ArcGIS. This Chapter also describes the technical implementation of *radproc*, shows a typical data processing workflow and discusses limitations and future developments.

In **Chapter 3**, the focus shifts to the intercomparison of two different radar-based QPEs with rain gauge station data for Germany. The chapter describes the derivation methodology and the benefits of a rainfall data intercomparison geodataset which has been published alongside the article. The dataset is a collection of precipitation statistics and several parameters that can potentially influence radar data quality. It allows for a straightforward comparison and analysis of the different precipitation datasets and can support a user's decision on which dataset is best suited for his or her application and study area. The Chapter also discusses several aspects of data processing and quality control such as outlier detection, handling missing data as well as georeferencing and projection issues.

The dataset described in Chapter 3 provides important input for **Chapter 4**, which concentrates on a detailed analysis and evaluation of developments, uncertainties and potentials of the operational and reanalysed German radar QPE products in comparison to rain gauge data. The advantages and disadvantages of all three datasets are discussed, their inherent bias and errors are assessed across various time scales ranging from annual and seasonal aggregations to hourly rainfall intensities in regard to their capability to map long-term precipitation distribution, to detect low intensity rainfall and to capture heavy rainfall. Furthermore, the impacts of season, orography and distance from the radar on long-term precipitation sums were examined in order to evaluate dataset performance. The analyses presented in this chapter aim to gain a better understanding of radar data quality, raise awareness of advantages and disadvantages of the respective datasets and help to correctly interpret results gained from analyses based on these data.

Chapter 5 presents a case study on radar composite data application for rainfall erosivity estimation. For estimating soil erosion by water using the Universal Soil Loss Equation (USLE), the R-factor serves as a measure of rainfall erosivity, which can be derived directly from temporally highly resolved precipitation time series. The case study was conducted for the German federal state of Hesse and compares several different methods for the derivation of the R-factor, which were used with radar climatology QPEs and rain gauge data in different temporal resolutions for intercomparison. Moreover, the impact of correction factors to compensate for systematic radar QPE errors and temporal rainfall data resolution, which were proposed in recent studies, was evaluated. Furthermore, the implications of the results for the practical application in the case study area are discussed and recommendations for further research and practical application are provided.

Finally, in **Chapter 6**, the outcomes of above-mentioned research are discussed, the related research questions are answered, conclusions are drawn and recommendations are given.

2

Facilitating Radar Precipitation Data Processing, Assessment and Analysis: A GIS-compatible Python Approach

J. Kreklow

Facilitating radar precipitation data processing, assessment and analysis: a GIS-compatible python approach

Jennifer Kreklow

Jennifer Kreklow
Leibniz Universität Hannover, Institute of Physical
  Geography and Landscape Ecology,
Schneiderberg 50, 30167 Hannover,
Germany
E-mail: kreklow@phygeo.uni-hannover.de

ABSTRACT

A review of existing tools for radar data processing revealed a lack of open source software for automated processing, assessment and analysis of weather radar composites. The ArcGIS-compatible Python package *radproc* attempts to reduce this gap. *Radproc* provides an automated raw data processing workflow for nationwide, freely available German weather radar climatology (RADKLIM) and operational (RADOLAN) composite products. Raw data are converted into a uniform HDF5 file structure used by *radproc*'s analysis and data quality assessment functions. This enables transferability of the developed analysis and export functionality to other gridded or point-scale precipitation data. Thus, *radproc* can be extended by additional import routines to support any other German or non-German precipitation dataset. Analysis methods include temporal aggregations, detection of heavy rainfall and an automated processing of rain gauge point data into the same HDF5 format for comparison to gridded radar data. A set of functions for data exchange with ArcGIS allows for visualisation and further geospatial analysis. The application on a 17-year time series of hourly RADKLIM data showed that *radproc* greatly facilitates radar data processing and analysis by avoiding manual programming work and helps to lower the barrier for non-specialists to work with these novel radar climatology datasets.

Key words | heavy rainfall, open source software, radar climatology, RADKLIM, *radproc*, weather radar

ABBREVIATIONS

API	Application Programming Interface
BUFR	Binary Universal Form for the Representation of meteorological data
CDC	Climate Data Center
DWA	Deutsche Vereinigung für Wasserwirtschaft, Abwasser und Abfall e.V.

DWD	Deutscher Wetterdienst (German Weather Service)
EUMETNET	European Meteorological Services Network
GIS	Geographic Information System
GRIB2	General Regularly-distributed Information in Binary form version 2
GUI	Graphical User Interface
HDF5	Hierarchical Data Format version 5
IDE	Integrated Development Environment
IDL	Interactive Data Language

NEXRAD	Next-Generation Radar
ODIM	OPERA Data Information Model
OPERA	Operational Program on the Exchange of Weather Radar Information
OSS	Open Source Software
RADKLIM	Radarklimatologie ('Radar Climatology')
RADOLAN	Radar-Online-Aneichung ('Radar Online Adjustment')
WSR-88D	Weather Surveillance Radar – 1988 Doppler

INTRODUCTION

Rainfall and especially heavy and extreme rainfall events are a major trigger for floods and flash floods (Gaume *et al.* 2009; Bouilloud *et al.* 2010; Alfieri *et al.* 2011; Wright *et al.* 2017), soil erosion (Wischmeier & Smith 1978; Panagos *et al.* 2015, 2017; Steinhoff-Knopp & Burkhard 2018), mud flows (Hänsel *et al.* 2018) and landslides (Guzzetti *et al.* 2007; Segoni *et al.* 2014) causing costly damage or even casualties. As the frequency and intensity of heavy rainfall events are likely to increase (IPCC 2013; Quirmbach *et al.* 2013; Panagos *et al.* 2017; Thorndahl *et al.* 2017) and seasonal and spatial distribution of rainfall is shifting due to climate change (Zolina *et al.* 2008; Panagos *et al.* 2017), there are growing needs for adaption and risk prevention measures (Alfieri *et al.* 2012; Winterrath *et al.* 2017).

The high spatial and temporal variability of rainfall (Ramos *et al.* 2005; Fischer *et al.* 2016) dictates that high resolution precipitation data are needed (Thorndahl *et al.* 2017; Winterrath *et al.* 2017). Weather radar observations can help to satisfy this demand and particularly improve severe weather detection and quantification of precipitation during storm events (Krajewski & Smith 2002; Heistermann *et al.* 2013; Wright *et al.* 2013). Moreover, technical developments in hardware and software engineering as well as an increasing availability of data, some of which are available even free of charge, allows a wider audience to apply radar products.

Working with radar data, however, presents a string of challenges which make many potential users still reluctant to take advantage of these data. Weather radar is an indirect measurement method suffering from numerous potential error sources and uncertainties in terms of precipitation quantification (Krajewski & Smith 2002; Gjertsen *et al.* 2003; Raghavan 2003; Meischner 2004; Sene 2010; Seo *et al.* 2011). Consequently, the use of radar-based precipitation estimates necessitates additional effort for data quality assessment and probably further corrections. Yet, many national weather services recently put much effort into re-analyses of radar data time series applying state-of-the-art bias correction and adjustment algorithms. Keupp *et al.* (2017) give an overview of current reanalysis activities in Europe aimed at the establishment of radar climatologies. These projects, such as the radar climatology RADKLIM (Winterrath *et al.* 2018a, 2018b) provided by the German Weather Service (Deutscher Wetterdienst, (DWD)) will open up new climatological application fields for radar data (Keupp *et al.* 2017; Winterrath *et al.* 2017) which include the characterisation of the spatial variability of long-term rainfall patterns, seasonal variations in rainfall, durations of dry periods and the study of rainfall extremes and their impacts (Overeem *et al.* 2009; Smith *et al.* 2012; Wright *et al.* 2014). Most likely, the derivation of these radar climatology datasets will also lead to an overall enhancement of data quality and a reduced necessity for individual bias corrections.

Beyond the outlined uncertainties regarding data quality, several technical barriers exist that can prevent potential users from working with radar data. These include different file formats for exchange and storage, provision in proprietary binary file formats, a scarcity of easy-to-use and free-of-charge processing software, spatial visualisation and clipping tools, missing compatibility or interfaces to Geographic Information Systems (GIS) and the vast amount of data (Heistermann *et al.* 2013, 2015; Fischer *et al.* 2016). As a consequence, the processing of radar data not only requires considerable expertise in data handling and programming, but it also takes much time to develop user-customised workflows, which discourages many potential users.

Despite initiatives such as the OPERA (Operational Program on the Exchange of Weather Radar Information) weather radar information model (Michelson *et al.* 2014), which has been widely adopted for international data exchange within Europe (Heistermann *et al.* 2015), many national weather authorities still provide weather radar

composites in their own custom formats. This also holds true for the German weather radar data products RADKLIM and its counterpart for operational applications called RADOLAN ('Radar Online Adjustment'). Consequently, software adaption and interfacing to support the processing of different data formats is still necessary on a national scale, and available tools for automated, GIS-compatible radar data processing, e.g., for American (Zhang & Srinivasan 2010) or Norwegian (Abdella & Alfredsen 2010) data, cannot be applied for the German weather radar products.

This paper presents the open source library *radproc* (Kreklow 2018) written in Python (van Rossum 2001–2019) as a possible solution to the bottlenecks in current weather radar data processing and assessment in Germany and beyond. *Radproc* intends to lower the barrier to radar data usage by automating radar and rain gauge data processing and providing an interface for data exchange with GIS. First, an overview of the data basis and existing tools for the processing of German weather radar composites is provided in order to illustrate the motivation and need for developing *radproc*. Moreover, a short outlook on software for the processing of radar data in other countries is given. Next, the development goals, the implementation of the technical framework and its potential for transferability to other precipitation data are presented. Afterwards, *radproc*'s functional scope is demonstrated based on a typical workflow including raw data processing, temporal aggregation, heavy rainfall detection and data export to ArcGIS. Finally, limitations are discussed, a perspective of future developments and improvements is given and conclusions are drawn.

MOTIVATION FOR THE DEVELOPMENT OF *RADPROC*

Data basis

The DWD operates a network of 17 ground-based C-band Doppler radar stations and, in 2005, launched the operational application of the RADOLAN programme to provide near real-time nationwide quantitative precipitation estimations on a 1 km^2 raster in temporal resolutions of 5 and 60 minutes (Winterrath *et al.* 2017). The hourly radar

rainfall composites are adjusted to precipitation measurements from a network of approximately 1,300 rain gauges (Bartels *et al.* 2004; Keupp *et al.* 2017).

In 2017, the DWD concluded its 'radar climatology' project, in which all available weather radar data have been re-analysed back to the year 2001 applying state-of-the-art bias correction and adjustment algorithms (Winterrath *et al.* 2017). The resulting dataset called RADKLIM initially offers a largely homogeneous, spatially and temporally highly resolved radar-based precipitation time series of 17 years for Germany. The final datasets of RADKLIM are called RW (60 minute resolution) and YW (5 minute resolution). The DWD intends to update the dataset annually to further extend the time series. Due to a law change in July 2017 (Deutscher Bundestag 2017), radar data are subject to an open access policy, which is why both RADKLIM products are provided free of charge in the DWD Climate Data Centre (CDC). This makes it a very interesting and promising dataset for various applications, for instance in hydrology, meteorology and geography.

Review of available software tools for RADOLAN and RADKLIM radar data processing

In recent years, a variety of processing tools supporting German weather radar data have been developed that contain different functions and target different user groups. The following review is structured according to the software distribution model since the availability, costs and customisability of a tool are factors strongly influencing a user's choice of software.

Open source software

According to the open source definition, a software is regarded as open source software (OSS), if its source code is made available and its license grants the rights to use and modify the software to anyone and for any purpose, including non-exclusive commercial exploitation and redistribution of derivate works of the software itself (St Laurent 2008).

Heistermann *et al.* (2015) give a detailed overview of five international, active OSS for radar data processing and analysis. Their review shows that these tools can help a great deal in coping with the import and management of

different file formats and can promote further research on data quality improvements through continuous community-based development. But all of these tools are mainly developed for and used by specialists since they require a significant technical understanding of data formats and radar data processing techniques as well as programming skills for application and the development and automation of data processing workflows. Thus, they are not primarily targeted at users outside the weather radar community, such as engineering offices, authorities or researchers and users from other water-related fields of application. Most of these are rather interested in the application, analysis and visualisation of quantitative precipitation estimations provided by the national meteorological authorities.

The Python library *wradlib* (Heistermann *et al.* 2013) is the only one of the reviewed tools, which supports Windows operating systems and the binary format of RADOLAN and, since the version 1.2 is available, also RADKLIM products. Moreover, it has an active and growing user community and a website with extensive documentation. Besides many functions dedicated to the typical tasks of weather radar raw data processing outlined above, *wradlib* provides some visualisation tools and a function for reading in a single binary RADOLAN or RADKLIM file into a *NumPy* array. *NumPy* (Oliphant 2006) is a widely used package for scientific computing with Python and provides an array object for efficient numerical computations. Nevertheless, the processing workflows beyond single file import as well as the data structure for storage and further analysis have to be developed and programmed by the user. For users with little programming skill, this is a difficult, time-consuming and most likely discouraging task. Furthermore, many users working with spatial data use GIS. *Wradlib* provides functions to export radar data as GeoTIFFs or ESRI ASCII files as well as a series of functions for georeferencing and reprojection, but it does not have any direct interface to any GIS nor does it support clipping the nationwide composites. However, the latter is an important feature to reduce the amount of data and to limit analyses to a desired study area. In addition, GIS users might encounter serious difficulties installing *wradlib* due to separate and possibly incompatible installations of GDAL (Geospatial Data Abstraction Library; http://www.gdal.org), which is indispensable for georeferencing.

In Germany, several other OSS have been developed in the last years that are supposed to lower the barrier for working with RADOLAN and providing processing functions, most of them being rather small projects for data conversion, visualisation or for solving some very specific tasks.

- The *radolan* Go library (https://gitlab.cs.fau.de/since/radolan) supports the parsing and visualisation of several RADOLAN products but does not provide any analysis functions.
- The *Java Radolan parser* (http://www.bitplan.com/index.php/Radolan) is a Java port and extension of the *radolan* Go library for interactive and animated visualisation of different RADOLAN products. Aggregation functions and RADKLIM support are in preparation.
- *Rdwd* (https://github.com/brry/rdwd) is an actively maintained R package (R Core Team 2018) to select, download and read DWD climate data into R. It does not support RADOLAN and RADKLIM data yet, but an extension is in preparation.
- The *C++ RADOLAN library* (https://github.com/meteo-ubonn/radolan) offers several functions for the import of RADOLAN files and conversion to NetCDF and Shapefile format, but it does not seem to be an actively maintained project anymore.
- The *RADAR* and *ArViRadDB* toolkit (https://www.hs-rm.de) is a collection of freely available compiled routines supporting the hourly RADOLAN RW product and targeted at some very specific needs in hydrological engineering as well as the detection of heavy rainfall intervals. RADAR yields GIS-compatible ESRI ASCII files as outputs, but it does not provide a real GIS integration that would allow data clipping.
- *IDLRaBiD* (ftp://ftp-cdc.dwd.de/pub/CDC/grids_germany/hourly/radolan/idlrabid/) is a software for RADOLAN visualisation last updated in 2011. It is freely available in the DWD Climate Data Center, but it requires an IDL (Interactive Data Language) license or Virtual Machine to run.

Of all reviewed OSS projects supporting RADOLAN or RADKLIM, *wradlib* offers by far the widest range of functions and the highest quality and quantity of documentation. Moreover, none of the presented tools except

wradlib supports RADKLIM data up to now and most of them do not support the RADOLAN composite product RY in 5 minute resolution.

None of the OSS provides any Graphical User Interfaces (GUI). They are either run from Integrated Development Environments (IDE) or executed in command line windows. Consequently, besides *wradlib*, which is primarily targeted at advanced users from the weather radar community, there is a scarcity of OSS for RADOLAN data processing and a total absence of OSS for the automated processing and analysis of RADKLIM and the temporally highly resolved RADOLAN and RADKLIM products.

Commercial software

To the best of the author's knowledge, there are currently six commercial software products available that support the processing of German radar data, each of them with different target groups and functionalities.

- The ArcGIS extension *NVIS* (http://www.itwh.de) is intended for RADOLAN visualisation, precipitation now-casting, analysis of heavy rainfall events and calibration of sewer system models. *NVIS* offers functions for operational or short-term analysis of hourly RADOLAN RW data and seamless GIS integration, but is neither targeted at long-term climatological analysis nor does it support any radar composites with 5 minute temporal resolution.
- The *HydroNET-SCOUT* toolkit (http://hydronet-scout.de/) supports the import and visualisation of several different radar data formats, radar raw data correction, precipitation nowcasting and warnings as well as the export of temporally or spatially aggregated precipitation data.
- *AquaZIS* (http://www.aquaplan.de) is a software that supports the analysis and management of a variety of meteorological data. It is primarily targeted at time series and heavy rainfall analysis for water management tasks and provides the possibility to export results into Shapefiles.
- The *KISTERS Meteo* and *HydroMaster* toolkit (https://water.kisters.de) is a collection of software products for water management tasks providing a wide range of analysis, nowcasting and visualisation tools for

many meteorological datasets including all presented RADOLAN and RADKLIM products.
- *Delft-FEWS* (https://publicwiki.deltares.nl/display/FEWSDOC) is a software for management of time series data and forecasting processes. According to its documentation, it supports several raw and intermediate RADOLAN products, but none of the final composite products like RW and RY.
- *NinJo* (http://www.ninjo-workstation.com/editions.0.html) is a basic software for visualisation and processing of meteorological data for operational weather observation and forecasting.
- *MDMS_Expert* (https://de.dwa.de/de/messdatenmanagement-expert.html) is a software for import, selection and display of meteorological data provided by DWA (Deutsche Vereinigung für Wasserwirtschaft, Abwasser und Abfall e.V.), which also supports statistical heavy rainfall and correlation analyses.

All commercial products have many different functions accessible via GUI and the engineering offices selling them provide support for installation and application. Nevertheless, specialised commercial software products like these are hardly affordable for many users. Water management authorities undoubtedly prefer these products for operational purposes due to their easy-to-use, reliable and tailor-made functionality. However, for smaller companies with little financial resources, companies striving to develop new technologies and methods and especially in research, the use of OSS could make the radar data more accessible and facilitate the development of new methods. Moreover, as most of the commercial software products seem to be completely based on GUIs, it is not obvious to what extent they allow for customisation and individual analysis of the data.

All reviewed commercial tools support the processing of some or all RADOLAN products, but up to now, none of them explicitly indicate the support of RADKLIM data on their websites or in their release notes.

Many of the presented open source and commercial tools aim to support either data visualisation, retrospective analysis of single rainfall events, operational rainfall now-casting or raw radar station data processing including the application of correction, merging and gauge adjustment

algorithms, whereas the number of tools supporting long-term climatological analysis of temporally highly resolved radar data is still rather small. Furthermore, the review revealed that there is a considerable gap in regard to the number of provided functions and ease of usability between open source and commercial software products.

Outlook on software tools for other radar data formats

Without claiming to be exhaustive, this section gives an overview of software tools for processing other radar data and of recent developments that should lead to a standardisation of radar data formats. The great variety of different radar data formats that exists internationally impedes data exchange and has led to the development of many software tools, which are only applicable in specific regions or individual countries. However, there are increasing efforts to foster data exchange and cooperation through a standardisation of data formats and the creation of regional radar composites. In Europe, this is coordinated by the European Meteorological Services Network's (EUMETNET) Operational Program on the Exchange of Weather Radar Information (OPERA) which developed the OPERA Data Information Model (ODIM) in order to facilitate data exchange and create a Pan-European radar composite. The OPERA community also provides several software packages to exchange data between other radar data formats and ODIM, which is implemented in HDF5 as well as in BUFR (Binary Universal Form for the Representation of meteorological data) format (Michelson et al. 2014; Saltikoff et al. 2018, http://eumetnet.eu/activities/observations-programme/current-activities/opera/). Moreover, the OSS BALTRAD (Henja et al. 2010) for radar data exchange and processing, which was developed and is used by several countries in the Baltic Sea region, is based on the ODIM formats. *Wradlib* also provides support for the import of ODIM for HDF5. For Norwegian radar data provided in HDF5, a GIS toolset for automated processing and evaluation has been developed (Abdella & Alfredsen 2010).

For the processing, visualisation and analysis of the American WSR-88D (Weather Surveillance Radar – 1988 Doppler) data, also referred to as NEXRAD (Next-Generation Radar), there are different available software tools. *HEC-MetVUE*, which was developed by the Hydrologic

Engineering Center (McWilliams 2017; Benson et al. 2018), and the *Weather and Climate Toolkit* (https://www.ncdc.noaa.gov/wct/) developed by the National Oceanic and Atmospheric Administration (NOAA), are software tools provided by national agencies. Furthermore, with *LROSE, TITAN, Py-ART* and *RSL,* a series of open source tools is available. Along with *BALTRAD*, these tools have been discussed in detail by Heistermann et al. (2015). Moreover, a GIS-based software to automatically create a NEXRAD precipitation database has been developed by Xie et al. (2005), the GIS software *NEXRAD-VC* allows for validation and calibration of NEXRAD data (Zhang & Srinivasan 2010) and *Hydro-NEXRAD* is a prototype software to provide hydrologists with radar-rainfall maps (Seo et al. 2011).

In Southeast Asia, radar data exchange is encouraged in order to create a regional radar composite for disaster risk reduction. This is supposed to be achieved by using the same data format, GRIB2 (General Regularly-distributed Information in Binary form) (Kakihara 2018). This can be used by *SATAID* (https://www.wis-jma.go.jp/cms/sataid/app.html), which is a software for daily weather analysis and forecasting widely used by meteorological service providers in Southeast Asia. It has been developed by the Japan Meteorological Agency's Meteorological Satellite Center. In South Korea, the web-based module *WERM-S* has been developed for rainfall erosivity index calculations from radar data provided in ASCII format (Risal et al. 2018).

The South African Weather Service uses the commercial *HydroNet* software for its rainfall monitoring and decision support based on radar data (http://www.weathersa.co.za/product-and-services/2-uncategorised/443-hydronet) and the application of this software is also endorsed in Australia (https://www.hydronet.com.au/). Moreover, NEXRAD, OPERA HDF5, GRIB2 and some other weather radar data formats are also supported by ICMLive (https://www.innoaqua.de/de/software/article/icmlive-638.html) for real-time operational hydraulic modelling and early warning applications.

DEVELOPMENT GOALS, IMPLEMENTATION AND TRANSFERABILITY OF *RADPROC*

Radproc has been developed with the intention to reduce the existing gap outlined in the software review and to

lower the entrance barrier for the usage of RADOLAN and RADKLIM data for GIS users with little or no programming skills. It is an open source tool that provides an automated data processing workflow based on flexible data structures and designed with high extensibility regarding additional functions and interfaces to other input data formats and GIS. Moreover, the hardware requirements and programming skills to use the tool are kept as low as possible, but individual analyses, modifications and the implementation of new precipitation datasets by advanced users are possible and welcome. The development of such a tool requires a balanced trade-off between necessary hardware, calculation speed and required programming skills for application.

As the programming language, Python was chosen as it is an open source language with a high and still increasing popularity for various applications, especially for Data Science, resulting in a large quantity of robust additional packages and a large and active community. Python is implemented in many GIS (e.g., ArcGIS and QGIS) and is

an easy to learn programming language. Moreover, the DataFrame introduced by the *pandas* package (Mckinney 2010) is a very flexible data structure well suited for time series data. Besides some implemented visualisation methods and full compatibility with several plotting libraries such as *matplotlib*, *seaborn* and *bokeh*, *pandas* also offers a direct interface to store DataFrames in HDF5 files (The HDF Group 2018), which allows for a structured and compressible storage of large datasets.

In order to reduce the data amount by clipping to a study area and to allow for geospatial analyses and sophisticated visualisations, a high compatibility to ArcGIS was sought as this software programme is one of the most mature and most widely used GIS in academia, hydrological engineering and public institutions. Since ArcGIS is a commercial software, which contradicts the open source approach, all ArcGIS-based functions were encapsulated in a separate module (see Figure 1). This way, a partial use of *radproc* without clipping and GIS export functions, is
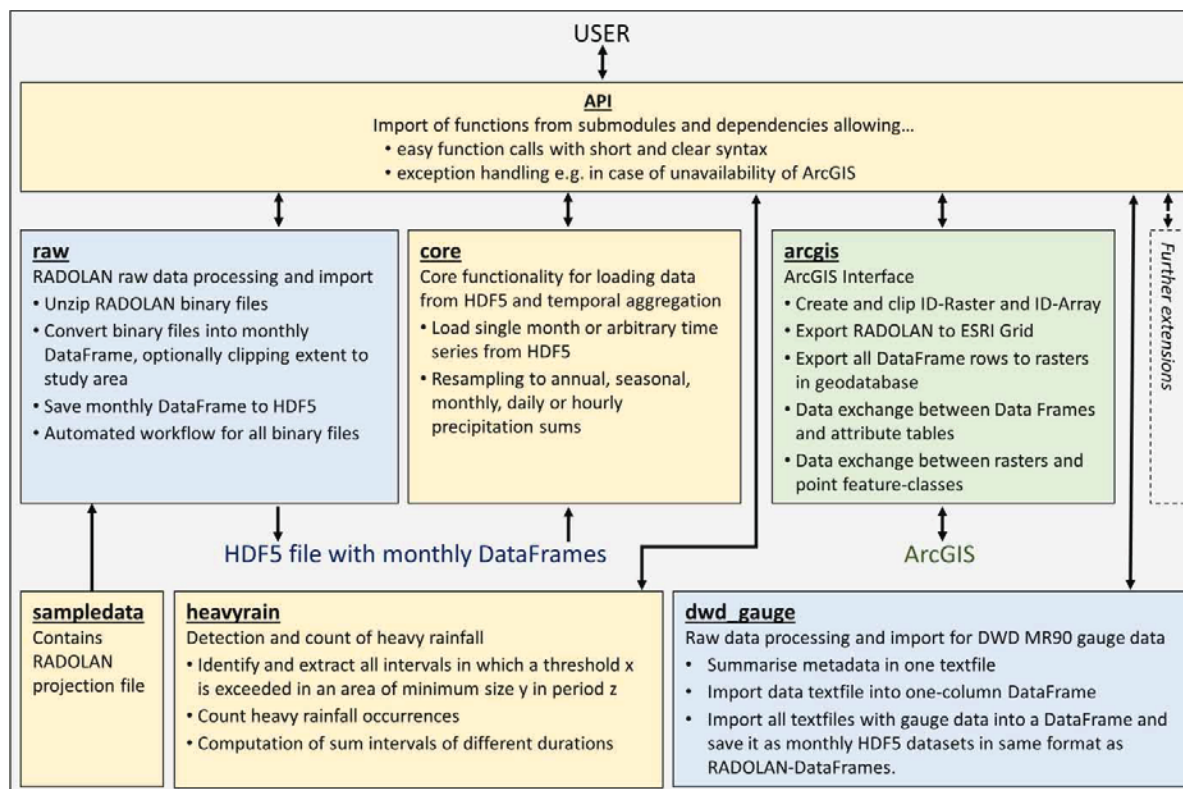

Figure 1 │ Module structure and interactions of *radproc*.

Table 1 │ *Radproc* development goals and decisions for implementation

Development goals	Implementation
➤ Open source	✓ Python as programming language
➤ Maximum compatibility with GIS to reduce data amount by clipping to study area and allow for custom visualisation and geoprocessing	
➤ Availability of tools for statistical analysis and visualisation to allow for custom analyses beyond *radproc*'s functions	✓ DataFrames from the *pandas* Python package as primary data structure
➤ Availability of a flexible, widely used and well-documented data format with support for statistical analyses and time series which is equally suitable for radar and rain gauge data	
➤ Structured, compressible data storage format enabling fast data access	✓ Data storage in HDF5 with one group per year and therein monthly *pandas* DataFrames as datasets
➤ Storage of processed data in a uniform data format on which all analysis and export functions are built in order to enable extensibility and interfacing to other precipitation data formats	
➤ Widely used, stable and well-documented GIS as a basis for all spatial analysis and visualisation tasks	✓ Choice of ArcGIS as the most mature and widely used GIS

still possible without ArcGIS and Python-based open source alternatives such as QGIS that can be implemented in the future.

Table 1 shows an overview of the defined development goals and the design decisions and the derived software choices.

In the current version 0.1.4, *radproc* consists of five modules for data processing and analysis as well as an API and a sample-data module (see Figure 1).

- The *raw* module comprises all functions for the automated processing and import of RADOLAN and RADKLIM raw data into HDF5. This includes extracting the binary data from compressed monthly or daily data archives, importing data into monthly DataFrames and saving these into *radproc*'s uniform HDF5 file structure.
- The *dwd_gauge* module offers automated processing and import of rain gauge data with 1 minute resolution provided by the DWD into the same HDF5 file structure as the radar data.
- The *core* module offers a variety of functions to load data from HDF5 and to resample them to annual, seasonal, monthly, daily or hourly precipitation sums. All functions of this module build solely upon the created HDF5 files and are thus independent from the original raw data formats.

- The *heavyrain* module contains functions for the calculation of duration sums as well as for the identification and counting of heavy rainfall events exceeding arbitrary thresholds. As it loads all data from HDF5 files via the *core* module, it is independent of the raw precipitation data formats.
- The *arcgis* module comprises all functions based on the ArcGIS *arcpy* package, e.g., functions for clipping data to a study area and for data exchange between DataFrames and raster datasets or attribute tables.
- The *API* module serves for more convenient function calls and takes care of exception handling, e.g., in case ArcGIS is not available.
- The *sampledata* module contains data for facilitating the use of *radproc* such as the projection file for the stereographic projection defined by DWD for RADO-LAN products.

Radproc's fundamental concept constitutes a conversion of all input data into a standardised HDF5 file containing a uniform structure with one group per year and therein monthly Dataframes as datasets. Thus, one HDF5 file contains the entire time series of a precipitation dataset for a defined study area split into monthly portions. The splitting is necessary in order to keep the required working memory to a manageable amount and to enable the processing of temporally highly resolved data for large study areas
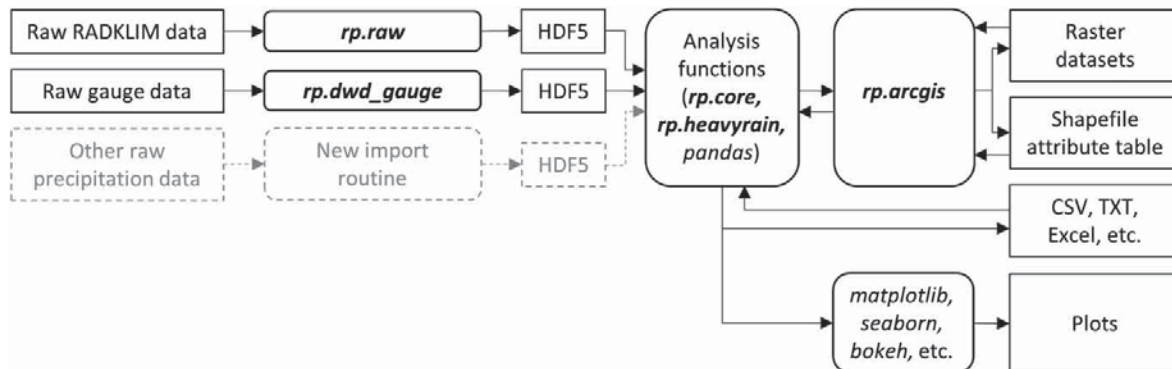
Figure 2 │ Extensible data processing workflow with multiple precipitation datasets. Radproc is abbreviated with rp and its modules are highlighted in bold.

on average workstation computers. Within these monthly DataFrames, each column corresponds to a spatial location, which can be either a grid cell or a point identifiable by means of a unique ID, whereas each row corresponds to a timestamp. This way, the selection of a DataFrame column yields a time series for a specific cell or point and the selection of a row yields the spatially distributed precipitation at a given time. After the creation of an HDF5 file for a precipitation dataset, the original input data are not required and accessed anymore. From this point onwards, all data, no matter whether gridded or point-scale data, are loaded from HDF5 and analysed with the same functions. Consequently, *radproc*'s entire analysis functionality is independent from the input data formats, which allows for a high extensibility in terms of new input data and analysis methods. As soon as new functions for the automated import of other precipitation datasets into the standardised HDF5 format have been developed, *radproc*'s whole functionality is available for this dataset. Such import functions can either be stand-alone scripts developed by individual users or functions added to a new or existing *radproc* module. In return, if a new analysis method is added, it can be applied on all datasets imported into HDF5. Moreover, since there is one separate HDF5 file for each precipitation dataset and study area, datasets are still independent of each other (see Figure 2). These are fundamental features since *radproc* is intended, among other applications, for data quality assessment, which necessarily involves the intercomparison of different datasets.

The only difference in data processing between gridded and point-scale data can be the export of results into GIS,

because data can either be exported to raster datasets or to new fields in attribute tables. As all environment settings during raster export (e.g., location, spatial reference) are derived from a so-called ID raster required as input parameter (see section on raw data processing below), this function is – as well as all analysis functions – neither limited to Germany nor to the RADOLAN, RADKLIM and gauge datasets currently implemented in *radproc*. Thus, *radproc*'s data processing workflow is transferable to any other precipitation time series dataset, provided that the required individual import routine converts the dataset into monthly *pandas* DataFrames, stores them into the described uniform HDF5 format and creates an ID raster for it in order to clip and export the data.

A TYPICAL DATA PROCESSING WORKFLOW USING *RADPROC*

In the following, a typical basic radar data processing and analysis workflow including raw data processing, temporal aggregation, heavy rainfall detection and data exchange with ArcGIS using *radproc* and the 17-year time series of the hourly RADKLIM RW product is illustrated and an overview of the most important functions is given. Whereas the RADKLIM and DWD gauge raw data processing is specific for Germany, the analyses and GIS exports shown in the other subsections are equally applicable for any other precipitation dataset imported into *radproc*'s standardised HDF5 file format, introduced above.

RADKLIM raw data processing and clipping

The raw RADOLAN and RADKLIM data are usually provided as gzip compressed monthly tar archives containing one uncompressed binary file per 5- (YW, RY) or 60-minute (RW) time interval. Every binary file starts with a metadata header and then contains 900×900 (RADOLAN) or $1{,}100 \times 900$ (RADKLIM) gridded precipitation values as integers in 1/10 mm for the whole of Germany, whereby every value describes the spatially averaged precipitation sum per time interval and 1 km grid cell.

As the RADKLIM data formats were adopted from RADOLAN, the data processing is very similar for both products and both will be referred to as RADOLAN throughout this section.

All raw data archives need to be unzipped for data import using the function *unzip_RW_binaries()* for hourly data or *unzip_YW_binaries()* for 5-minute data from *radproc*'s raw module. Both functions automatically generate a folder structure of yearly and monthly directories for the available time series, and gzip compress all unzipped binary files. The latter is a relatively slow process because of the large number of files but it is necessary to save hard drive space.

Subsequently, the new folder with all unpacked, compressed binary files can be passed to the overarching function *create_idraster_and_process_radolan_data()* which automates the entire process of data import, conversion to DataFrames and saving to HDF5. Internally, this function calls a series of helper and wrapper functions dividing the task into separate parts. The underlying binary file import into a two-dimensional *NumPy* array and a metadata dictionary is based on a slightly modified version of *wradlib's* *read_RADOLAN_composite()* function. Consecutively, all binary data are imported and the row order is reversed for each array. The latter is necessary in order to avoid the data grid to be upside down because the binary data block starts in the lower left grid corner whereas ESRI grids are created starting in the upper left corner. Next, the reversed arrays are reshaped to one-dimensional arrays and these are inserted into monthly DataFrames by another function. The RADOLAN pixels are numbered and converted to DataFrame columns whereas every DataFrame row is labelled with the corresponding timestamp from the

RADOLAN metadata. These monthly DataFrames are saved as datasets in the specified HDF5 file.

Optionally, if ArcGIS is available, a polygon GIS shapefile or feature class containing the outline of a study area can be passed to the processing function. In that case, *radproc*'s *arcgis* module is accessed to create a so-called ID raster for the national RADOLAN grid in stereographic projection which allows for spatial localisation of the numbered RADOLAN pixels. Each ID value of this raster corresponds to a DataFrame column since these are labelled with the ID numbers. The tool automatically detects the input radar data product and applies the corresponding grid size and location. The ID raster is then clipped to the extent of the given shapefile to obtain the IDs located within the study area. Finally, the clipped ID raster is converted into a one-dimensional *NumPy* array called ID array, and NoData values are removed (see Figure 3). The resulting ID array is used to select the RADOLAN pixels within the study area upon DataFrame creation.

The generated HDF5 file with monthly datasets, which is compressed by default to save hard drive space, can be directly and quickly accessed by *pandas* and is the basis for all other *radproc* functions. The entire workflow of raw data processing is illustrated in Figure 4.

Temporal aggregation

Besides the use of precipitation sums for climatological or hydrological analysis or as model inputs, the aggregation of longer time periods should always be one of the first steps in a workflow using weather radar data in order to assess data quality in a given study area. Many systematic measurement and correction errors which cause bias such as spokes, clutter pixels or areas of missing data, are visible, e.g., in a map showing the mean annual precipitation sum.

From any HDF5 file having the structure described above, single monthly DataFrames can be loaded with *radproc*'s *load_month()* function or longer periods can be loaded with *load_months_from_hdf5()* for further analysis, plotting or data exports.

Furthermore, the *core* module offers several functions for automated temporal aggregation to hours, days, months, years or hydrological seasons. These functions access the
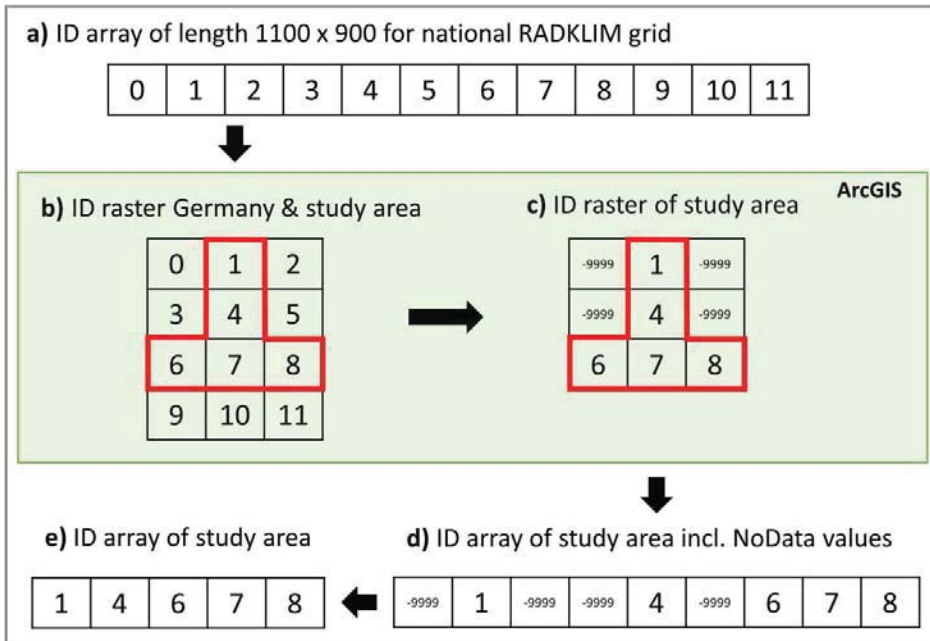
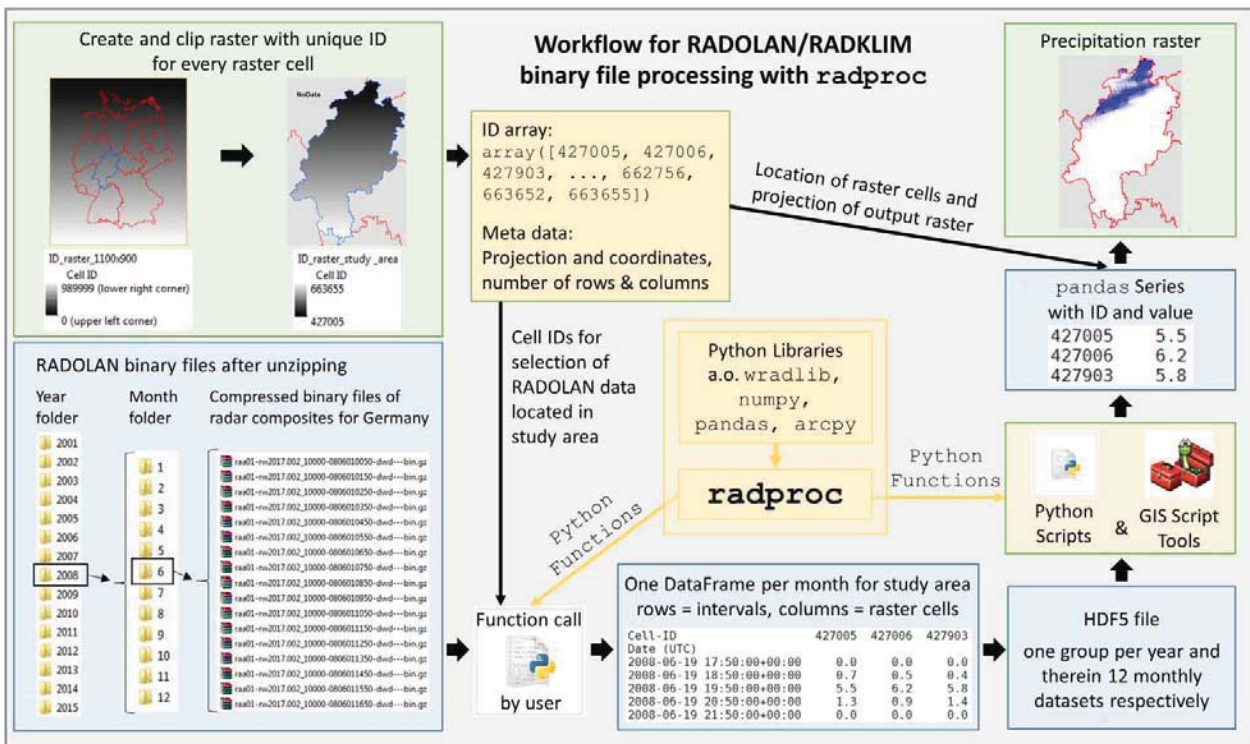**Figure 3** │ Methodology for data clipping using an ID raster.

Figure 4 │ Workflow for RADOLAN and RADKLIM data processing with radproc.

25

HDF5 file via the load functions and iteratively load and resample all data within the specified time period. For example, a call of the function *hdf5_to_years()* with the parameters *year_start* and *year_end* set to 2012 and 2017, respectively, returns a DataFrame with six rows, each of them containing the annual precipitation sum per pixel. A subsequent call of this DataFrames' *mean()* method yields – depending on the specified axis – either the spatially or temporally averaged annual precipitation.

Figure 5 shows the function call described above and an excerpt of the created output DataFrame located in the Harz Mountains, a low mountain range in the transition area between Northern and Central Germany, in a Jupyter Notebook (https://jupyter.org/).

Internally, *hdf5_to_years()* is only a wrapper function that calls *load_years_and_resample()*, which is actually used by all of *radproc*'s resampling functions. It iterates over all months within all years of the specified time period, whereby the DataFrame for each month is loaded and resampled individually in order to reduce the required memory. The DataFrames are either resampled to the respective target frequency or, if the latter is equal to or lower than 'month', they are resampled to a single-row DataFrame with the monthly precipitation sum. The first resampled month DataFrame of the first year is initialised as the future output DataFrame and afterwards, one after the other, all resampled month DataFrames are appended. After the loops, the output DataFrame is finally resampled to the target frequency.

Data exchange with ArcGIS

Radproc's *arcgis* module provides a set of functions for data exchange between ArcGIS and Python as well as some geospatial analysis functions, e.g., for extended zonal statistics and data extraction from raster cells to points.

For the export of radar data from DataFrames to single raster datasets, the function *export_to_raster()* can be used, whereas the function *export_dfrows_to_gdb()* handles the export of entire DataFrames into new File Geodatabases. The latter function exports every DataFrame row to one raster dataset, whereby it automatically derives the file names from the DataFrame index. Additionally, a list of statistical parameters can be passed to the function to calculate some statistical characteristics from the input DataFrame and export these, too. For example, a *statistics* list with the entries 'mean' and 'max' yields two additional exported raster datasets, each of them containing the mean and maximum value per cell, respectively. Figure 6 shows the function call and its results for exporting the DataFrame with the annual precipitation sums generated in the 'temporal aggregation' subsection.

Moreover, feature-class attribute tables can be directly imported into *pandas* DataFrames with *attribute_table_to_df()* and, in return, a list of DataFrame columns can be joined to an attribute table using *join_df_columns_to_attribute_table()*. Besides data exchange with other geodata, this provides a seamless integration of point feature-classes, which is the typical geodata format for rain gauge
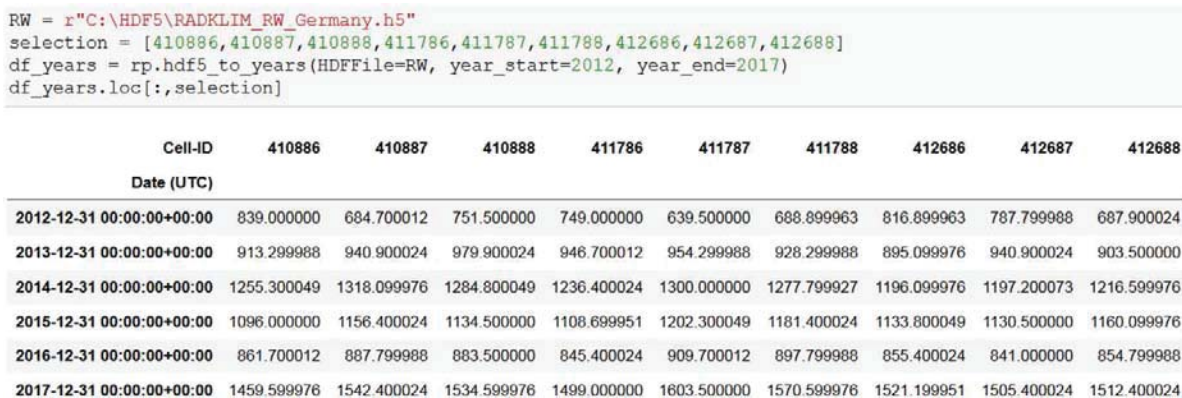
```
RW = r"C:\HDF5\RADKLIM_RW_Germany.h5"
selection = [410886,410887,410888,411786,411787,411788,412686,412687,412688]
df_years = rp.hdf5_to_years(HDFFile=RW, year_start=2012, year_end=2017)
df_years.loc[:,selection]
```

Cell-ID	410886	410887	410888	411786	411787	411788	412686	412687	412688
Date (UTC)									
2012-12-31 00:00:00+00:00	839.000000	684.700012	751.500000	749.000000	639.500000	688.899963	816.899963	787.799988	687.900024
2013-12-31 00:00:00+00:00	913.299988	940.900024	979.900024	946.700012	954.299988	928.299988	895.099976	940.900024	903.500000
2014-12-31 00:00:00+00:00	1255.300049	1318.099976	1284.800049	1236.400024	1300.000000	1277.799927	1196.099976	1197.200073	1216.599976
2015-12-31 00:00:00+00:00	1096.000000	1156.400024	1134.500000	1108.699951	1202.300049	1181.400024	1133.800049	1130.500000	1160.099976
2016-12-31 00:00:00+00:00	861.700012	887.799988	883.500000	845.400024	909.700012	897.799988	855.400024	841.000000	854.799988
2017-12-31 00:00:00+00:00	1459.599976	1542.400024	1534.599976	1499.000000	1603.500000	1570.599976	1521.199951	1505.400024	1512.400024

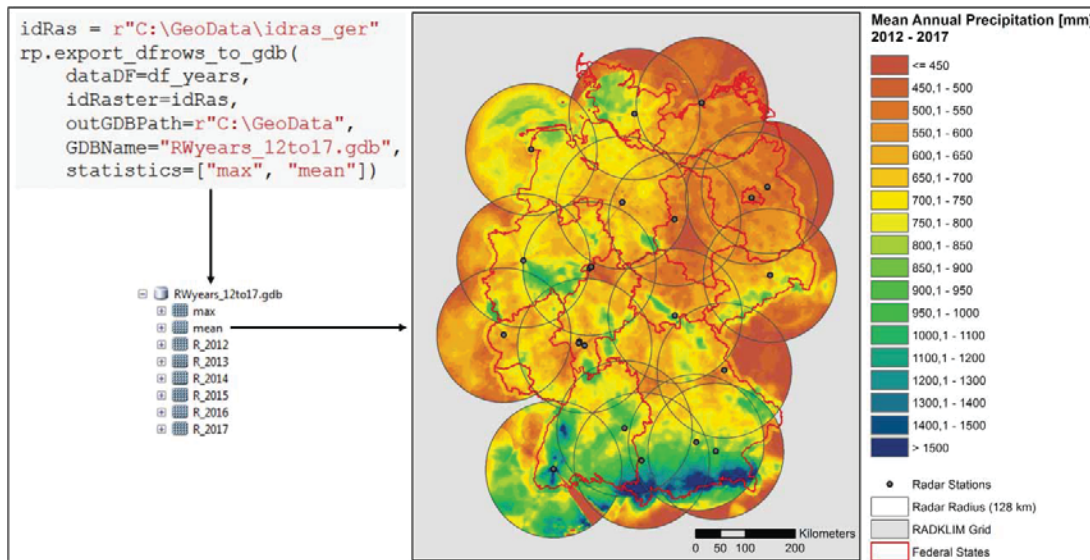**Figure 5** │ Aggregating RADKLIM RW data to annual precipitation sums.

Figure 6 │ Exporting the annual precipitation sums to raster datasets.

measurements, into the data analysis workflow. This is an important feature for comparison of gauge and radar datasets. To complete this data exchange circle, the function *rastervalues_to_points()* receives a list of raster datasets and a point feature-class and, by location, extracts all corresponding raster values to fields in the attribute table.

Detection and count of heavy rainfall

One of the primary reasons for developing RADKLIM was to provide a highly resolved nationwide dataset for the analysis of recent changes in rainfall-related extreme weather events (Winterrath *et al.* 2017). As a starting point for heavy rainfall analysis, *radproc* currently offers three functions providing an overview of the heavy rainfall behaviour and frequency in a given study area.

The function *find_heavy_rainfalls()* checks a time period for the exceedance of a given rainfall intensity threshold and returns a DataFrame with all intervals meeting the given criteria. This way, the exact time and location of heavy rainfall intervals can be identified and the selected intervals can subsequently be exported for visualisation.

Using the same iterative approach as the resampling functions, *find_heavy_rainfalls()* accesses a given HDF5 file via the load functions in the *core* module and checks the time series between the parameters *year_start* and

year_end for rainfall intervals exceeding specific thresholds. Here, the parameter *thresholdValue* defines the rainfall intensity threshold in mm per time unit (given by input data) to be checked for exceedance independently for each raster cell. Additionally, the parameter *minArea* specifies the number of raster cells in which the threshold must be exceeded for the interval to be selected, whereby these cells do not need to be adjacent. This parameter can be used to consider the surface area of rainfall cells, but also to take potentially known cells biased by clutter into account. Finally, the time period to be checked can be described in more detail by setting the *season* parameter to periods such as year, summer, winter or any single month or range of months.

As an example, Figure 7 shows a function call, which checks whether a precipitation amount of 100 mm/h (as the input dataset RW has an hourly resolution) has been exceeded in at least one cell anywhere in the nationwide $1,100 \times 900$ grid in any month of May in the period 2001 to 2017. If this holds true, the respective interval is contained in the output DataFrame. The last two lines of code select all columns (cells) containing any value greater than 100 in order to reduce the number of displayed columns. Moreover, this cell selection gives an idea, in how many cells such high rainfall amounts occurred.

As a result, this short analysis of the RADKLIM RW dataset reveals that, throughout the entire dataset, a

precipitation amount of 100 mm has occurred in nine hourly intervals between 2001 and 2017 in the month of May with a total number of 97 cells exceeding this threshold at least once.

Taking the same parameters into account, the function *count_heavy_rainfall_intervals()* also checks a time period for exceedances meeting the given criteria, but returns a single-row DataFrame with a count of exceedances per cell instead of the intervals themselves. This count gives a good overview of the heavy rainfall frequency and its spatial distribution in the study area.

Finally, the third function *duration_sum()* computes the rolling precipitation sum from data in 5 minute resolution for a defined duration D and saves the resulting DataFrames to a new HDF5 file. The calculation considers transitions between subsequent months and yields monthly DataFrames in 5 minute resolution, whose intervals contain the respective precipitation sum of the last D minutes, that is, the last $D/5$ intervals. Due to the standardised format, the resulting HDF5 file can be used as input for

find_heavy_rainfalls() to further detect and analyse extreme rainfall events which may have been separated and thus attenuated by the artificial interval boundaries in data with a lower temporal resolution such as RW. Nevertheless, when analysing the results, it has to be taken into account that subsequent intervals are not statistically independent because a single original 5 minute interval influences several intervals in the duration dataset. As duration sums are a commonly used method in hydrologic engineering, further analysis methods building upon them might be implemented to *radproc* in future.

DWD MR90 rain gauge data processing

In order to facilitate data comparison and, thus, data quality assessment, *radproc*'s *dwd_gauge* module provides functions for automated rain gauge data processing. Currently, only 1-minute gauge data in the DWD MR90 format are supported, but further functions to support other input

```
RW = r"C:\HDF5\RADKLIM_RW_Germany.h5"
hr = rp.find_heavy_rainfalls(HDFFile=RW, year_start=2001, year_end=2017,
                    thresholdValue=100, minArea=1, season="May")
cellsExceeding100mm = hr[hr>100].dropna(axis='columns', how='all').columns
hr.loc[:,cellsExceeding100mm]
```

Cell-ID Date (UTC)	285040	286844	467863	467864	470547	470548	471446	471447	471448	471449	...
2007-05-26 19:50:00+00:00	0.000000	0.000000	0.000000	0.000000	0.0	0.0	0.000000	0.000000	0.000000	0.0	...
2008-05-31 14:50:00+00:00	0.000000	0.000000	0.000000	0.000000	0.0	0.0	0.000000	0.000000	0.000000	0.0	...
2008-05-31 18:50:00+00:00	0.000000	0.000000	115.099998	104.400002	6.8	4.7	6.400000	6.200000	7.500000	6.1	...
2009-05-26 14:50:00+00:00	0.000000	0.000000	0.000000	0.000000	0.6	0.3	0.700000	0.600000	0.600000	0.5	...
2009-05-26 15:50:00+00:00	0.000000	0.000000	0.300000	0.400000	0.6	0.6	0.400000	0.500000	0.600000	0.7	...
2011-05-19 19:50:00+00:00	0.000000	0.000000	0.000000	0.000000	0.0	0.0	0.000000	0.000000	0.000000	0.0	...
2016-05-23 18:50:00+00:00	0.000000	0.000000	1.100000	0.600000	110.5	102.5	102.400002	110.400002	105.400002	104.0	...
2016-05-27 19:50:00+00:00	0.000000	0.000000	0.000000	0.000000	0.0	0.0	0.000000	0.000000	0.000000	0.0	...
2017-05-29 23:50:00+00:00	109.099998	106.800003	0.000000	0.000000	0.0	0.0	0.000000	0.000000	0.000000	0.0	...

9 rows × 97 columns

Figure 7 │ Detecting rainfall intervals exceeding 100 mm/h.

formats, especially the freely available data from DWD Climate Data Centre, are currently under development.

A MR90 rain gauge dataset comprises one data file and one metadata file. These two files per gauge station need to be saved in separate directories. To support the creation of a point feature-class from the metadata, the function *summarize_metadata_files()* summarises the information on station ID, station name, geographic coordinates and height above sea level from the metadata files into one single text file. A single data file can be imported into a one-column DataFrame with *stationfile_to_df()*.

Finally, the function *dwd_gauges_to_hdf5()* offers an automated iterative processing and import of all data files in a directory. The gauge data are converted into the same DataFrame format as the radar data. To make the data formats completely match, the time zone of the gauge data is converted to UTC and the data are resampled to the same 5-minute intervals as the 5-minute RADKLIM product YW. The final DataFrame contains one column per rain gauge. Finally, it is divided into monthly DataFrames, which are saved to the standardised HDF5 file format. As described above, *radproc*'s analysis and resampling functions work for all datasets converted this way. Consequently, the function calls for resampling and heavy rainfall detection shown in Figures 5 and 7 are exactly the same for the gauge data except for a different input HDF5 file path. However, instead of exporting the rows of the output DataFrame to rasters as shown in Figure 6, the rows can be exported to new fields of a feature class attribute table using *join_df_columns_to_attribute_table()*.

FUTURE DEVELOPMENTS, LIMITATIONS AND CONCLUSIONS

In this paper, the Python library *radproc* providing a GIS-compatible platform for automated radar data processing and analysis was introduced.

The software review revealed that there is a considerable gap concerning functionality and ease of usability between open source and commercial software products for weather radar data processing and analysis in Germany, and the outlook on software for other radar datasets indicated a similar situation in other parts of the world. Moreover,

only a small number of tools – none of which are OSS – support long-term climatological analysis of RADOLAN and RADKLIM data, yet.

The development of the RADKLIM dataset and other radar climatologies has opened up new application fields which, along with the vast amount of data, require new, innovative processing frameworks and analysis methods. These are probably most likely to develop in community-based open source research software projects, which could be demonstrated by the development of the *wradlib* library (Heistermann *et al.* 2013). Moreover, OSS helps users to build upon each other's work and to increase the reproducibility of research results.

The development of *radproc* is an attempt to reduce the gap identified in the review of existing tools by providing a highly extensible OSS that facilitates and largely automates data processing and converts data into flexible, widely used data formats. *Radproc* is the first OSS to provide support for long-term 5-minute RADOLAN and RADKLIM data processing and analysis. The developed modules and the innovative processing workflow with a focus on the unification of different data formats are a solid foundation to turn the project into a community-based platform for radar data processing, analysis and conversion in future. In order to enable a wide usage and support collaboration for further development, *radproc* is distributed under the permissive MIT license, complemented with an additional provision, which requires the source code of modified versions of the software to be made freely available in a public repository   (http://www.pgweb.uni-hannover.de/licensing.html). The software is being used by several working groups in the fields of geography, hydrology and natural hazards risk assessment throughout Germany, primarily for detection and reanalysis of past heavy rainfall events and for the provision of model inputs. Along with the feature requests and feedback the author received, this shows, that there is considerable demand for such a project. Due to the same programming language and the usage of *NumPy* arrays as common fundamental data structure, *radproc* is also compatible with *wradlib* and allows the application of, e.g., *wradlib*'s georeferencing and visualisation functions. Consequently, both libraries can be combined for individual radar data analysis workflows and complement each other.

Nevertheless, the chosen implementation of *radproc* still has some technical limitations. The most important one is that all data processing operations are performed in working memory. Unfortunately, in HDF5 files, the space reserved for column header information in flexible 'table' datasets is limited to approximately 2,000 columns, which is by far exceeded by the number of cells in most study areas. Consequently, the monthly DataFrames need to be stored as 'fixed' tabular datasets, which do not support flexible operations such as searching and selecting subsets of the data. Instead, the DataFrames need to be loaded into working memory entirely. For the hourly RW products, this is not a major issue, but for 5-minute radar data, the size of the study area that can be processed is scaled with the available memory. Furthermore, the *pandas* HDF5 API does not yet provide options for flexible metadata storage, which spills over to *radproc*.

Like all other reviewed OSS, *radproc* does not provide any GUI, yet. Hence, its application still requires a certain readiness by the user to learn some very basic Python syntax. But with the increasing number of online courses and *radproc*'s extensive documentation including an installation guide, a full library reference and tutorials directly generated from Jupyter Notebooks, this is feasible without much effort even for users without any prior programming skills.

However, due to the tight integration of ArcGIS, it could be an option to develop a *radproc* GIS toolbox to facilitate application. So far, this has been tested, but the connection between the separate Python installations of ArcGIS and a scientific distribution like Anaconda (https://www.anaconda.com), which is necessary to access all of *radproc*'s dependencies and the ArcGIS *arcpy* module, is rather difficult to establish. Enabling an Anaconda IDE such as Spyder or the Jupyter Notebook to import *arcpy* is easy and quickly done, but enabling the import of any additional site-packages into ArcGIS, which is necessary to execute GIS tools accessing *radproc*, is much more complicated and sparsely documented. This might become easier through the planned porting to Python 3 and the implementation of ArcGIS Pro and will be pursued within this context.

Another option for future developments and a repeated request is the addition of a module to support QGIS as an alternative to ArcGIS in order to turn the entire workflow into an open source project. Due to *radproc*'s extensible modular structure, such a QGIS module or any other modules to support further radar or gauge data formats could be added, but neither of these is specifically planned, yet, except for the additional DWD gauge data import routines described in the previous section. Currently, an additional module for the calculation of rainfall erosivity, the R factor of the Universal Soil Loss Equation (Wischmeier & Smith 1978), is being developed and will be added in future.

Radproc constitutes a powerful open source tool for automated weather radar data processing and analysis and has considerable potential for further development and improvement. It contributes to facilitating radar data processing, allowing non-specialised users to cope with the vast amount of binary data and put the novel RADKLIM dataset to use. Thus, *radproc* can help to enable radar data usage for all applications that benefit from high resolution precipitation data, e.g., in research, hydrological engineering, disaster control, erosion and flood protection and environmental planning.

REFERENCES

Abdella, Y. & Alfredsen, K. 2010 A GIS toolset for automated processing and analysis of radar precipitation data.

Computers & Geosciences **36** (4), 422–429. https://doi.org/10.1016/j.cageo.2009.08.008.

Alfieri, L., Velasco, D. & Thielen, J. 2011 Flash flood detection through a multi-stage probabilistic warning system for heavy precipitation events. *Advances in Geosciences* **29**, 69–75. https://doi.org/10.5194/adgeo-29-69-2011.

Alfieri, L., Salamon, P., Pappenberger, F., Wetterhall, F. & Thielen, J. 2012 Operational early warning systems for water-related hazards in Europe. *Environmental Science & Policy* **21**, 35–49. https://doi.org/10.1016/j.envsci.2012.01.008.

Bartels, H., Weigl, E., Reich, T., Lang, W., Wagner, A., Kohler, O. & Gerlach, N. MeteoSolutions GmbH 2004 *Projekt RADOLAN – Routineverfahren zur Online-Aneichung der Radarniederschlagsdaten mit Hilfe von Automatischen Bodenniederschlagsstationen (Ombrometer) (Project RADOLAN – Operational Procedures for an Online-Adjustment of Radar Precipitation Data Using Automated Rain Gauges)*. Zusammenfassender Abschlussbericht für die Projektlaufzeit von 1997 bis 2004, Deutscher Wetterdienst, Offenbach am Main, Germany.

Benson, S., Hunter, J. & McWilliams, C. D. 2018 HEC-Metvue – Tool for Real-Time Forecasting; Analyzing and Manipulating Gridded Datasets; Development of Design Storms for Probable Maximum Precipitation Estimation. In *American Meteorological Society 98th Annual Meeting*, 8 January 2018, Austin, TX, USA. https://ams.confex.com/ams/98Annual/webprogram/Paper336164.html (accessed 19 February 2019).

Bouilloud, L., Delrieu, G., Boudevillain, B. & Kirstetter, P.-E. 2010 Radar rainfall estimation in the context of post-event analysis of flash-flood events. *Journal of Hydrology* **394** (1–2), 17–27. https://doi.org/10.1016/j.jhydrol.2010.02.035.

Deutscher Bundestag 2017 *Erstes Gesetz zur Änderung des Gesetzes über den Deutschen Wetterdienst*: DWD-Gesetz (DWD Law), 2017 **Teil I**.

Fischer, F., Hauck, J., Brandhuber, R., Weigl, E., Maier, H. & Auerswald, K. 2016 Spatio-temporal variability of erosivity estimated from highly resolved and adjusted radar rain data (RADOLAN). *Agricultural and Forest Meteorology* **223**, 72–80. https://doi.org/10.1016/j.agrformet.2016.03.024.

Gaume, E., Bain, V., Bernardara, P., Newinger, O., Barbuc, M., Bateman, A., Blaškovičová, L., Blöschl, G., Borga, M., Dumitrescu, A., Daliakopoulos, I., Garcia, J., Irimescu, A., Kohnova, S., Koutroulis, A., Marchi, L., Matreata, S., Medina, V., Preciso, E., Sempere-Torres, D., Stancalie, G., Szolgay, J., Tsanis, I., Velasco, D. & Viglione, A. 2009 A compilation of data on European flash floods. *Journal of Hydrology* **367** (1–2), 70–78. https://doi.org/10.1016/j.jhydrol.2008.12.028.

Gjertsen, U., Salek, M. & Michelson, D. B. 2003 Gauge-adjustment of radar-based precipitation estimates – a review. *Cartographic Perspectives* **45**, 1. https://doi.org/10.14714/CP45.494.

Guzzetti, F., Peruccacci, S., Rossi, M. & Stark, C. P. 2007 Rainfall thresholds for the initiation of landslides in central and southern Europe. *Meteorology and Atmospheric Physics* **98** (3–4), 239–267. https://doi.org/10.1007/s00703-007-0262-7.

Hänsel, P., Kaiser, A., Buchholz, A., Böttcher, F., Langel, S., Schmidt, J. & Schindewolf, M. 2018 Mud flow reconstruction by means of physical erosion modeling, high-resolution radar-based precipitation data, and UAV monitoring. *Geosciences* **8** (11), 427. https://doi.org/10.3390/geosciences8110427.

Heistermann, M., Jacobi, S. & Pfaff, T. 2013 Technical Note: an open source library for processing weather radar data (*wradlib*). *Hydrology and Earth System Sciences: HESS* **17** (2), 863–871. https://doi.org/10.5194/hess-17-863-2013.

Heistermann, M., Collis, S., Dixon, M. J., Giangrande, S., Helmus, J. J., Kelley, B., Koistinen, J., Michelson, D. B., Peura, M., Pfaff, T. & Wolff, D. B. 2015 The emergence of open-source software for the weather radar community. *Bulletin of the American Meteorological Society* **96** (1), 117–128. https://doi.org/10.1175/BAMS-D-13-00240.1.

Henja, A., Szewczykowski, M., Ernes, S. & Michelson, D. B. 2010 The BALTRAD technical platform. In: *ERAD 2010 - The Sixth European Conference on Radar in Meteorology and Hydrology*. http://erad2010.com/pdf/oral/wednesday/dataex/02_ERAD2010_0232.pdf (accessed 19 February 2019).

IPCC 2013 *Climate Change 2013: The Physical Science Basis*. Contribution of Working Group I to the Fifth Assessment Report of the Intergovernmental Panel on Climate Change, Cambridge University Press, Cambridge, UK and New York, NY. http://www.climatechange2013.org/images/report/WG1AR5_ALL_FINAL.pdf (accessed 16 April 2018).

Kakihara, K. 2018 Radar Network in Southeast Asia. In *Japan Meteorological Agency, WMO/ASEAN Training Workshop on Weather Radar Data Quality and Standardization*, 5 February 2018, Bangkok, Thailand. https://www.jma.go.jp/jma/en/photogallery/WMO-ASEAN_Radar_Workshop_Feb2018/1-2_Keynote_WIGOS-Project (accessed 19 February 2019).

Keupp, L., Winterrath, T. & Hollmann, R. 2017 *Use of Weather Radar Data for Climate Data Records in WMO Regions IV and VI*. https://www.wmo.int/pages/prog/wcp/ccl/opace/opace2/documents/TT-URSDCM_Use_Remote_Sensing_DataClimateMonitoringRAIV-VI.pdf

Krajewski, W. F. & Smith, J. A. 2002 Radar hydrology: rainfall estimation. *Advances in Water Resources* **25**, 1387–1394.

Kreklow, J. 2018 *Radproc – A Gis-Compatible Python-Package For Automated Radolan Composite Processing And Analysis*. https://doi.org/10.5281/zenodo.1316376. Zenodo.

Mckinney, W. 2010 Data Structures for Statistical Computing in Python. In: *Proceedings of the 9th Python in Science Conference*, Austin, TX, USA, pp. 51–56. https://conference.scipy.org/proceedings/scipy2010/pdfs/mckinney.pdf (accessed 15 November 2018).

McWilliams, C. D. 2017 *HEC-MetVue Implementation*, 19 January 2017. https://acwi.gov/hydrology/minutes/MetVue_Presentation-19Jan2017.pdf (accessed 19 February 2019).

Meischner, P. 2004 *Weather Radar: Principles and Advanced Applications*, 1st edn. Springer, Berlin, Heidelberg, Germany.

Michelson, D. B., Lewandowski, R., Szewczykowski, M. & Beekhuis, H. 2014 *EUMETNET OPERA Weather Radar Information Model for Implementation with the HDF5 File Format: Version 2.2*. EUMETNET, Brussels. http://eumetnet. eu/wp-content/uploads/2017/01/OPERA_hdf_description_ 2014.pdf (accessed 16 November 2018).

Oliphant, T. E. 2006 *A Guide to NumPy*. Trelgol Publishing, USA.

Overeem, A., Holleman, I. & Buishand, A. 2009 Derivation of a 10-year radar-based climatology of rainfall. *Journal of Applied Meteorology and Climatology* **48** (7), 1448–1463. https://doi.org/10.1175/2009JAMC1954.1.

Panagos, P., Ballabio, C., Borrelli, P., Meusburger, K., Klik, A., Rousseva, S., Tadic, M. P., Michaelides, S., Hrabalikova, M., Olsen, P., Aalto, J., Lakatos, M., Rymszewicz, A., Dumitrescu, A., Begueria, S. & Alewell, C. 2015 Rainfall erosivity in Europe. *Science of the Total Environment* **511**, 801–814. https://doi.org/10.1016/j.scitotenv.2015.01.008.

Panagos, P., Ballabio, C., Meusburger, K., Spinoni, J., Alewell, C. & Borrelli, P. 2017 Towards estimates of future rainfall erosivity in Europe based on REDES and WorldClim datasets. *Journal of Hydrology* **548**, 251–262. https://doi.org/ 10.1016/j.jhydrol.2017.03.006.

Quirmbach, M., Einfalt, T., Langstädtler, G., Janßen, C., Reinhardt, C. & Mehlig, B. 2013 Extremwertstatistische Untersuchung von Starkniederschlägen in NRW (ExUS) (A study of extreme value statistics of heavy rainfalls in NRW). *Korrespondenz Abwasser und Abfall* **60** (7), 591–599.

Raghavan, S. 2003 *Radar Meteorology*, 1st edn. Springer Science + Business, Dordrecht, Germany.

Ramos, M. H., Creutin, J.-D. & Leblois, E. 2005 Visualization of storm severity. *Journal of Hydrology* **315** (1–4), 295–307. https://doi.org/10.1016/j.jhydrol.2005.04.007.

R Core Team 2018 *R: A Language and Environment for Statistical Computing*. R Foundation for Statistical Computing, Vienna, Austria. https://www.R-project.org (accessed 20 November 2018).

Risal, A., Lim, K. J., Bhattarai, R., Yang, J. E., Noh, H., Pathak, R. & Kim, J. 2018 Development of web-based WERM-S module for estimating spatially distributed rainfall erosivity index (EI30) using RADAR rainfall data. *Catena* **161**, 37–49. https://doi.org/10.1016/j.catena.2017.10.015.

Saltikoff, E., Haase, G., Leijnse, H., Novák, P. & Delobbe, L. 2018 OPERA – past, present and future. In: *ERAD 2018 – 10th European Conference on Radar in Meteorology and Hydrology*, 2 July 2018, Utrecht, The Netherlands. http:// projects.knmi.nl/erad2018/ERAD2018_extended_ abstract_025.pdf (accessed 18 February 2019).

Segoni, S., Rossi, G., Rosi, A. & Catani, F. 2014 Landslides triggered by rainfall: a semi-automated procedure to define consistent intensity–duration thresholds. *Computers & Geosciences* **63**, 123–131. https://doi.org/10.1016/j.cageo.2013.10.009.

Sene, K. 2010 *Hydrometeorology*. Springer, Dordrecht, The Netherlands.

Seo, B.-C., Krajewski, W. F., Kruger, A., Domaszczynski, P., Smith, J. A. & Steiner, M. 2011 Radar-rainfall estimation algorithms of Hydro-NEXRAD. *Journal of Hydroinformatics* **13** (2), 277–291. https://doi.org/10.2166/hydro.2010.003.

Smith, J. A., Baeck, M. L., Villarini, G., Welty, C., Miller, A. J. & Krajewski, W. F. 2012 Analyses of a long-term, high-resolution radar rainfall data set for the Baltimore metropolitan region. *Water Resources Research* **48** (4), 616. https://doi.org/10. 1029/2011WR010641.

Steinhoff-Knopp, B. & Burkhard, B. 2018 Soil erosion by water in Northern Germany: long-term monitoring results from Lower Saxony. *Catena* **165**, 299–309. https://doi.org/10. 1016/j.catena.2018.02.017.

St Laurent, A. M. 2008 *Understanding Open Source and Free Software Licensing*. O'Reilly Media, Sebastopol, CA, USA.

The HDF Group 2018 *Hierarchical Data Format*. https://portal. hdfgroup.org (accessed 18 December 2018).

Thorndahl, S., Einfalt, T., Willems, P., Nielsen, J. E., Veldhuis, M.-C. t., Arnbjerg-Nielsen, K., Rasmussen, M. R. & Molnar, P. 2017 Weather radar rainfall data in urban hydrology. *Hydrology and Earth System Sciences: HESS* **21** (3), 1359–1380. https://doi.org/10.5194/hess-21-1359-2017.

van Rossum, G. 2001–2019 *Python*. Python Software Foundation, Beaverton, USA. https://www.python.org/ (accessed 27 February 2019).

Winterrath, T., Brendel, C., Hafer, M., Junghänel, T., Klameth, A., Walawender, E., Weigl, E. & Becker, A. 2017 *Erstellung Einer Radargestützten Niederschlagsklimatologie (Creation of A Radar-Based Precipitation Climatology)*. Berichte des Deutschen Wetterdienstes 251, Deutscher Wetterdienst, Offenbach am Main, Germany. https://www.dwd.de/DE/ leistungen/pbfb_verlag_berichte/pdf_einzelbaende/251_pdf. pdf?__blob=publicationFile&v=2 (accessed 10 October 2018).

Winterrath, T., Brendel, C., Hafer, M., Junghänel, T., Klameth, A., Lengfeld, K., Walawender, E., Weigl, E. & Becker, A. 2018a *Radar Climatology (RADKLIM) Version 2017.002 (RW); Gridded Precipitation Data for Germany*. https://doi.org/ 10.5676/DWD/RADKLIM_RW_V2017.002.

Winterrath, T., Brendel, C., Hafer, M., Junghänel, T., Klameth, A., Lengfeld, K., Walawender, E., Weigl, E. & Becker, A. 2018b *Radar Climatology (RADKLIM) Version 2017.002 (YW); Gridded Precipitation Data for Germany*. https://doi.org/10. 5676/DWD/RADKLIM_YW_V2017.002.

Wischmeier, W. H. & Smith, D. D. 1978 Predicting Rainfall Erosion Losses. A guide to conservation planning. U.S. Department of Agriculture, Agriculture Handbook No. 537, Washington, USA.

Wright, D. B., Smith, J. A., Villarini, G. & Baeck, M. L. 2013 Estimating the frequency of extreme rainfall using weather radar and stochastic storm transposition. *Journal of Hydrology* **488**, 150–165. https://doi.org/10.1016/j.jhydrol.2013.03.003.

Wright, D. B., Smith, J. A., Villarini, G. & Baeck, M. L. 2014 Long-term high-resolution radar rainfall fields for urban hydrology. *Journal of the American Water Resources Association* **50** (3), 713–734. https://doi.org/10.1111/jawr.12139.

Wright, D. B., Mantilla, R. & Peters-Lidard, C. D. 2017 A remote sensing-based tool for assessing rainfall-driven hazards. *Environmental Modelling & Software* **90**, 34–54. https://doi.org/10.1016/j.envsoft.2016.12.006.

Xie, H., Zhou, X., Vivoni, E. R., Hendrickx, J. M. H. & Small, E. E. 2005 GIS-based NEXRAD Stage III precipitation database: automated approaches for data processing and visualization. *Computers & Geosciences* **31** (1), 65–76. https://doi.org/10.1016/j.cageo.2004.09.009.

Zhang, X. & Srinivasan, R. 2010 GIS-based spatial precipitation estimation using next generation radar and raingauge data. *Environmental Modelling & Software* **25** (12), 1781–1788. https://doi.org/10.1016/j.envsoft.2010.05.012.

Zolina, O., Simmer, C., Kapala, A., Bachner, S., Gulev, S. & Maechel, H. 2008 Seasonally dependent changes of precipitation extremes over Germany since 1950 from a very dense observational network. *Journal of Geophysical Research* **113** (D6), D05109. https://doi.org/10.1029/2007JD008393.

3

A Rainfall Data Intercomparison Dataset of RADKLIM, RADOLAN, and Rain Gauge Data for Germany

J. Kreklow, B. Tetzlaff, G. Kuhnt, B. Burkhard

Data (2019), 4(3)

data

MDPI

Data Descriptor

A Rainfall Data Intercomparison Dataset of RADKLIM, RADOLAN, and Rain Gauge Data for Germany

Jennifer Kreklow [1],* , **Björn Tetzlaff [2], Gerald Kuhnt [1] and Benjamin Burkhard [1,3]**

[1] Institute of Physical Geography and Landscape Ecology, Leibniz Universität Hannover, Schneiderberg 50, 30167 Hannover, Germany

[2] Institute of Bio- and Geosciences IBG-3, Forschungszentrum Jülich GmbH, 52425 Jülich, Germany

[3] Leibniz Centre for Agricultural Landscape Research ZALF, Eberswalder Straße 84, 15374 Müncheberg, Germany

* Correspondence: kreklow@phygeo.uni-hannover.de; Tel.: +49-0511-762-19798

check for updates

Abstract: Quantitative precipitation estimates (QPE) derived from weather radars provide spatially and temporally highly resolved rainfall data. However, they are also subject to systematic and random bias and various potential uncertainties and therefore require thorough quality checks before usage. The dataset described in this paper is a collection of precipitation statistics calculated from the hourly nationwide German RADKLIM and RADOLAN QPEs provided by the German Weather Service (Deutscher Wetterdienst (DWD)), which were combined with rainfall statistics derived from rain gauge data for intercomparison. Moreover, additional information on parameters that can potentially influence radar data quality, such as the height above sea level, information on wind energy plants and the distance to the next radar station, were included in the dataset. The resulting two point shapefiles are readable with all common GIS and constitutes a spatially highly resolved rainfall statistics geodataset for the period 2006 to 2017, which can be used for statistical rainfall analyses or for the derivation of model inputs. Furthermore, the publication of this data collection has the potential to benefit other users who intend to use precipitation data for any purpose in Germany and to identify the rainfall dataset that is best suited for their application by a straightforward comparison of three rainfall datasets without any tedious data processing and georeferencing.

Dataset: Available at Zenodo data repository, DOI:10.5281/zenodo.3262172. (https://zenodo.org/record/3262172)

Dataset License: CC-BY-SA 4.0

Keywords: weather radar; rain gauge; precipitation; QPE; RADOLAN; RADKLIM; GIS

---

1. Summary

Rainfall is a major driver for many environmental processes. The operational monitoring and management of water resources as well as the modeling of many water-related processes require spatially and temporally highly resolved rainfall data [1].

Weather radar systems can provide such highly resolved data, but due to the indirect measurement technique, radar data are also subject to systematic and random bias and various potential uncertainties. In the last two decades, much progress has been achieved in the derivation of quantitative precipitation estimates (QPE) from weather radar reflectivity data through the development of new algorithms. These led to improvements in reflectivity data correction (removal of clutter, e.g., due to wind energy

plants, ground echoes, attenuation correction, detection of spokes and erroneous bright band echoes, etc.), conversion from reflectivity to precipitation heights, adjustment to rain gauge data and the creation of gridded composites from the local radar station data (e.g., [2–7]).

In Germany, the operational RADOLAN ("Radar Online Adjustment") program was launched by the German Weather Service (Deutscher Wetterdienst (DWD)) in June 2005 [8,9]. It provides hourly radar-based QPEs adjusted to rain gauge data on a nationwide 1 km grid (called RW product) as well as unadjusted QPEs with temporal resolutions up to 5 min. Though these RADOLAN composite data are a considerable improvement for spatially and temporally highly resolved rainfall monitoring, the QPEs still contain systematic errors and significant clutter. Moreover, data processing and correction algorithms as well as the radar hardware have been continuously developed since the launch of the program, which is why the RADOLAN dataset constitutes an inhomogeneous time series [10]. The data are mainly used for rainfall monitoring and operational water management and warning procedures, whereas they are still rather sparsely used in scientific research.

In 2018, the DWD published a reanalysis of all their radar data back to the year 2001 using consistent processing techniques, several new correction algorithms, and more rain gauges for adjustment. This radar climatology dataset called RADKLIM has been developed with the intent to enable radar-based climatological research and especially heavy rainfall analyses [10]. Besides hourly gauge-adjusted QPEs (are also called RW) [11], the radar climatology also comprises quasi-adjusted QPEs in a 5-minute resolution called YW [12].

The dataset described in this paper is a collection of precipitation statistics we calculated from the hourly nationwide RADKLIM and RADOLAN RW products which were combined with rainfall statistics we derived from DWD rain gauge data for intercomparison. The precipitation statistics include annual precipitation sums for the years 2006 to 2017, mean annual sums, mean seasonal sums per hydrologic half-year, the number and mean rainfall height of days exceeding a daily precipitation amount of 1 mm and 20 mm sub-divided by half-years, the number of NoData values, and several additional information on parameters that can potentially influence radar data quality. These include the height above sea level, the number, average height and diameter of wind energy plants per pixel and the distance to the next radar.

The rainfall data intercomparison dataset is shared via two vector format point shapefiles collected in a zip archive hosted at Zenodo data repository. The dataset was collected and is currently being analyzed as part of a study aimed at the evaluation of the German radar climatology. The publication of this data collection has the potential to benefit others who intend to use precipitation data for any purpose in Germany and who need to know which rainfall dataset is best suited for their analysis period and study area. The quality and completeness of precipitation datasets differs in time and space due to missing or erroneous data, changes or gaps in the network of measuring devices as well as seasonal and environmental influences such as topography, temperature or origin and type of precipitation. With a range of different datasets available (which also include satellite-based and spatially interpolated precipitation data not considered in this data collection), researchers often need to identify the best suited rainfall dataset for their application, which may be a time-consuming task that already involves a significant amount of data processing. The dataset presented in this paper can help researchers make a decision by providing a straightforward comparison of three rainfall datasets without any tedious raw data processing and georeferencing. Though, when evaluating the datasets against each other, it has to be considered that they are not independent. Most or probably all of the DWD gauge data have been used for radar data adjustment, while RADOLAN and RADKLIM share the same reflectivity measurements and some of their processing and correction algorithms. However, the rainfall data intercomparison dataset can be used to evaluate the quality of the radar data products by analyzing their spatial and temporal distribution in any individual study area within Germany and by comparison with the additional collected information. This way, it is possible to describe and assess the spatially and temporally varying radar data quality regarding the reflectivity and the applied conversions, corrections and gauge adjustment. Thus, the dataset presented in this paper can help to

build confidence for using radar data or also support the decision not to use them due to data quality issues in the respective study area. Furthermore, it also constitutes a spatially highly resolved rainfall statistics geodataset for the period 2006 to 2017, which can be used for statistical rainfall analyses or to derive model inputs.

The generated dataset is described in Section 2, and in Section 3, information on the original input data sources, a detailed description of the data processing, the calculated precipitation statistics and additional parameters, as well as an evaluation on the quality and completeness of the dataset are provided. Finally, in Section 4, further notes on the usage of the dataset and a brief application example are provided.

2. Data Description

The generated rainfall data intercomparison dataset described in this paper consists of two vector format point shapefiles, which can be read by all common Geographic Information Systems (GIS). The spatial extent of both files covers the area of the Federal Republic of Germany and the temporal period ranges from 2006 to 2017.

The dataset comprises the following shapefiles *radar_comparison.shp* and *gauge_comparison.shp*.

- *Radar_comparison.shp*: Point data of the centroids of the RADKLIM data grid (1 km resolution) clipped to Germany. The spatial reference is a polar-stereographic projected Cartesian coordinate system defined by DWD for their radar composite products (see [13] for more details on this custom projection referred to as 'radar projection' throughout this paper). This file is subsequently referred to as 'RADKLIM and RADOLAN radar precipitation dataset' or 'radar shapefile'.
- *Gauge_comparison.shp*: Point data of rain gauges with the geographic coordinate system WGS 84 as a spatial reference. This shapefile is subsequently referred to as 'rain gauge precipitation dataset' or 'rain gauge shapefile'.

The objective of the data collection was to provide an easy-to-use dataset that enables also nonspecialists from different communities (geosciences, hydrology, meteorology, and environmental planning) to get quick insights into the properties of the radar datasets and, thus, to help improve the usability of RADKLIM and RADOLAN. Consequently, the dataset was published in the widespread shapefile geodata format in order to provide all collected information in one attribute table and enable an easy and straightforward usage in all common GIS as well as data exports to other tabular data formats. Both shapefiles contain a variety of attribute fields including a series of aggregated rainfall statistics calculated from all three precipitation datasets for comparison as well as metadata on gauge and radar pixel ID numbers, height above sea level, and some dataset-specific metadata such as distance to next radar, full gauge station names, and gauge measurement periods.

A summary of the most important attribute fields of the dataset is provided in Table 1 and the entire list of attribute fields is included in the metadata description [14].

Table 1. Overview and description of the most important attribute fields contained in the rainfall data intercomparison dataset. All fields marked with * were calculated for all three precipitation datasets, fields marked with ** were calculated only for the two radar datasets. These fields are prefixed with "RK_" (derived from the hourly RADKLIM RW product), "RO_" (RADOLAN RW) or "G_" (rain gauge data) in the attribute table.

Field Name	Parameter Description	Unit
*MAP	Mean annual precipitation sum 2006–2017	mm
**MAPc	Mean annual precipitation sum cleaned from extreme outliers	mm
*MAPc_l	Mean annual precipitation sum cleaned from extreme lower outliers	mm
*MSP	Mean summer precipitation sum (May–October)	mm
*MWP	Mean winter precipitation sum (November–April)	mm
*2006, … , *2017	Precipitation sum of the year 2006, 2007, … , 2017	mm
*nnan	Total number of NoData entries in the period 2006–2017	-
*s_nd_1	Number of days exceeding a precipitation sum of 1 mm in the summer	-
*s_MDP_1	Mean precipitation of all days exceeding a precipitation sum of 1 mm in the summer	mm
*s_nd_20	Number of days exceeding a precipitation sum of 20 mm in the summer	-
*s_MDP_20	Mean precipitation of all days exceeding a precipitation sum of 20 mm in the summer	mm
*w_nd_1	Number of days exceeding a precipitation sum of 1 mm in the winter	-
*w_MDP_1	Mean precipitation of all days exceeding a precipitation sum of 1 mm in the winter	mm
*w_nd_20	Number of days exceeding a precipitation sum of 20 mm in the winter	-
*w_MDP_20	Mean precipitation of all days exceeding a precipitation sum of 20 mm in the winter	mm
height_dem	Average height above sea level per radar pixel	m
nwep	Number of wind energy plants in the respective radar pixel	-
wep_height	Average hub height of all wind energy plants per pixel	m
wep_dia	Average rotor diameter of all wind energy plants per pixel	m
**dist10	Distance to closest radar station in the year 2010	km
**dist17	Distance to closest radar station in the year 2017	km

3. Materials and Methods

In the following sections, input data sources and data availability are explained, data processing, data aggregation, and validation procedures are also described for each input dataset, and, finally, an explanation of the merging procedure applied to obtain the resulting dataset is provided.

3.1. RADKLIM and RADOLAN Radar Precipitation Dataset

3.1.1. Data Sources and Accessibility

The data basis for the radar shapefile consists of the following freely available datasets.

(a)   The hourly RADOLAN RW composite
(b)   The hourly RADKLIM RW composite
(c)   A Shuttle Radar Topography Mission (SRTM) Digital Elevation Model
(d)   A dataset on the distribution and properties of wind energy plants

(a) The RADOLAN RW dataset intended for operational, near real-time rainfall monitoring contains hourly precipitation heights for Germany adjusted to rain gauge measurements on a 900 km * 900 km grid. The product code "RW" refers to the final, hourly-resolved result of the RADOLAN radar data processing chain which includes the conversion from reflectivity to precipitation heights, various correction algorithms (e.g., for clutter and orographic beam blockage), the merging of local radar station data to a nationwide gridded composite, as well as the adjustment to rain gauge measurements using a weighted average of radar-gauge differences and ratios. The RADOLAN RW product is available at the DWD

Climate Data Centre (ftp://ftp-cdc.dwd.de/pub/CDC/grids_germany/hourly/radolan/historical/bin/) and covers the period from June 2005 until now, with the most recent file being provided ~20 min after the end of the last measurement interval. For comparability with the other datasets, the period 2006 – 2017 was used for the dataset presented in this paper. RADOLAN data are provided in a custom binary format with one file per hourly composite, which are collected in monthly zip archives. Additional information on data format, projection and radar locations is provided in the accompanying project report and file format description [8,15].

(b) The RADKLIM RW dataset [11] which is available at the DWD Open Data Portal (https://open data.dwd.de/climate_environment/CDC/grids_germany/hourly/radolan/reproc/2017_002/bin/) contains hourly precipitation heights for Germany adjusted to rain gauge measurements on a 1100 km * 900 km grid. This radar-based precipitation climatology dataset is a reanalyzed and temporally extended version of RADOLAN using consistent processing techniques, several new correction algorithms (e.g., for distance- and height-dependent signal reduction and for spokes) and more rain gauges for adjustment. The dataset currently covers the period of 2001 to 2017, but only the years from 2006 onwards have been used for the dataset presented in this paper in order to allow for a comparison to the shorter RADOLAN time series. The file format is similar to RADOLAN, except for the extended grid size and the files containing more header information.

(c) The Digital Elevation Model (DEM) derived by the Shuttle Radar Topography Mission (SRTM) contains the height above sea level in meters with a grid resolution of 25 meters and is freely available for researchers at the EOWEB Geo Portal (https://geoservice.dlr.de/egp/).

(d) The wind energy dataset contains information on the spatial distribution and properties of wind energy plants in Germany. It is part of a renewable energy dataset collected by [16] and provided in shapefile format by the Helmholtz Centre for Environmental Research (Umweltforschungszentrum, UFZ) (https://www.ufz.de/record/dmp/archive/5467/de/). Information on wind energy plants was included in the dataset since they may cause false echoes and, thus, clutter and noise in the radar measurements.

3.1.2. Data Processing, Aggregation, and Validation

Step 1: RADKLIM and RADOLAN raw data processing

Using the Python package *radproc* [17], the raw RADOLAN and RADKLIM datasets were both unzipped separately, clipped to the Federal Republic of Germany, imported into monthly *pandas* DataFrames [18] with one column per radar pixel and one row per hour and saved to two identically structured HDF5 files [19] with one group per year and therein twelve monthly datasets.

During this process, so-called ID rasters with the locations of the numbered data pixels were generated, one raster for the 900 km * 900 km RADOLAN grid and one for the 1100 km * 900 km RADKLIM grid. The ID rasters are clipped to Germany and used as a basis for the raw precipitation data clipping and for the subsequent export of results to raster datasets. A more detailed description of the raw data processing methodology is provided by [20].

Step 2: Calculation of precipitation statistics

The calculations for all precipitation statistics are based on the generated HDF5 file and functions from the Python packages *radproc*, *pandas*, and *numpy* [21]. Most of the calculated statistics are self-explaining or comprehensively outlined in Table 1 and the metadata description (e.g., precipitation sums per year or hydrological half-year and number of days exceeding a precipitation sum of 1 mm or 20 mm), which is why the following sections are limited to describing data cleaning and validation approaches as well as some dataset-specific parameters.

The calculated mean annual precipitation sums showed significant differences between RADKLIM and RADOLAN with much higher values in several thousand RADOLAN cells. These are due to a series of extremely high outliers in the annual precipitation sums before 2010, primarily in the year 2009, which contains sums of up to 43,155 mm. Overall, 199 cells throughout Germany exceed a precipitation

sum of 5000 mm in 2009 in the RADOLAN dataset and a total of 928 cells exceeds 2000 mm (field 'RO_2009'), whereas the mean annual precipitation sum for Germany amounts to ~785 mm and the average for 2009 is still 40 mm lower (fields 'G_MAP' and 'G_2009'). The outliers are caused by a combination of false echoes (clutter) and the spreading of maximum values to their surrounding raster cells by the so-called push-method used until July 2010 to transform radar data points from polar coordinates to Cartesian coordinates in the gridded composite [22–24]. The term clutter refers to errors in the radar data that are characterized by reflectivities greater than zero over longer time periods. They are caused by reflections from, e.g., wind energy plants, high buildings, or mountains. The aggregation of these numerous mainly low values, which can also be spread to some or all neighboring pixels by the push-method, can result in high sums. However, these extreme values are part of the RADOLAN RW product, which is why they have been included in the intercomparison dataset. It is important to be aware that RADOLAN contains such extreme values. However, in order to obtain more realistic and comparable annual precipitation sums as well as an indicator for the presence of outliers, an additional data cleaning has been conducted, which is highlighted by a 'c' in the respective field names. To exclude extreme outliers from the average calculation, the Interquartile Range (IQR) method for outlier detection, which was developed by Tukey [25] and is also used for visualizations in box–whisker plots, has been applied across both axes (rows/pixels and columns/years). A value x was regarded as a valid value if it is located inside the range

$$Q_1 - 1.5 \cdot (Q_3 - Q_1) < x < Q_3 + 1.5 \cdot (Q_3 - Q_1) \tag{1}$$

with Q1 = first quartile and Q3 = third quartile. The thresholds were calculated for each cell across both axes separately. If a value lies outside this range across both axes, it is flagged as an outlier and removed from the average calculation. Using both axes was necessary in order to take local spatial effects as well as temporal changes such as particularly dry or wet years into account.

For RADOLAN, this data cleaning affected a total of 25,282 cells. The annual averages were reduced in 21,324 RADOLAN cells (high outliers, e.g., due to clutter were removed) with a reduction between 2 mm and 3677 mm, whereas in 3958 cells averages were raised by 4.6 mm to 146.5 mm (low outliers, e.g., due to missing data were removed). For RADKLIM, 32,883 cells were affected by the outlier removal. In 12,742 RADKLIM pixels, the averages were reduced by 0.9 mm to 192.5 mm, whereas in 20,141 pixels, the averages were raised by 0.6 to 126.3 mm. All in all, the affected RADOLAN cells show a mean reduction of 80.4 mm, whereas the RADKLIM cells exhibit a mean raise of 9.9 mm.

Consequently, the data cleaning serves well to work out one of the major differences between the two radar datasets. RADOLAN has a higher number of cells affected by clutter and, thus, by high outliers, which are also much more pronounced than in RADKLIM. Thus, on the contrary, the latter has a much higher number of cells affected by lower outliers by missing data or very low values.

Step 3: Derivation of additional parameters for radar data quality evaluation

As additional parameters that may have an influence on radar data quality, the height above sea level, the distance from the nearest radar, and the number and properties of wind energy plants were derived for each radar pixel.

The height above sea level can affect the radar reflectivity signal in several ways. Especially in mountainous regions, sources of error include an overshooting of orographic precipitation, ground clutter, partial beam blockage, and a high share of snow and ice particles, which are more difficult to quantify than rainfall due to their larger surface and melting effects, known as the bright band. These effects can lead either to underestimation or overestimation of the precipitation amount [4,26,27].

The distance of a pixel from the radar can also affect data quality and is mostly related to significant underestimation of rainfall amounts at larger distances from the radar. This is due to the attenuation of the reflectivity signal, which can be caused by the radar beam geometry, the scattering and absorption of the radar signal by hydrometeors and potential beam blockage [7,27].

The Digital Elevation Model was used to calculate the average height above sea level for each 1 km^2 radar pixel. Averaging was necessary in order to obtain a representative height value for each 1 km^2 radar pixel as the radar measurements actually also represent the average precipitation per square kilometer. The single tiles of the DEM were merged, reprojected to the radar projection, clipped to Germany, and aggregated by calculating the mean height per pixel in the RADKLIM ID raster, which the aggregated DEM was snapped to in order to obtain congruent pixel locations and extent.

The quality of the derived height was validated against the height of the gauge stations taken from the gauge metadata considering all pixels that contain a gauge. As shown in Figure 1, both datasets show a high conformity with a Pearson correlation coefficient of r = 0.98, but slightly higher DEM values and expectedly higher differences in higher altitude.
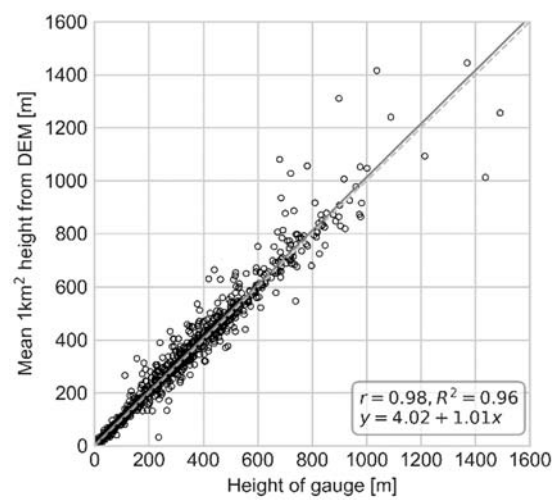
Figure 1. Comparison of height above sea level derived from the gauge metadata (field 'G_height') and from the Shuttle Radar Topography Mission (SRTM) Digital Elevation Model (DEM) aggregated to 1 km^2 ('height_dem') for the 997 points in the gauge shapefile.

The distance to the nearest radar is split into four separate fields, which is due to changes in the radar network (new stations or altered locations) and the difference in the radar radius used for RADKLIM (128 km) and RADOLAN (150 km). As there were no changes to the radar hardware in the years 2010 and 2017, the radar stations for these two years were digitized from the coordinates given in [13] and the Euclidean distance of each pixel to the nearest radar within the given radius and year was calculated in the radar projection for RADKLIM and RADOLAN, respectively. However, the calculated maximum distances did not match the radar ranges that are visible in the precipitation composites since the calculated radius was too small. Consequently, the radius was extended in order to fill out the entire radar range and to obtain valid distance values for each pixel. As a result, the maximum distance values exceed the respective radius given by DWD by between 3.5 km in Northern Germany and up to 10 km in Southern Germany. This effect can be explained by the polar-stereographic radar projection's increasing distortion of area towards the south and the differences between planar and geodesic distance calculations. Whereas the planar Euclidean distance corresponds to the length of a straight line on a plane surface, the geodesic line is the distance between two points on a curved surface, such as the Earth. Since the geodesic distance is greater and a projection to a planar surface tends to stretch surfaces in order to obtain a Cartesian grid, a geodesic line transformed into a planar projected coordinate system (such as the radar projection defined by DWD) is longer than a straight line drawn on a planar surface. The assumption, that the radar radius given by DWD is actually a geodesic distance and does not correspond to 128 or 150 km in their custom projected stereographic coordinate system could be confirmed by a comparison of planar and geodesic buffers around the radar locations with aggregated precipitation composites (see Figure 2). A geodesic buffer with a distance of 128 km around the radar locations is perfectly aligned with the radar ranges observed from

the precipitation composites, but the maximum distance measured in the radar projection was 3.5 to 10 km higher. In contrast to this, a planar buffer of 128 km is too small and does not cover the actual radar range.
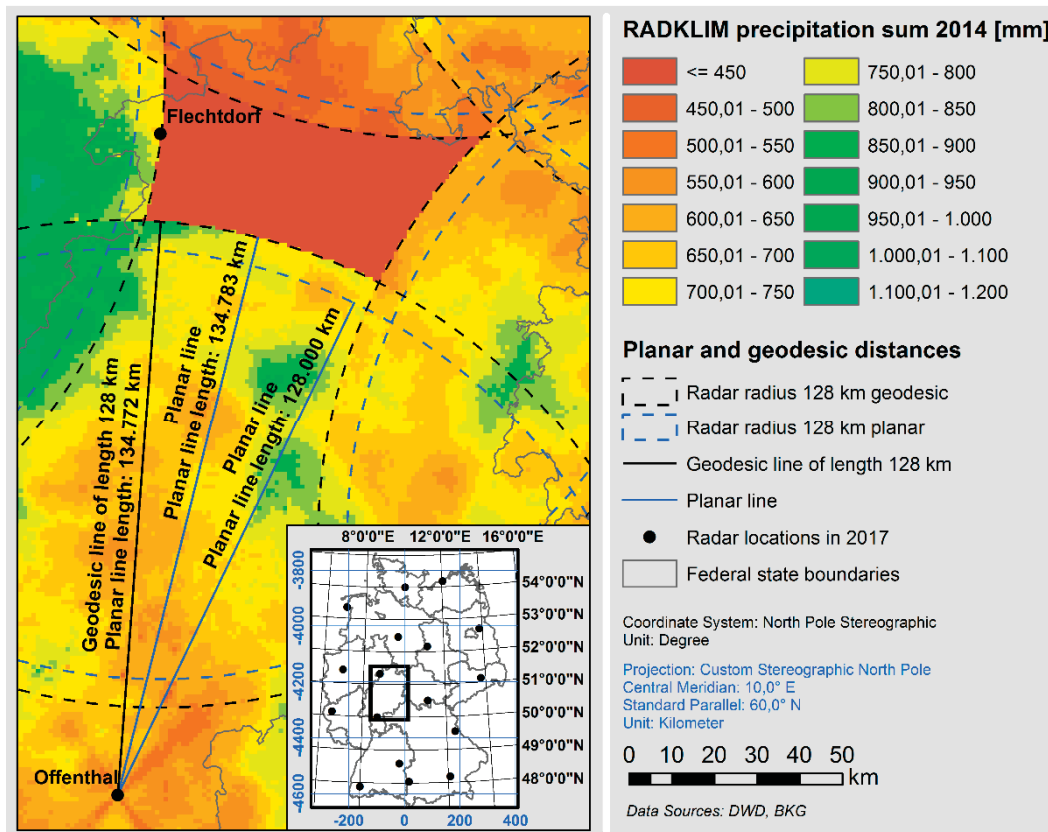
Figure 2. Differences between planar and geodesic distance calculation in the projected, Cartesian stereographic coordinate system defined for the radar products by Deutscher Wetterdienst (DWD). The very low precipitation values in the northern area, which are due to several months of missing data during the upgrade of the radar Flechtdorf in 2014, provide an ideal radar range for the distance validation.

For the derivation of the three parameters related to wind energy plants (count, mean hub height and mean rotor diameter per radar pixel), the RADKLIM IDs were extracted to the wind energy point shapefile and summary statistics for each pixel were calculated. Subsequently, the statistics were exported to three separate rasters based on the RADKLIM ID raster.

Step 4: Creation of the output dataset

In order to prepare the concluding data collection step, the RADKLIM ID raster for Germany was converted to an ArcGIS file geodatabase point feature class containing the centroids of all 1 km^2 RADKLIM grid cells. Subsequently, a list of all rasters which are supposed to be included in the dataset was created and their pixel values were extracted to the respective point features based on location.

The resulting dataset comprises 392,529 point features (rows in the attribute table) on a regular 1 km grid and the attribute table contains 67 fields (columns).

3.2. Rain Gauge Precipitation Dataset

3.2.1. Data Source and Accessibility

The rain gauge RR data in 1-minute resolution used for this dataset are freely available in the DWD Open Data Portal (https://opendata.dwd.de/climate_environment/CDC/observations_germany/climate/1_minute/precipitation/). Measurement data are provided as zipped text files with one file per station and month and sorted in year folders. Downloading the dataset can be rather tedious as there is no option to automatically download an entire year folder although there are thousands of files per year which are not collected in any zip archives. The data files have an aperiodic structure, which means hours or days without precipitation are summarized in one line. Next to the precipitation data are zip archives with several metadata text files for each station containing information on measurement periods, devices, and time zones as well as station coordinates, height above sea level, and full station names. An additional metadata text file provides a summary of all gauges describing their coordinates, height, names and measurement periods.

For the analysis period 2006 to 2017, the precipitation was measured by tipping bucket or OTT Pluvio rain gauges at most of the stations and the data are provided in UTC time zone since the year 2000.

3.2.2. Data Processing, Aggregation and Validation

Step 1: Data availability check, data processing, and data cleaning

All precipitation data files for the period 2006 to 2017 were downloaded and unzipped into year folders using Python. Subsequently, all data were imported and converted into periodic monthly *pandas* DataFrames with one column per gauge and one row per minute. These DataFrames were then saved into the same uniform HDF5 file format as the radar data with one group per year and therein twelve monthly datasets. Internally, the data import and preprocessing is divided into several consecutive parts. First, data availability and completeness were checked and a dictionary with lists of files for import sorted by month was generated. For every year and station, the number of available month files was counted. If one or more month files were missing, the remaining files for this station were removed from the lists and all values for this station were set to *pandas'* missing data value NaN throughout the entire year. This resulted in a loss of between 0.9 % of gauges in 2014 up to 20.8% in 2006 with an average loss of 4% (37 gauges) for the above period, but this data cleaning is necessary in order to reduce the bias of subsequent aggregated statistics due to incomplete time series and to obtain more reliable data for comparison. Next, each file was imported, and the three precipitation data columns representing weighing method (RS_01), dropper (RTH_01), and tipping bucket (RWH_01) measurement devices were merged and converted into a single-column DataFrame. Usually, only one data column contains valid values at a time, but in some cases, e.g., due to device changes or due to the use of ombrometers providing a combination of dropper and tipping bucket, there can be two columns with non-NaN values. With respect to the measurement accuracy and resolution, the value from the 'RS_01' column (weighing method), which was measured by Pluvio rain gauges in most cases, was selected where available. If it is NaN at the respective interval, the value from the 'RTH_01' (dropper) column was selected and if values in both of these columns are NaN, the value from the 'RWH_01' (tipping bucket) column was selected. Upon resampling, all gaps in the aperiodic data were filled with zeros since—assuming the data are correct—only rainless periods are summarized and NaN intervals are indicated by the value −999 in the original data. Finally, for each month, all single-column DataFrames were concatenated and the monthly DataFrames were saved to HDF5.

However, data validation showed that the raw gauge data contain a series of erroneous or at least questionable values, which could be summarized into three classes outlined below. Whereas comparable values were kept in the RADKLIM and RADOLAN data, they need to be corrected in the gauge dataset, which is regarded as ground-truth reference for the evaluation of the radar datasets.

Consequently, an additional iterative data cleaning procedure has been applied to the HDF5 file containing the processed gauge data in order to account for each of these error types (see Figure 3):

1. Several extremely high minute values (121 min intervals between 312.44 and 487.56 mm at station 01669 in January 2008), which are regarded as impossible. Consequently, all intervals exceeding 100 mm were replaced by NaN in the HDF5 file without any further checks. The high threshold of 100 mm was chosen in order to ensure that no heavy rainfall events that may have been saved as aggregated value (e.g., a daily sum), e.g., due to hardware issues, are erased from the data without any further checks.

2. Very high values with missing entries or zeros in the raw data several minutes or hours beforehand (e.g., 57.27 mm at station 07104 at 06.06.2011 10:49 with previous entry 0.0 mm at 10:02; 55.17 mm at station 05158 at 30.09.2006 13:08 with previous entries all 0.0 mm). Such high values could be either erroneous data or also sum values for a previous time period during which a malfunction of the gauge occurred and the precipitation sum was added later. For such values, it is difficult to tell which of these cases holds true and how long the summarized period has been. However, as the gauge dataset needs to be reliable at least at an hourly temporal resolution for subsequent comparison to the radar data, a three-step validation was applied: First, all intervals exceeding 4 mm/min were regarded as potentially erroneous and identified from the HDF5 file. Second, for all exceeding intervals, the precipitation values of the gauge during the previous hour were checked. If there are any non-zero precipitation values, the gauge was assumed to have worked correctly and the value was kept. Third, if the gauge indicated no precipitation during the previous hour, the precipitation amount of the two adjacent hours of the corresponding RADKLIM pixel was consulted. If any of these indicated precipitation, the gauge value was kept. If both hours have a value of 0.0 mm at the RADKLIM pixel, the exceeding gauge value was set to NaN since it can either be considered as erroneous or the actual precipitation may have occurred at some unknown time in the past and the value is not representative for the point of time under review.

3. Sequences of several consecutive minutes with remarkably high values (e.g., at station 02532 on 15.06.2006, there are four consecutive entries with 10.75 mm/min between 8:01 and 8:04 AM). To address potential errors due to value repetitions in the data and their potentially significant effects on data aggregation results, the intervals exceeding 4 mm/min were additionally checked for the time between exceedances. If there are more than two consecutive intervals exceeding 4 mm/min, all intervals starting from the third were set to NaN.
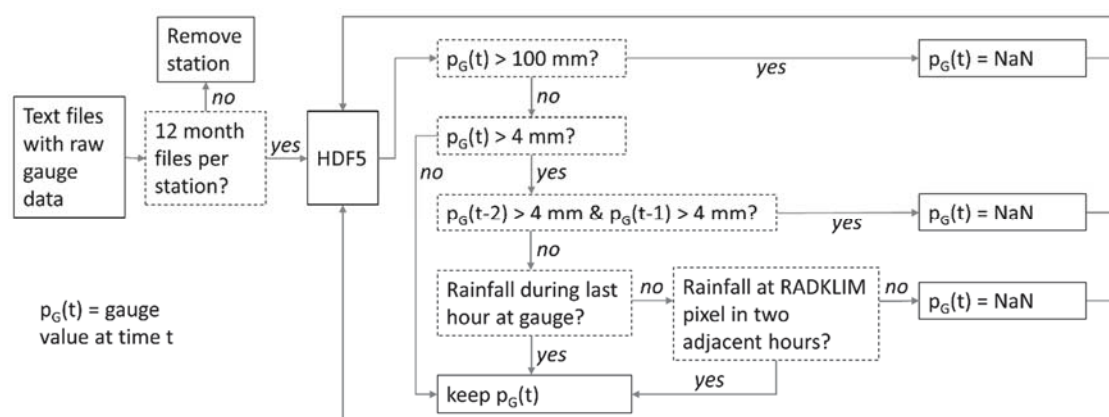

Figure 3. Schematic rain gauge data cleaning workflow.

The reasons for the observed errors and uncertainties are largely unknown and not indicated in the sparse gauge data documentation. It can be assumed, though, that several of the high outliers are actually sum values of longer time periods due to temporary malfunctions of the devices. Especially

during heavy rainfall events measured by tipping bucket gauges, there may be design-inherent difficulties to continuously detect rain rates with high intensities. Errors related to missing NoData values (see Step 3 below), however, can most likely be attributed to data processing issues.

All in all, the number of gaps as well as unexpected and unexplainable errors in the raw gauge data is much higher than in the radar data, whereas the documentation of gauge data formats is much sparser and less comprehensive. Consequently, the gauge data processing necessitates a much higher effort for the handling of missing or erroneous data. Regarding the missing data, 435 out of 997 gauges in the final dataset have a largely complete time series without any hours regarded as NaN (field 'G_nnan', see Step 3 below). Moreover, for 598 gauges the number of NaN values is sufficiently low to have all annual precipitation sums for the entire period of 2006 to 2017 calculated. As for the radar data, all precipitation statistics calculated in the following are based on the generated HDF5 file.

Step 2: Creation of a point shapefile with gauge locations

Besides the precipitation data preprocessing, an ArcGIS file geodatabase point feature class with all gauge locations as well as metadata on beginning and end of the measurement period, station name, and number; height above sea level; and the federal state was generated from the metadata summary file. Since the gauge locations are provided as geographic coordinates, the spatial reference of this feature class is the Geographic Coordinate System WGS 84. Moreover, the RADKLIM and RADOLAN cell IDs corresponding to each station were extracted from the RADKLIM and RADOLAN ID rasters. The new ID fields added to the attribute table are the basis for the final merging of the gauge and radar datasets described in Section 3.3, since they provide the information in which RADKLIM or RADOLAN cell the respective gauges are located.

Step 3: Calculation of precipitation statistics

Most of the precipitation statistics calculated and the functions applied on the gauge dataset are identical to those for the radar datasets. But, in contrast to the calculations for the radar data, results are exported to the feature class attribute table directly from the DataFrames and without storage of intermediate files. The only major difference in the data exported to the feature classes pertains to the annual precipitation sums. In contrast to the radar dataset, the cleaned sums after the removal of low outliers, which is explained in Section 3.1.2, were exported for the gauge dataset. This is necessary due to erroneous values in the original gauge data. For gauge no. 01346, the data files contain the value 0.0 throughout the entire years 2006, 2007, and most of 2008 resulting in incorrect annual precipitation sums of 0 mm, 0 mm, and 32.29 mm, respectively. As this leads to heavily biased annual averages and because the gauge dataset values need to be regarded as a ground truth for subsequent data comparisons, these values must not be exported to the final dataset and were removed as outliers beforehand. Yet, a comparison of the cleaned and uncleaned annual sums showed that only one other gauge, no. 04501, which has an annual precipitation sum of 21.9 mm in the year 2006, is affected by comparable errors.

For the count of NaN values (field 'G_nnan'), the different temporal resolutions of gauge (1 min) and radar datasets (60 min) had to be equalized in order to obtain comparable values. Hence, the gauge data were aggregated to hours whereby an hour was set to NaN if more than 10 out of 60 min intervals contain NaN values. Additionally, as stations with less than 12 monthly data files for one year are not contained in the HDF5 file for the respective year, the number of hours per missing year was added to the calculated NaN counts. Consequently, the total NaN count is the sum of NaN values actually contained in the HDF5 file plus the number of hours of each year removed by data cleaning procedures.

Step 4: Removal of gauge points with incomplete data collection

After the export of the annual precipitation sums, gauge points without precipitation data or without corresponding RADKLIM or RADOLAN cell ID—which can happen if they are close to the

national border in an area not covered by radar—are deleted in order to keep only gauges with a complete dataset for comparison with the radar data.

The resulting rain gauge point shapefile comprises 997 point features (rain gauges) spread over Germany with a total of 37 fields in the attribute table.

3.3. Merging the Datasets

3.3.1. Methodology

In order to merge both precipitation datasets to the final rainfall data intercomparison dataset, both feature class attribute tables were joined to each other based on the RADKLIM ID. On the one hand, the gauge values were joined to the radar feature class by performing an outer join to keep all radar values. For radar pixels that contain a gauge, the respective gauge values were appended to the attribute table, whereas, for radar pixels without a gauge, the fields for gauge data contain NoData values (<Null>). On the other hand, the values of radar pixels containing a gauge were joined to the gauge feature class using an inner join that only keeps features with common RADKLIM IDs. Consequently, the gauge feature class is actually a subset of the radar feature class which contains only complete data collections for intercomparison as well as accurate gauge locations instead of radar grid cell centroids.

Finally, for publication, both feature classes were exported to shapefiles which can be read by all common GIS. However, shapefiles are not able to store the feature class-specific <Null> values (these are replaced by 0 upon export). Since in the radar feature class, <Null> values represent the status 'no coverage' (a pixel is either not covered by any radar or does not contain a gauge), which can be important for intercomparison, this information needs to be kept. Hence, to distinguish the actual value 0 from <Null> values, the latter were replaced by the value −99999 in both feature classes before export. Contrary to the radar shapefile, in the gauge shapefile, missing annual precipitation sums received the value 0 because the years are not necessarily uncovered but the data may have been removed due to incompleteness or erroneous data. Consequently, this shapefile contains −99999 only for parameters which could not be calculated such as the mean daily precipitation exceeding 20 mm if there is actually no such day.

3.3.2. Resulting Dataset

The final radar shapefile still comprises 392,529 point features (rows in the attribute table) on a regular 1 km grid, but after joining the gauge attribute fields, the attribute table now contains 98 fields (columns). The final gauge shapefile comprises 997 point features with exactly the same 98 fields as the radar shapefile in its attribute table.

All parameters that were calculated for two or all three rainfall datasets were prefixed with RK_ (RADKLIM), RO_ (RADOLAN), or G_ (Gauges) to identify the data origin. Thus, to compare, e.g., the mean precipitation sum in the hydrological winter half-year between all three precipitation datasets, the fields 'RK_MWP', 'RO_MWP', and 'G_MWP' need to be selected.

4. Data Use and Application

The rainfall data intercomparison dataset presented in this paper can be directly imported into all common GIS due to its shapefile format. It can be used for the creation of maps at any scale within Germany in order to, e.g.,

- compare the rainfall datasets with each other and evaluate their quality,
- identify the dataset best-suited for the respective study area and application,
- improve the understanding of the inherent bias and error structure, especially of the two radar datasets, and to
- provide precipitation maps and statistics as well as model inputs for the covered time period.

As an example for a straightforward comparison of the gauge and RADKLIM datasets, Figure 4 shows the cleaned mean annual precipitation sums of the gauges (gauge shapefile, field 'G_MAPc_l') as well as the RADKLIM mean annual precipitation sums (radar shapefile, field 'RK_MAP').
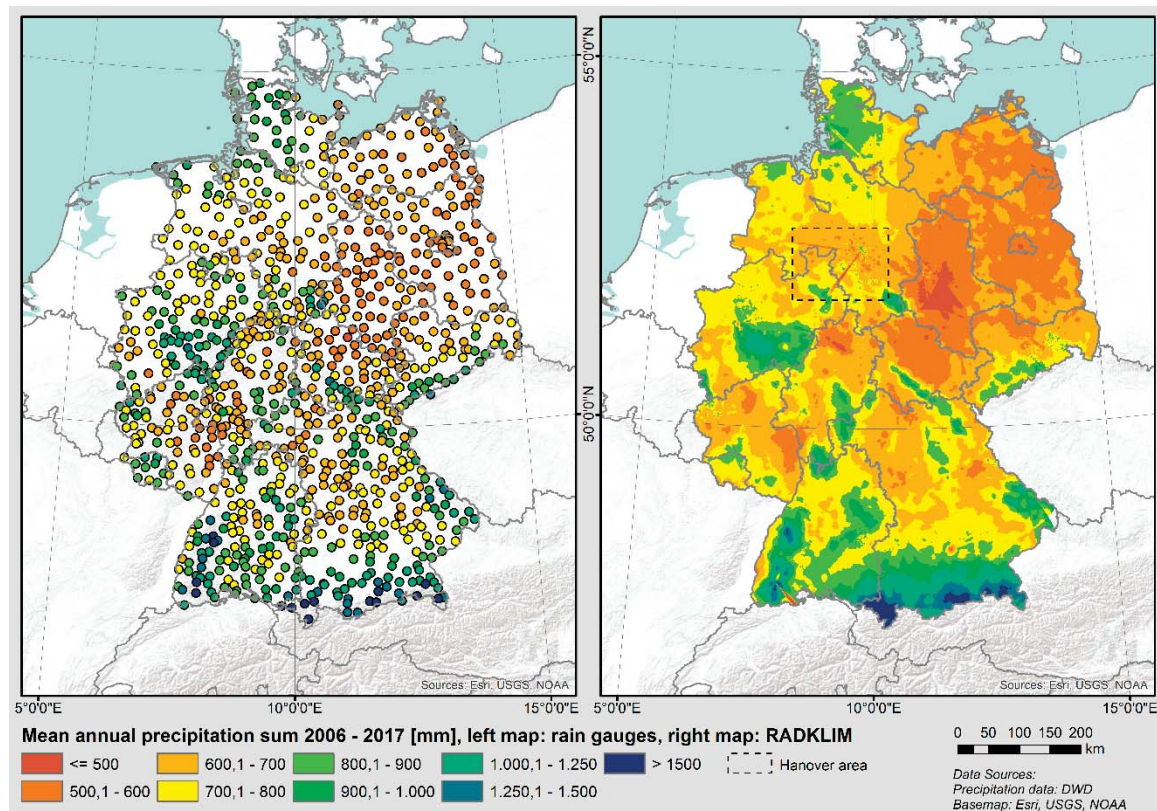
Figure 4. Mean annual precipitation sum 2006–2017 calculated from rain gauges (map on the left) and RADKLIM (map on the right). The dashed rectangle in the RADKLIM map indicates the area around the radar station in Hanover discussed in the text.

Besides the precipitation averages, the rain gauge data-based map (Figure 4 on the left) also shows the nationwide spatial distribution of gauge stations in the gauge shapefile, whereas the RADKLIM map (Figure 4 on the right) shows the clipped 1 km^2 grid of the radar shapefile. The comparison of both maps shows a mainly consistent spatial precipitation distribution in the gauge and RADKLIM datasets with mountain ranges being distinguishable and a decrease of precipitation amounts from west to east, which is characteristic for the transition from a maritime to a more continental climate in Germany. However, the maps also indicate slightly higher gauge values in some regions and the RADKLIM map shows several spatial structures that can be attributed to radar artifacts. As an example, there is a series of striking clusters of pixels with outstandingly low and high values around the radar station in Hanover, Lower Saxony, as well as two lines of pixels with remarkably low values running from the radar station in western and southwestern directions. The former are insufficiently corrected or overcorrected ('Reverse Speckle') false echoes, which are a common problem due to the low radar beam height at close range from the radar, whereas the latter are so-called spokes, which can occur if the radar beam is blocked close to the radar or if an azimuth angle is not scanned at all [10].

Beyond the applications presented above, the rainfall data intercomparison dataset can also be used for statistical analyses. Examples include the calculation of differences and ratios between precipitation datasets, exploratory data analysis, plotting or the fitting of regression models in order to analyze the correlations and dependencies between the RADKLIM and RADOLAN data and other parameters such as the height above sea level or the distance to the next radar. A straightforward way for users of ArcGIS to import the intercomparison dataset into the Python ecosystem, which provides

rich functionality for statistical analyses, is shown in Figure 5. It shows the import of the gauge shapefile attribute table into a DataFrame in Python using the *radproc* package in a Jupyter Notebook [28] and how to plot selected data columns against each other as a scatter plot. This quick analysis confirms the assumption derived from the map comparison (see Figure 4) that gauge and RADKLIM values match quite well in general, but the gauge values tend to be higher than the RADKLIM values.

```
import radproc as rp
import pandas as pd
gaugeShp = r'O:\IntercomparisonDataset\gauge_comparison.shp'
#import attribute table to pandas DataFrame
gaugeDF = rp.attribute_table_to_df(gaugeShp)
#replace all -99999 NoData values by numpy's nan
gaugeDF = gaugeDF.replace(-99999.0, np.nan)
gaugeDF
```

	FID	Statnr	radklim_id	radolan_id	start_date	end_date	Statname	State	latitude	longitude	...	RKw_nd_20
0	0	03217	96687.0	6767.0	20060704	20181212	Weesby	Schleswig-Holstein	54.8373	9.1481	...	4.0
1	1	02907	101174.0	11254.0	19990201	20181212	Leck	Schleswig-Holstein	54.7903	8.9514	...	2.0
2	2	05732	111046.0	21126.0	20050607	20181212	Wrixum/Föhr	Schleswig-Holstein	54.6928	8.5271	...	0.0
3	3	04405	112918.0	22998.0	20060129	20181212	Satrup	Schleswig-Holstein	54.6854	9.6261	...	7.0
4	4	04896	114730.0	24810.0	20050517	20181212	Wagersrott	Schleswig-Holstein	54.6654	9.8050	...	5.0
5	5	00791	117373.0	27453.0	20051206	20181212	Bordelum	Schleswig-Holstein	54.6328	8.9370	...	3.0
6	6	05930	117445.0	27525.0	19941102	20181212	Schönhagen	Schleswig-	54.6410	10.0238	...	6.0

```
%matplotlib inline
gaugeDF.plot(x='G_MAPc_l',y='RK_MAP',kind='scatter')
```

```
<matplotlib.axes._subplots.AxesSubplot at 0x36acb390>
```


Figure 5. Importing the gauge shapefile into a DataFrame and plotting the mean annual precipitation sums of gauges and RADKLIM against each other.

References

1.   Thorndahl, S.; Einfalt, T.; Willems, P.; Nielsen, J.E.; Veldhuis, M.C.T.; Arnbjerg-Nielsen, K.; Rasmussen, M.R.; Molnar, P. Weather radar rainfall data in urban hydrology. *Hydrol. Earth Syst. Sci.* **2017**, *21*, 1359–1380. [CrossRef]
2.   Krajewski, W.F.; Kruger, A.; Smith, J.A.; Lawrence, R.; Gunyon, C.; Goska, R.; Seo, B.C.; Domaszczynski, P.; Baeck, M.L.; Ramamurthy, M.K.; et al. Towards better utilization of NEXRAD data in hydrology: An overview of Hydro-NEXRAD. *J. Hydroinformatics* **2011**, *13*, 255–266. [CrossRef]
3.   Seo, B.C.; Krajewski, W.F.; Kruger, A.; Domaszczynski, P.; Smith, J.A.; Steiner, M. Radar-rainfall estimation algorithms of Hydro-NEXRAD. *J. Hydroinformatics* **2011**, *13*, 277. [CrossRef]
4.   Leijnse, H.; Uijlenhoet, R.; Hazenberg, P. Radar rainfall estimation of stratiform winter precipitation in the Belgian Ardennes. *Water Resour. Res.* **2011**, *47*, 257.
5.   Gjertsen, U.; Salek, M.; Michelson, D.B. Gauge-adjustment of radar-based precipitation estimates–a review. *Cartogr. Perspect.* **2003**, *1*. [CrossRef]
6.   Goudenhoofdt, E.; Delobbe, L. Evaluation of radar-gauge merging methods for quantitative precipitation estimates. *Hydrol. Earth Syst. Sci.* **2009**, *13*, 195–203. [CrossRef]
7.   Berne, A.; Krajewski, W.F. Radar for hydrology: Unfulfilled promise or unrecognized potential? *Adv. Water Resour.* **2013**, *51*, 357–366. [CrossRef]
8.   MeteoSolutions GmbH. Projekt RADOLAN–Routineverfahren zur Online-Aneichung der Radarniederschlagsdaten mit Hilfe von Automatischen Bodenniederschlagsstationen (Ombrometer). Zusammenfassender Abschlussbericht für die Projektlaufzeit von 1997 bis 2004. Available online: https://www.dwd.de/DE/leistungen/radolan/radolan_info/abschlussbericht_pdf.pdf?__blob=publicationFile&v=2 (accessed on 19 April 2018).
9.   Winterrath, T.; Rosenow, W.; Weigl, E. On the DWD Quantitative Precipitation Analysis and Nowcasting System for Real-Time Application in German Flood Risk Management. *IAHS Publ.* **2012**, *351*, 323–329.
10. Erstellung Einer Radargestützten Niederschlagsklimatologie; Berichte des Deutschen Wetterdienstes No. 251. 2017. Available online: https://www.dwd.de/DE/leistungen/pbfb_verlag_berichte/pdf_einzelbaende/251_pdf.pdf?__blob=publicationFile&v=2. (accessed on 29 March 2019).
11. RADKLIM Version 2017.002: Reprocessed Gauge-Adjusted Radar Data, One-Hour Precipitation Sums (RW). Available online: https://opendata.dwd.de/climate_environment/CDC/grids_germany/hourly/radolan/reproc/2017_002/bin (accessed on 25 June 2019).
12. RADKLIM Version 2017.002: Reprocessed Quasi Gauge-Adjusted Radar Data, 5-Minute Precipitation Sums (YW). Available online: https://opendata.dwd.de/climate_environment/CDC/grids_germany/5_minutes/radolan/reproc/2017_002/bin/ (accessed on 25 June 2019).
13. Deutscher Wetterdienst. RADKLIM: Beschreibung des Kompositformats und der Verschiedenen Reprozessierungsläufe. Version 1.0. 2018. Available online: https://www.dwd.de/DE/leistungen/radarklimatologie/radklim_kompositformat_1_0.pdf;jsessionid=0889B3A8CB74341FAA652DB2A4FB7F63.live11041?__blob=publicationFile&v=1 (accessed on 26 March 2019).
14. A Rainfall Data Inter-Comparison Dataset for Germany: Version 1.0. Available online: https://zenodo.org/record/3262172 (accessed on 29 June 2019).
15. Deutscher Wetterdienst. RADOLAN und RADVOR: Beschreibung des Kompositformats. Version 2.4.4. 2018. Available online: https://www.dwd.de/DE/leistungen/radolan/radolan_info/radolan_radvor_op_komposit_format_pdf.pdf?__blob=publicationFile&v=11 (accessed on 26 March 2019).
16. Eichhorn, M.; Scheftelowitz, M.; Reichmuth, M.; Lorenz, C.; Louca, K.; Schiffler, A.; Keuneke, R.; Bauschmann, M.; Ponitka, J.; Manske, D.; et al. Spatial Distribution of Wind Turbines, Photovoltaic Field Systems, Bioenergy, and River Hydro Power Plants in Germany. *Data* **2019**, *4*, 29. [CrossRef]
17. Radproc–A Gis-Compatible Python-Package for Automated Radolan Composite Processing and Analysis; Zenodo. 2018. Available online: https://zenodo.org/record/2539441 (accessed on 25 June 2019).
18. Mckinney, W. pandas: A Foundational Python Library for Data Analysis and Statistics. Available online: https://www.dlr.de/sc/Portaldata/15/Resources/dokumente/pyhpc2011/submissions/pyhpc2011_submission_9.pdf (accessed on 31 July 2019).
19. Hierarchical Data Format. Available online: https://portal.hdfgroup.org (accessed on 18 December 2018).

20. Kreklow, J. Facilitating radar precipitation data processing, assessment and analysis: A GIS-compatible python approach. *J. Hydroinformatics* **2019**, *21*, 652–670. [CrossRef]

21. Oliphant, T.E. *A Guide to NumPy*; CreateSpace: Scotts Valley, CA, USA, 2006.

22. Stephan, K. Erfahrungsbericht zur Verwendung des PULL-Kompositverfahrens zur Erstellung des Radolan-Komposits (RZ-Komposit). *DWD Interner Ber.* **2007**, in press.

23. RADOLAN-Information Nr. 17. Available online: https://www.dwd.de/DE/leistungen/radolan/radolan_info/radolan_info_nr_17.pdf?__blob=publicationFile&v=3 (accessed on 17 June 2019).

24. Weigl, E.; Winterrath, T. Radargestützte Niederschlagsanalyse und –vorhersage (RADOLAN, RADVOR-OP). *Promet* **2009**, *35*, 78–86.

25. Tukey, J. *Exploratory Data Analysis*; Addison-Wesley: Reading, MA, USA, 1977.

26. Germann, U.; Galli, G.; Boscacci, M.; Bolliger, M. Radar precipitation measurement in a mountainous region. *Q. J. R. Meteorol. Soc.* **2006**, *132*, 1669–1692. [CrossRef]

27. Meischner, P. *Weather Radar: Principles and Advanced Applications*, 1st ed.; Springer: Berlin/Heidelberg, Germany, 2004.

28. Project Jupyter. Jupyter Notebook, 2014–2019. Available online: https://jupyter.org/ (accessed on 17 June 2019).

4

Radar-Based Precipitation Climatology in Germany – Developments, Uncertainties and Potentials

J. Kreklow, B. Tetzlaff, B. Burkhard, G. Kuhnt

atmosphere

MDPI

Article

Radar-Based Precipitation Climatology in Germany—Developments, Uncertainties and Potentials

Jennifer Kreklow [1,*] **, Björn Tetzlaff** [2] **, Benjamin Burkhard** [1,3] **and Gerald Kuhnt** [1]

[1]   Institute of Physical Geography and Landscape Ecology, Leibniz Universität Hannover, Schneiderberg 50, 30167 Hannover, Germany; burkhard@phygeo.uni-hannover.de (B.B.); kuhnt@phygeo.uni-hannover.de (G.K.)

[2]   Institute of Bio- and Geosciences IBG-3, Forschungszentrum Jülich GmbH, 52425 Jülich, Germany; b.tetzlaff@fz-juelich.de

[3]   Leibniz Centre for Agricultural Landscape Research ZALF, Eberswalder Straße 84, 15374 Müncheberg, Germany

*   Correspondence: kreklow@phygeo.uni-hannover.de; Tel.: +49-0511-762-19798

check for updates

Abstract: Precipitation is a crucial driver for many environmental processes and weather radars are capable of providing precipitation information with high spatial and temporal resolution. However, radar-based quantitative precipitation estimates (QPE) are also subject to various potential uncertainties. This study explored the development, uncertainties and potentials of the hourly operational German radar-based and gauge-adjusted QPE called RADOLAN and its reanalyzed radar climatology dataset named RADKLIM in comparison to ground-truth rain gauge data. The precipitation datasets were statistically analyzed across various time scales ranging from annual and seasonal aggregations to hourly rainfall intensities in regard to their capability to map long-term precipitation distribution, to detect low intensity rainfall and to capture heavy rainfall. Moreover, the impacts of season, orography and distance from the radar on long-term precipitation sums were examined in order to evaluate dataset performance and to describe inherent biases. Results revealed that both radar products tend to underestimate total precipitation sums and particularly high intensity rainfall. However, our analyses also showed significant improvements throughout the RADOLAN time series as well as major advances through the climatologic reanalysis regarding the correction of typical radar artefacts, orographic and winter precipitation as well as range-dependent attenuation.

Keywords: weather radar; rain gauge; rainfall; QPE; RADOLAN; RADKLIM; GIS; radar climatology; uncertainties

1. Introduction

Precipitation is one of the main drivers of hydrologic and energy cycles and induces a variety of environmental processes such as runoff, erosion or floods and has been acknowledged as an Essential Climate Variable. Due to the high spatiotemporal variability of precipitation, a spatially distributed quantitative estimation of rainfall rates is a challenging task. Thus, the "unbiased estimation of high temporal resolution precipitation amount, especially over the oceans, and over areas of complex orography" [1] has been identified as an outstanding scientific and technological challenge.

Direct rainfall measurements with rain gauges on the ground can only provide local point scale information. As rain gauges are scarce in many regions, this approach is not sufficient to capture spatial rainfall distribution, especially for smaller-scale convective storm events [2–4]. In the last decades, ground-based weather radar and space-borne satellite observations have emerged as alternative

Improving Usability of Weather Radar Data in Environmental Sciences: Potentials, Challenges, Uncertainties and Applications   J. Kreklow

Atmosphere **2020**, *11*, 217   2 of 19

measurement techniques capable of producing temporally and spatially highly resolved gridded precipitation estimates. Despite their undisputed potential to satisfy the increasing demand of research and planning institutions, insurance companies, policy and operational communities for reliable, highly resolved precipitation data, these data also cause new uncertainties [5]. Both remote sensing-based products are estimates derived from indirect measurements, which are subject to various potential sampling errors causing systematic bias and random errors [6]. Consequently, there are numerous studies that have evaluated radar [7–13] and satellite [14] products against rain gauges, conducted comparisons between radar and satellite products [15–18] or between all three methods [19,20].

An excellent overview of radar basics and the main sources of uncertainty is given in [21], whereas [22] provides an overview of the basics and uncertainties of satellite observations. However, up to now, satellite-based quantitative precipitation estimates (QPE) have been less suitable for climatological analyses due to their comparably low spatial and/or temporal resolution [23].

The uncertainties in QPE derived from C-Band radars in the midlatitudes include various different effects, many of them causing an underestimation of rainfall depth. The attenuation of the radar beam by heavy precipitation or a wet radome can lead to a decrease in reflectivity with increasing distance from the radar. The conversion from the measured reflectivity to precipitation depths is hampered by the vertical variability of the drop size distribution and the non-uniform vertical profile of reflectivity. Moreover, the radar beam can be (partially) blocked by obstacles such as buildings or mountains, which cause linear artifacts of regions with underestimated rainfall, the so-called negative spokes. In areas with a diverse and in some regions, complex terrain such as Germany and especially during the winter season, precipitation quantification is a challenge due to differing hydrometeor types, bright-band effects and overshooting. The higher proportion of snow and ice particles at higher altitudes and during wintertime can cause bright-band effects at the melting layer and lead to strong reflectivity signals, whereas the signal above the bright-band may decrease significantly. Moreover, especially rainfall of stratiform and orographic character can be underestimated due to overshooting, which is a source of uncertainty in mountainous areas and at long ranges from the radar caused by the increasing height of observation due to the beam elevation angle and the Earth's curvature [9,24].

Besides the main sources of uncertainty and various potentials of radar data for hydrological applications, Berne and Krajewski [21] also stated in 2013 that radar data are not used as extensively in the field of hydrology as one would expect. This also holds true for the operational radar-based and gauge-adjusted German QPEs, which have been operationally derived and continuously further developed by the German Weather Service (Deutscher Wetterdienst, DWD) since June 2006 within the RADOLAN ("Radar Online Adjustment") programme [25]. Despite the fact that these temporally (up to 5 min) and spatially (1 km^2) highly resolved data have been available for fourteen years now, RADOLAN is still sparsely used in scientific studies. Studies using RADOLAN comprise the analysis of extreme flash floods and heavy rainfalls [26,27], forecasting of water levels and floods [12,28], the intercomparison to satellite-based QPEs [16,18] and the estimation of rainfall erosivity [29,30]. However, an increased use of RADOLAN data could be observed as most of these studies have been published within the last four years. This tendency might go along with an improvement of data quality since the correction and adjustment algorithms used for RADOLAN have been continuously further developed. In 2018, the radar-based QPE time series was extended back to the year 2001 and reanalyzed using consistent processing techniques and several new correction algorithms. The resulting dataset called RADKLIM ("Radar Climatology") should open up new climatological application fields for radar composite data such as statistical heavy rainfall analyses, erosion modelling and the use of aggregated precipitation sums for precipitation statistics or as model inputs. Up to now, this dataset has primarily been used by the DWD itself for studies on heavy rainfall frequency and extent [31,32], but also for rainfall erosivity analyses [33,34].

However, to the best of the authors' knowledge, no nationwide evaluation of the RADOLAN and RADKLIM composites and their inherent error structure has been published yet. This study provides a nationwide comparative evaluation of the recently published RADKLIM dataset in comparison

to RADOLAN and rain gauge data. The aim was not to provide a quantitative error matrix, which would require much more independent reference data. Instead, we wanted to map out the differences, developments, advantages and shortcomings of the compared datasets and gain a better understanding of the systematic and random error structure of the RADKLIM and RADOLAN radar composite datasets.

The goal of this study was to support a user's decision on which of the datasets is best suited depending on the individual study area, time period and intended application and to raise awareness of the potential bias that varies in space and time. Special attention was paid to developments in the RADOLAN processing routines and their impact on data quality as well as to the impacts of the additional correction algorithms applied to derive the RADKLIM dataset.

Resulting from the issues outlined above, the following research questions were addressed and discussed in this study:

1. Which developments in the German radar-based QPE derivation procedure have taken place since the launch of the RADOLAN programme in 2006 and how did they affect data quality?
2. How did the additional climatological correction algorithms used for RADKLIM affect the data quality compared to RADOLAN and the gauge dataset?
3. Which challenges, advantages and limitations do users need to take into account when using RADKLIM and RADOLAN in comparison to gauge data?

2. Materials and Methods

2.1. Study Area

The investigated area for this study comprises the state territory of Germany (see Figure 1), which covers about 357,021 km^2 extending from 47° N to 55° N and from 5° E to 16° E. Consequently, the country is located in the humid midlatitudes in a transition zone between a maritime climate in the western part and a humid continental climate in the east. Atmospheric circulation and, thus, the distribution of precipitation is influenced by humid westerly winds, which decrease towards the eastern part of Germany. Additionally, the distribution of precipitation amounts is characterized by the diverse topography of the study area with the summits and foothills of the Alps in the south, a variety of low mountain ranges in the central part and lowlands in the north.
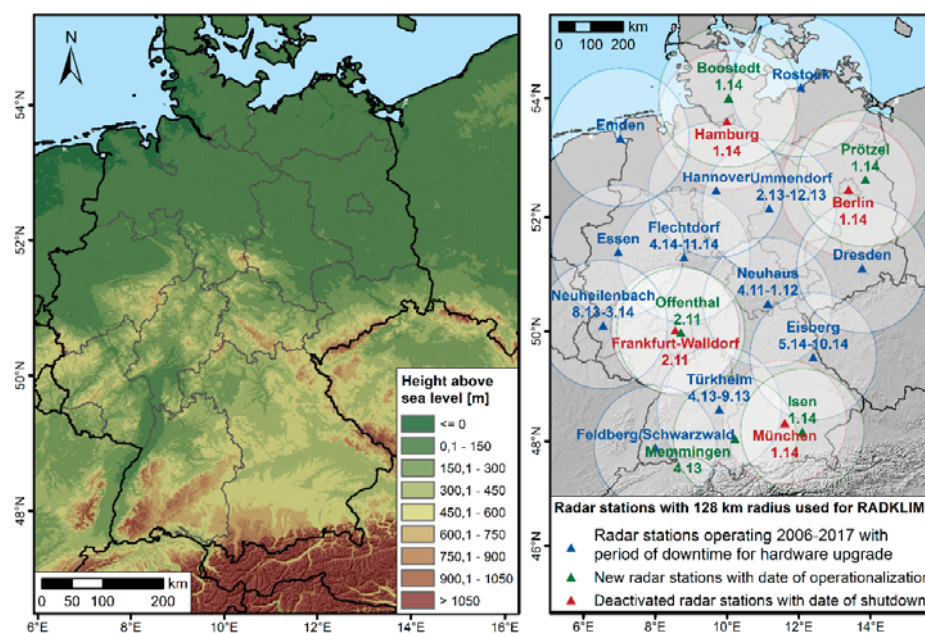
Figure 1. Height above sea level (m) of Germany based on a SRTM Digital Elevation Model (**left map**) and German radar station network with 128 km radius as used for RADKLIM (**right map**).

2.2. Data Basis

2.2.1. RADOLAN

The German Weather Service (DWD) operates a network of currently 17 ground-based C-Band radar stations. The reflectivity data obtained by this network have been processed to QPEs on a nationwide 900 km × 900 km grid in 1 km^2 resolution within the operational RADOLAN ("Radar Online Adjustment) programme since June 2006.

Data processing and correction algorithms include:

- The elimination of clutter pixels;
- Orographic shading correction;
- Smoothing with gradient filters;
- A transformation of the reflectivity Z to rain rates R using a custom refined Z-R-relation;
- Merging the local radar station data to a national gridded composite;
- The adjustment of the radar-based rain rates to ground-truth automated rain gauge measurements using a weighted average of adjustment differences and factors [25].

The final RADOLAN product RW has an hourly resolution and is freely available at the Open Data DWD server [35] with the most recent interval being provided within 30 min after the end of the measurement interval. The composite with the highest temporal resolution (5 min) is the RY product, which is neither adjusted to gauges nor freely available online.

However, the RADOLAN routine as well as the radar network have been continuously developed, which causes significant changes in the data quality throughout the time series. The first major change in the processing routine took place in December 2007. It comprised the inclusion of foreign gauges and German gauges located close to the border beyond any radar radius as well as a gauge-based interpolation of gaps in the RW product. Two other important changes were the increase of the radar radius from 128 km to 150 km in March 2010 [36,37] and the use of RY data for the derivation of the RW product since May 2010, which introduced additional quality checks for clutter removal and replaced the "push"-method for composite creation by the more mitigating "pull"-method [38,39]. When converting the local radar data in polar projection to a Cartesian composite grid, the size of the polar grid cells becomes larger at longer ranges from the radar. Consequently, close to the radar, several polar cells are located in one Cartesian cell, whereas, at long ranges from the radar, several Cartesian cells may be located within one polar cell. Moreover, in areas with overlapping polar grids, one value has to be selected for the Cartesian grid cell. The "push"-method uses a search radius of one cell in each direction to fill gaps and selects the maximum value of all available values. As a consequence, high values may be spread to all adjacent cells and a characteristic cross-shaped artefact is visible on the composite. The "pull"-method does not apply a search radius and directly selects the value of the closest polar cell. In case of overlaps, the maximum value is selected [40]. In August 2016, a further software update introduced additional clutter corrections, a filter that prevents biased rain gauge values from being used for adjustment, a reduction of edges and inconsistencies at radar borders and additional rain gauges in the Czech Republic for adjustment [41]. Finally, the use of new polarimetric radar data as an input for all composite products since October 2017 constituted the latest major change in the RADOLAN routine [42].

2.2.2. RADKLIM

In 2018, the DWD published a reanalyzed version of their radar reflectivity data archive dating back to the year 2001 using consistent processing techniques and more rain gauges for adjustment [43]. Additionally, new climatological algorithms for the detection and correction of radar-specific artefacts such as clutter and spokes as well as for the correction of signal reduction with distance and height have been developed and applied. In this context, the radius of local radar data used for the composite

has been reduced to 128 km. Moreover, the first major change in the RADOLAN routine has been partly revoked for RADKLIM, so that gaps in the radar data are not filled with interpolated gauge data anymore. Instead, gaps are contained in the dataset as no data values. In contrast to the RADOLAN RY product in 5-min resolution, the RADKLIM counterpart called YW [44] has been quasi-adjusted based on the RW product to improve its precipitation quantification. Moreover, the height of the composite has been extended by 200 rows, 100 each in the north and south, and the grid has been shifted eastwards by 80 km in order to cover the entire country and to provide some additional buffer to each side [45].

Table 1 provides an overview of the four final RADOLAN and RADKLIM composite products. Due to the unavailability of the RADOLAN RY product, this study only evaluated the hourly RW products.

Table 1. Overview of the final RADKLIM and RADOLAN composite datasets.

Radar Product	Open Access	Time Period	Temporal Resolution [min]	Radar Radius [km]	National Grid [km]
RADKLIM RW	Yes	2001–2018	60	128	1100×900
RADKLIM YW	Yes	2001–2018	5	128	1100×900
RADOLAN RW	Yes	Since June 2005	60	125/150	900×900
RADOLAN RY	No	Since June 2005	5	125/150	900×900

2.2.3. Rain Gauge Data

Rain gauge data in 1-min resolution were used as ground-truth precipitation data for validation. These data are freely available in the DWD Open Data Portal [46]. For more details on these data, the processing and the applied quality checks, please refer to [47].

2.3. Methodology

2.3.1. Data Preparation

For the analysis of all precipitation datasets, a processing framework consisting of ArcGIS and Python developed by Kreklow [48] using the radproc version 0.1.4 [49] was used. Moreover, parts of the analyses of this study were based on a rainfall data intercomparison geodataset of RADKLIM, RADOLAN and rain gauge data [50], which provided data pairs of each station and radar pixel for a wide range of precipitation statistics and additional parameters relevant for data quality evaluation.

2.3.2. Dataset Completeness and Outliers

The completeness of the dataset and the occurrence of outliers are two major properties determining the reliability and usability of a dataset as well as the additional effort necessary for raw data processing and data preparation. Both may cause strongly biased precipitation statistics.

In order to assess dataset completeness, the NoData counts, that is, the number of hourly intervals with NoData values, for all 997 gauge-radar data pairs were statistically analyzed.

The occurrence of outliers and their effect on annual precipitation sums were also evaluated based on the intercomparison dataset. Following the definition by Tukey [51], Kreklow et al. [47] defined outliers as annual precipitation sums lying outside 1.5× Interquartile Range (IQR) and calculated cleaned mean annual precipitation (MAP) sums without these outliers. In order to assess the effect of this cleaning process as well as the spatial and temporal distribution of outliers in the datasets, we calculated the differences between cleaned MAP and original MAP.

2.3.3. Precipitation Statistics and Interrelations to Potential Error Sources

Many typical weaknesses of radar measurements such as clutter, spokes and underestimations with increasing distance from the radar and increasing altitude only become apparent through the aggregation of longer time periods. Moreover, the reliable mapping of precipitation amounts is a key requirement for a dataset that is to be used for climatological applications. We put particular emphasis

on investigating the seasonal differences between the datasets in order to evaluate the improvements of RADKLIM in quantifying precipitation in winter, when there is a higher prevalence of snowfall.

Thus, precipitation sums and means for varying periods including years, hydrologic half-years, months and days were calculated for each dataset in order to map typical spatial distributions and assess temporal variability. For direct quantitative comparisons, the ratios between RADKLIM and RADOLAN as well as between RADKLIM and gauge data were calculated. All comparative analyses were conducted either for RADKLIM–gauge data pairs (n = 997) or for RADKLIM–RADOLAN pixel pairs (n = 392,529).

In order to assess the level of consistency between the datasets as well as the impacts of altitude and distance from the radar on the QPEs, linear regression models were fitted to the data pairs using the ordinary least squares method and the Pearson correlation coefficient r was calculated for the respective data pairs with the following formula:

$$r = \frac{\sum_{i=1}^{n}\left(X_i - \overline{X}\right)\left(Y_i - \overline{Y}\right)}{\sqrt{\sum_{i=1}^{n}\left(X_i - \overline{X}\right)^2}\ \sqrt{\sum_{i=1}^{n}\left(Y_i - \overline{Y}\right)^2}} \tag{1}$$

where X and Y are the respective observed precipitation sums, $\overline{Y}$ and $\overline{X}$ are the mean precipitation sums, n is the total number of data pairs and i denotes the ith data pair. For the correlation analyses between precipitation sums and altitude or distance from radar, the former is the dependent variable Y and the latter is the independent variable X.

The coefficient of determination r^2 was used to evaluate the model fit since it is a measure for the proportion of the variance in the data that can be explained by the model.

$$r^2 = \frac{\text{Model Sum of Squares}}{\text{Total Sum of Squares}} = \frac{\sum_{i=1}^{n}\left(\hat{Y}_i - \overline{Y}\right)^2}{\sum_{i=1}^{n}\left(Y_i - \overline{Y}\right)^2} \tag{2}$$

where $\hat{Y}_i$ is the modeled or predicted value associated to Y_i.

For perfect linearity between the datasets, both parameters equal the value 1, whereas values close to 0 indicate a very weak correlation or none at all.

Furthermore, the Root Mean Squared Error (RMSE) was calculated to represent the average magnitude of the error, whereby higher weight is given to larger errors, that is, deviations between the datasets.

$$\text{RMSE} = \sqrt{\frac{1}{n}\sum_{i=1}^{n}(X_i - Y_i)^2} \tag{3}$$

2.3.4. Rainfall Detection and Intensity

In addition to the long-term precipitation statistics, the capability to detect rainfall as well as to capture different rainfall intensities up to heavy rainfall was investigated on a daily and hourly time scale for the different precipitation datasets.

On a daily scale, the precipitation detection rate of each precipitation dataset was inferred by counting the days with precipitation sums greater than 1 mm and by calculating the mean precipitation amounts of these rainy days. As an indicator for the capability of a dataset to detect heavy rainfall occurrence, the number of days with precipitation amounts greater than 20 mm and their mean precipitation sums were calculated.

Moreover, the distribution of hourly rainfall intensities was analyzed for RADKLIM and the gauge dataset in order to assess their capability to detect rainfall and to capture rainfall of high intensity. First, the gauge data were resampled from minute to hourly resolutions. Second, all hourly intervals of the resampled gauge dataset and the RADKLIM RW product were classified according to their rainfall

intensity and the frequency per class was counted. Finally, the absolute and relative differences of the class frequencies between both datasets were calculated.

3. Results

3.1. Spatiotemporal Distribution and Impacts of Outliers and Missing Data

The distribution of outliers varies considerably in space and time as well as between the two datasets. The original RADOLAN data suffer from many high outliers actually causing a positive bias in the mean annual precipitation sum (MAP, see Figure 2). Outliers are particularly frequent at close range around the radars, but also tend to occur in mountainous areas. Visual inspection of the spatial distributions of outliers and wind energy plants revealed that many of the outliers are related to the presence of wind energy plants at the respective pixel if the latter is located at close range to the radar or at mountain ranges. There, the radar beam has a relatively low height above ground and the wind turbine rotors can disturb the radar signal by causing constant noise. These effects could be reduced significantly in RADKLIM.
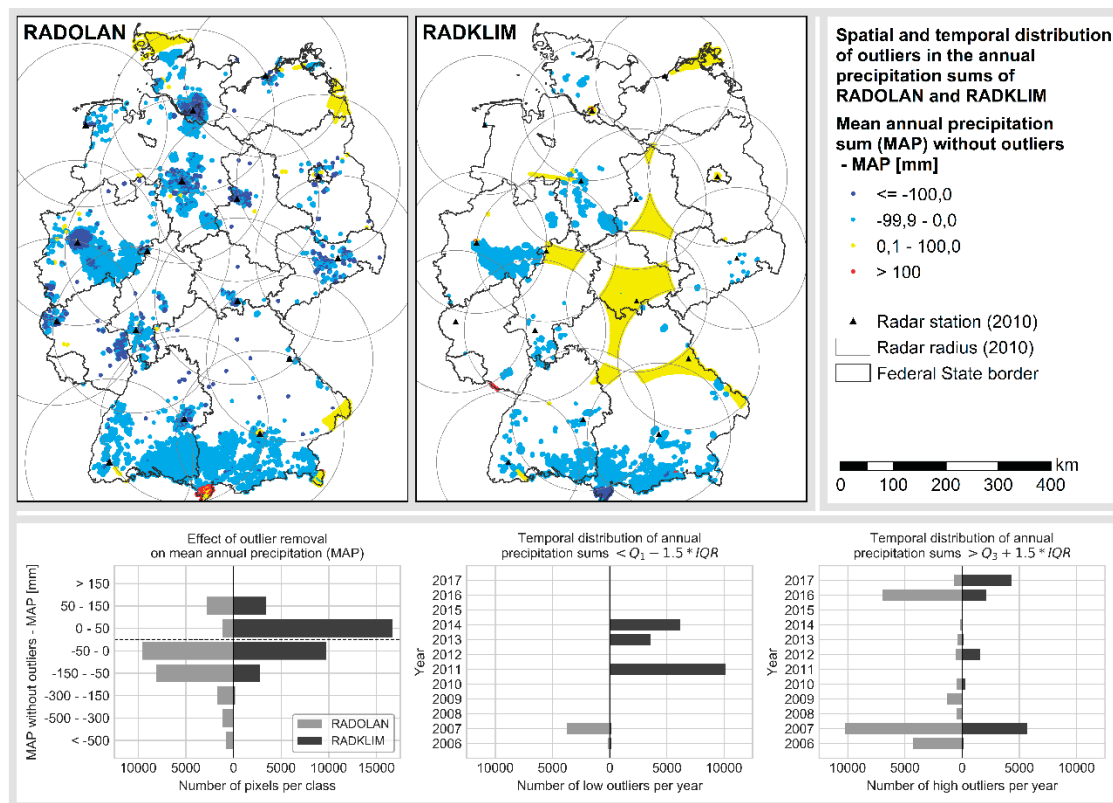
Figure 2. Spatiotemporal distribution of outliers in the annual precipitation sums of RADOLAN and RADKLIM. Blue values represent high outliers (MAP > cleaned MAP), yellow and red values represent low outliers (cleaned MAP > MAP).

Figure 2 also shows large areas of low outliers in RADKLIM, which are clearly delineated by radar borders. The occurrence of these data gaps is limited to the years 2011, 2013 and 2014, which correspond to the periods during which some of the radars were replaced by Dual-Pol radars (see Figure 1). These gaps do not occur in RADOLAN since the 150 km radar radia overlap in these areas and there were no temporary backup radars installed while upgrading the operational radars. However, since the radius was reduced to 128 km and the gaps were not filled with interpolated data in RADKLIM, these gaps occur as NoData periods in the RADKLIM dataset. Further reasons for missing data in both radar datasets include radar downtimes due to hardware maintenance work, which is

usually conducted during the night in periods without rainfall, as well as several azimuth angles, that may not be scanned by any radar due to radiation protection regulations.

In RADOLAN, low outliers are limited to areas close to the national border that are not covered by any radar. Like the majority of high outliers, they only occur in the years 2006 and 2007, which shows the improvement achieved by the use of additional gauges and the filling of gaps with data interpolated from gauge measurements since December 2007. However, a large portion of the high outliers in RADOLAN and all high outliers in RADKLIM in the very wet year of 2007 can be attributed to a series of heavy rainfall events in central and northern Germany (Figure 2: Light blue dots in RADKLIM map in range of the radars Essen and Hannover) in August and September 2007 [52]. A further decrease of high outliers in RADOLAN could be achieved in 2010 since additional quality checks for clutter removal were introduced and high reflectivity values are no longer spread to the adjacent pixels by the "push"-method when merging and converting local radar data to the gridded Cartesian composite.

The strikingly high number of high outliers in 2016 in both radar datasets, however, was not caused by any changes in the radar data processing but actually by a year of extraordinarily large differences in precipitation distribution. While the overall annual precipitation amount over Germany only reached 93% of the long-term average, Southern Germany suffered from a series of extreme rainfall events in May and June, which caused several flash floods and also casualties. Consequently, most of the light blue pixels in Figure 2 located in the two southernmost Federal States Bavaria (Southeast) and Baden-Württemberg (Southwest) can be associated to these events in 2016, which significantly raised the annual precipitation amount [53].

Similarly, most of the high outliers in RADKLIM in 2017, which are primarily located in Southern Bavaria were caused by a series of heavy rain and snowfall events throughout the entire year and not by radar errors [53]. However, despite the indisputable impact of the heavy rainfalls in Bavaria in the years 2016 and 2017, the increase of values flagged as outliers in this mountainous area in the RADKLIM dataset (especially compared to RADOLAN in 2017) may also be attributed to a better quantification of precipitation in higher altitudes of the Alps, which was additionally improved by a better coverage through the new radar that was established in Memmingen in 2013.

*3.2. Annual and Seasonal Precipitation Sums*

The overall spatial distribution of the MAP of all three precipitation datasets show similar patterns with mountainous areas being clearly visible and also the transition from a maritime climate in the northwest to a more continental climate with lower precipitation amounts towards the south and east of Germany is well mapped (see Figure 3). However, the actual precipitation amounts differ considerably between the datasets. Taking the gauge MAP of 784.6 mm as a ground-truth, RADKLIM on average underestimates the MAP by 7.9%, whereas RADOLAN overestimates it by 0.9%. The very close match for RADOLAN, however, results from averaging values, which vary heavily in space and time. The temporal development (see Figure 4) shows a significant decrease of precipitation amounts between 2006 and 2011 for RADOLAN, which was caused by the changes in the processing routine discussed above. However, the errors and clutter in the first years of the time series caused such an extreme bias that the maximum MAP in RADOLAN still amounts to 7533 mm and many pixels with very high MAP are located at close range from the radars. These biased MAP values, which could be completely removed in RADKLIM, are also clearly visible in Figure 5.
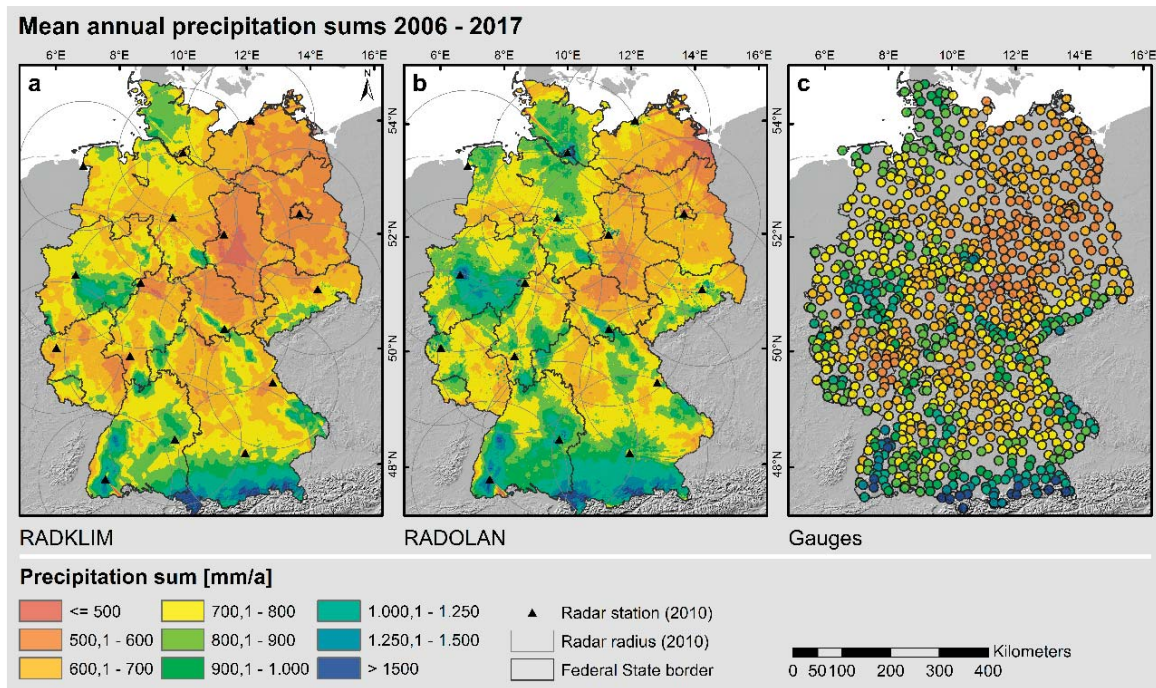
Figure 3. Mean annual precipitation sums for the period 2006 to 2017 derived from (**a**) RADKLIM, (**b**) RADOLAN and (**c**) gauge data.
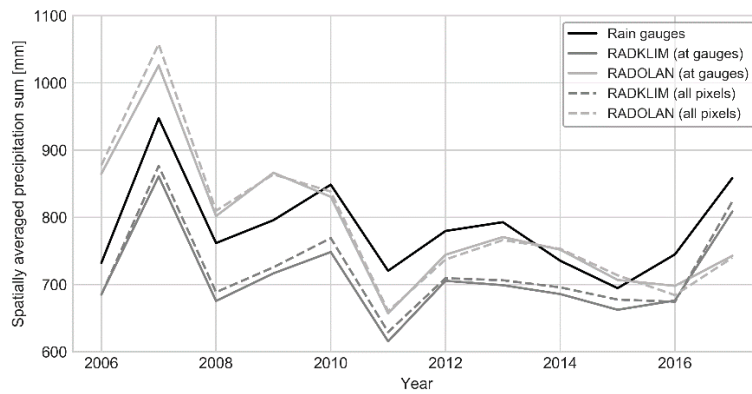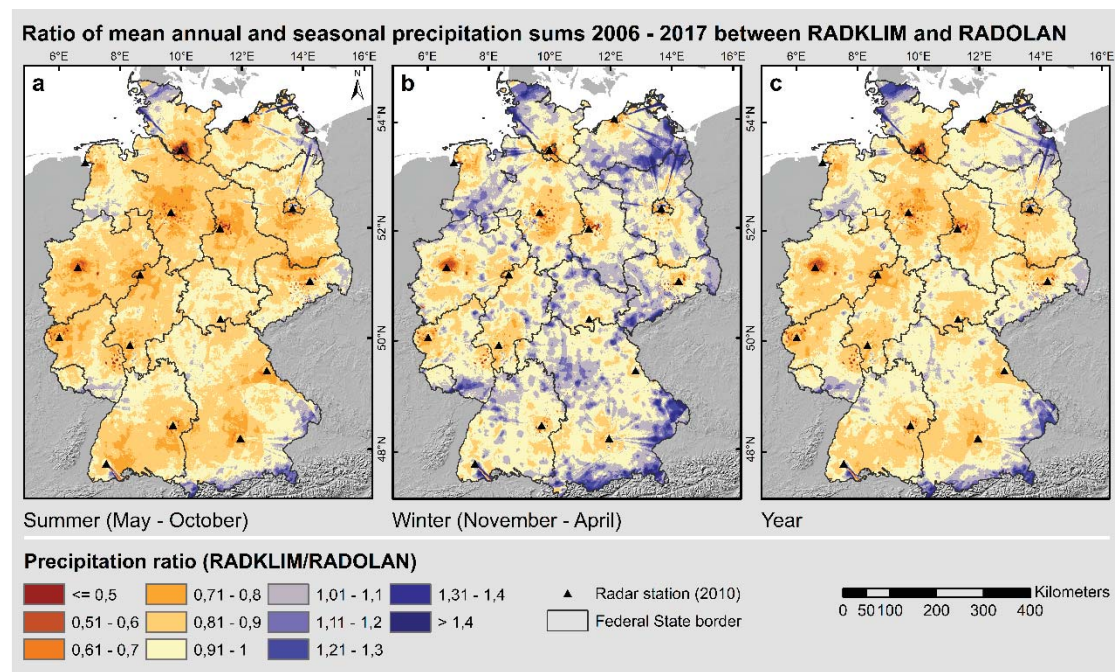

Figure 4. Mean annual precipitation sums of Germany between 2006–2017.
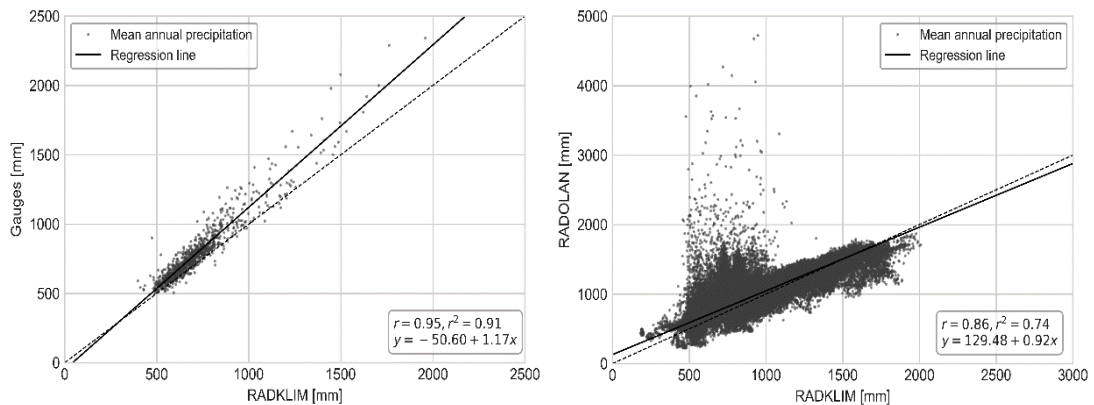
Figure 5. Comparison of mean annual precipitation sums from the 997 rain gauges and the corresponding RADKLIM pixels (**left plot**) as well as from the 392529 RADOLAN-RADKLIM pixel pairs (**right plot**).

RADKLIM, on the contrary, shows a much lower MAP, especially in lowland areas in the east and south of Germany. The data gaps identified in the previous section are also clearly visible and explain the very low minimum MAP of 180.9 mm. Moreover, many of the high clutter values around the radars visible in RADOLAN, which are particularly pronounced around the radars in Hannover, Dresden and Frankfurt, were corrected and show below-average values in RADKLIM. In return, many of the spokes, which are clearly visible in RADOLAN, could be successfully corrected in RADKLIM. As a consequence, the overall RADKLIM image shows significantly fewer radar artefacts than RADOLAN. The effects of both corrections (clutter pixels and spokes) became particularly evident by calculating the ratio between RADKLIM and RADOLAN MAP (see Figure 6). The ratio also revealed that almost nationwide the mean summer precipitation sum in RADKLIM is lower than in RADOLAN with the largest differences in close proximity to the radars. During the winter half-year, though, there is a much more differentiated distribution of the ratio. At greater distances from the radars, the ratio becomes positive, so the RADKLIM winter precipitation sums are higher than in RADOLAN. This effect is particularly pronounced in mountainous areas far from the radars. This indicates that the underestimation of precipitation due to attenuation and the lower reflectivity of snowflakes, which are common problems of radar measurements, could be reduced significantly in RADKLIM. Both effects are investigated in more detail in the following section.

Figure 6. Ratio of mean annual and seasonal precipitation sums 2006–2017 between RADKLIM and RADOLAN.

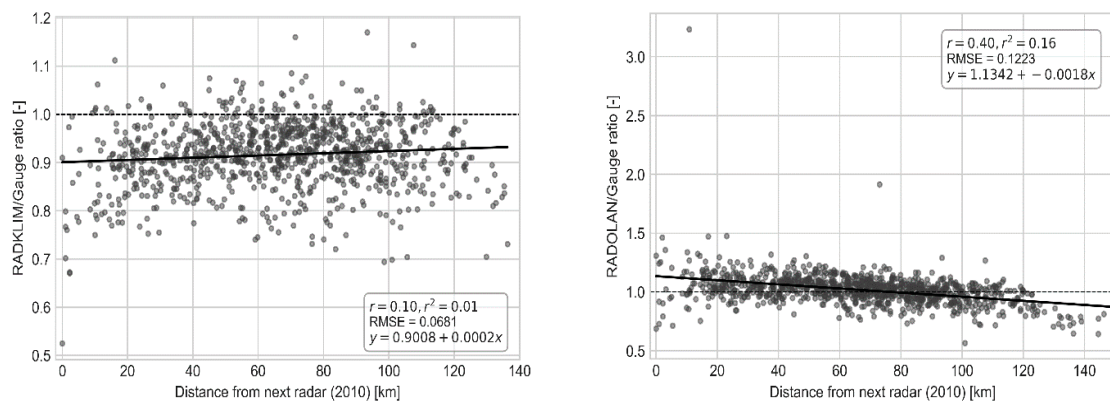### 3.3. Impacts of Elevation and Distance from Next Radar

For all three datasets, a quadratic linear regression was best suited to describe the relation between heights above sea level and seasonal precipitation sums (see Figure 7). The better fit of the quadratic model is due to the extraordinarily high elevation of the Alps compared to the rest of Germany, which has a significant positive impact on the precipitation sums. All datasets show higher precipitation sums and correlation coefficients for the summer half-year than for the winter half-year. RADKLIM and the gauge data actually show similar correlation coefficients with a slightly better fit for the gauges and also the RMSEs are almost similar for the summer precipitation sum. For winter, however, the RADKLIM regression line has a more moderate slope and a much lower RMSE indicating less variability in the RADKLIM data. Especially at lower elevations up to about 550 m, the winter precipitation sums

Improving Usability of Weather Radar Data in Environmental Sciences: Potentials, Challenges, Uncertainties and Applications   J. Kreklow

Atmosphere **2020**, *11*, 217   11 of 19

of the gauge data tend to be higher than the RADKLIM sums. Both regression lines are less steep for RADKLIM, which indicates that the increase of precipitation amounts with increasing altitude is slightly underestimated in RADKLIM. Furthermore, the higher spread between the summer and winter regression lines shows that this effect is somewhat stronger in winter than in summer. However, these effects are not very pronounced and the overall distributions of gauges and RADKLIM show very similar patterns and both map the increase of precipitation with increasing elevation. The results for RADOLAN, however, show a much poorer performance and coincide with the observations shown in Figure 6. There is a much stronger underestimation of winter precipitation at higher altitudes with a very weak coefficient of determination $r^2 = 0.19$. In summer, the overall relation between precipitation and altitude is comparable to RADKLIM, but less reliable for the individual pixel as the high RMSE indicates.
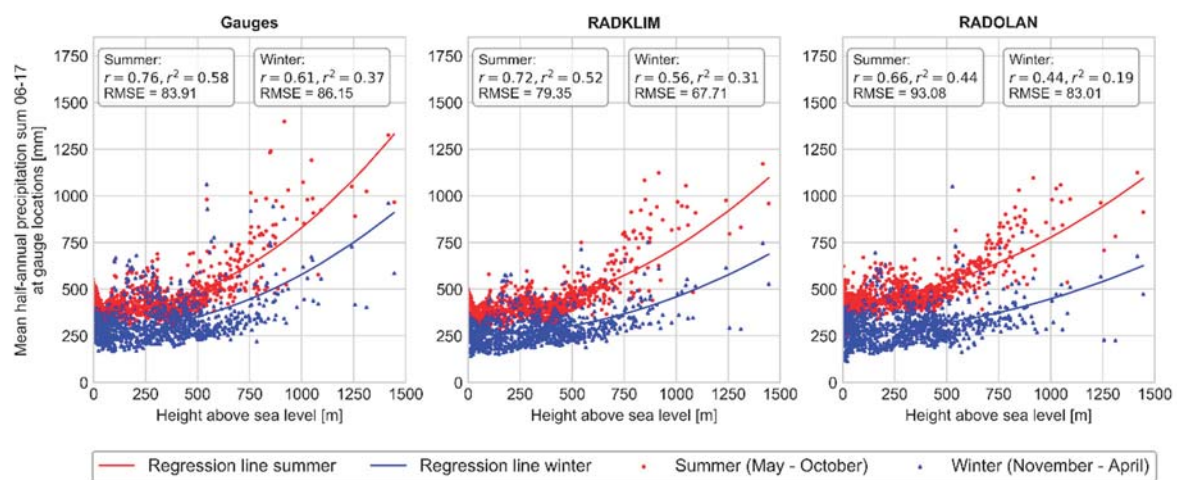
Figure 7. Quadratic regression between seasonal precipitation sums and altitude for gauges (**left plot**), RADKLIM (**centre**) and RADOLAN (**right**).

The impact of the distance from the radar was assessed using the MAP ratios between the radar products and the gauges since these are independent from the actual precipitation amounts. The regression analysis (see Figure 8) showed a significant difference between RADKLIM and RADOLAN in terms of attenuation correction. The RADOLAN/gauge ratio decreases considerably with increasing distance from the next radar. The turning point from a predominantly positive to a predominantly negative ratio is located at an approximately 70 km distance from the radar. Besides some extreme outliers close to the radars, an additional drop of the ratio beyond about 120 km distance from the radar became apparent. In order to assess the impact of the larger radius used for RADOLAN, we removed all 19 value pairs beyond a 128 km distance from the radar and recalculated the regression (not shown). The slope of the recalculated regression line ($y = 1.1214 - 0.000015x$) differed only slightly from the original regression using the entire value range. The coefficient of determination decreased to $r^2 = 0.11$ and the turning point from predominantly positive to predominantly negative values shifted to an about 80 km distance from the radar. Thus, the larger radius for RADOLAN does have a slight impact on the decrease of radar rainfall at far ranges from the radar, but this decrease is governed by a systematic bias in the RADOLAN data. In contrast to this, with a coefficient of determination of $r^2 = 0.01$, the RADKLIM/gauge ratio shows no correlation at all to the distance from the radar. Instead, independently from the distance to the radar, the ratio averages almost constantly at about 0.91. Consequently, the additional attenuation correction algorithms developed for the radar climatology in conjunction with the decrease of the radar radius to 128 km led to a significant improvement in data quality.

Improving Usability of Weather Radar Data in Environmental Sciences: Potentials, Challenges, Uncertainties and Applications   J. Kreklow

*Atmosphere* **2020**, *11*, 217
12 of 19

Figure 8. Linear regression between the distance from the next radar and the RADKLIM/gauge MAP ratio (**left plot**) as well as the RADOLAN/gauge MAP ratio (**right plot**).

3.4. Rainfall Detection Rates, Heavy Rainfall Days and Rainfall Intensities

In the summer half-year, RADKLIM and RADOLAN detected more days with rainfall > 1 mm than in winter, whereas the gauge dataset showed very little difference between seasons in terms of count and average precipitation (see Figure 9, left). In RADKLIM, however, the mean precipitation per rainy day is almost 40% higher in summer than in winter, which, again, indicates an underestimation of winter precipitation. RADOLAN showed the highest count in both seasons but by far the lowest precipitation average, especially in summer. On the one hand, this is due to the clutter in the first years of the time series, which are characterized by frequent weak radar echoes caused by, for example, wind energy plants, that are converted into many intervals with very weak precipitation. On the other hand, the count of rainfall days is influenced by the unequal completeness of the time series. While RADOLAN has very few NoData intervals due to the filling of gaps with interpolated data, RADKLIM has the clearly outlined gaps caused by the reduction of the radar radius. The gauge dataset suffers additionally from a relatively incomplete time series due to frequent changes in the gauge network. For a more detailed discussion of the reasons for the much higher number of missing data in the rain gauge dataset, which becomes apparent in Figure 10, please refer to [47].
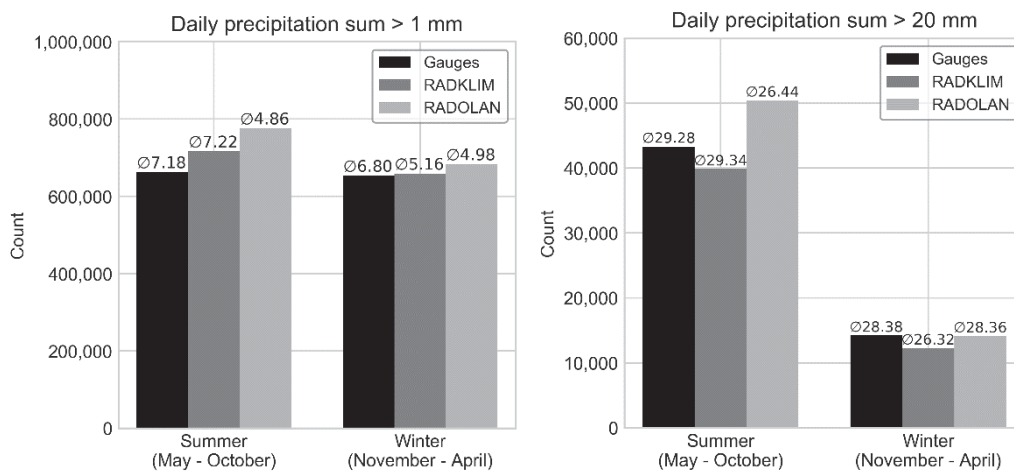
Figure 9. Number of days with precipitation amounts >1 mm (**left plot**) and >20 mm (**right plot**) in summer and winter half-years for gauges, RADKLIM and RADOLAN data. The numbers above the bars indicate the average daily precipitation sum of all days exceeding the respective threshold.
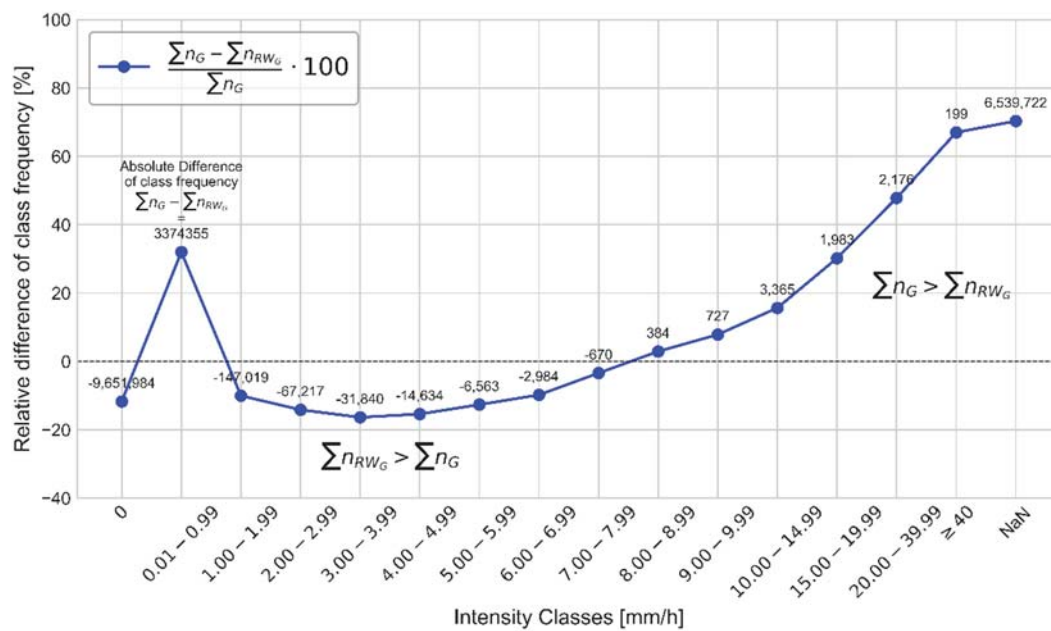
Figure 10. Difference of intensity class frequency between all point-pixel data pairs (n = 997) of the period 2006–2017 of gauge data (n_G) and RADKLIM RW product (n_{RW_G}).

The analysis of heavy rainfall days (see Figure 9, right) showed, as expected, much higher counts in the summer half-year, during which more small-scale convective heavy rainfall events add to large-scale frontal systems that occur throughout the entire year. More surprisingly, the mean precipitation per heavy rainfall day is largely similar between all datasets as well as between seasons. However, despite the almost identical average precipitation in summer and the lower NoData count, RADKLIM counted fewer heavy rainfall days than the gauge dataset. This can be partly explained by the distribution of hourly rainfall intensities (see Figure 10) and the related differences in spatial scale of both measurement methods. In the intensity classes between 1 and 8 mm, more intervals were recorded in RADKLIM than in the gauge dataset. On the one hand, chances are higher that rainfall occurs anywhere within the air column above the 1 km^2 area of the radar pixel than within the 200 cm^2 small opening of the gauge. On the other hand, this is a logical consequence of the higher NaN count of the gauges, which lack rainfall intervals in return. The divergent ratio for the lowest class < 1 mm can most likely be attributed to an erroneous filtering of low reflectivities during clutter correction and to a shading of light precipitation, e.g., behind other rainfall cells. However, in the classes ≥ 8 mm, the gauges contained more intervals and there was a constantly increasing difference between the datasets.

It has to be mentioned that, despite careful data cleaning, the gauge data might still contain several values representing aggregations of longer time periods due to temporary malfunctions of the gauges. This could slightly overemphasize the difference between datasets for the high intensity classes, but the amount of questionable values is too small to bias the overall distribution in a significant way. Instead, the latter results from the difference in measurements scales and methods. While the radar covers a larger area, the final value of the pixel actually represents the average precipitation of the entire 1 km^2 pixel area. Consequently, the different spatial measurement scales inevitably cause deviations between the recorded precipitation intensities. The chance to detect precipitation is higher within the radar pixel, but the averaging of the larger area is likely to cause a lower intensity compared to the gauges. In addition, especially for heavy rainfall events, the radar underestimates rainfall intensity due to signal loss behind heavy rainfall cells. According to [27], the underestimation caused by path-integrated rainfall-induced attenuation along the radar beam can reach a factor of three for uncorrected reflectivity during extreme rainfall events, which is hard to correct adequately.

4. Discussion

All three datasets analyzed in this study showed different advantages and disadvantages, but also positive developments throughout the last years. For example, the considerable improvements in the RADOLAN routines, especially in terms of clutter removal, have to be highlighted. An additional improvement is to be expected due to the polarimetric information added to the precipitation estimation procedure since October 2017, which could not be addressed in this study. Dual-polarised Doppler radar systems allow a better distinction between meteorological and non-meteorological signals (e.g., insects, birds, airplanes, buildings, terrain) and help to classify different hydrometeor types such as raindrops, hail and snow [21,54]. On the one hand, since RADOLAN is an operational QPE product for which time series consistency is not a primary issue, it allows a steady implementation of new technologies and research results. On the other hand, features such as the attenuation correction and additional disaggregated gauge data for adjustment, which require long-term observations and need to be applied retrospectively, cannot be implemented into the RADOLAN routines. Consequently, for operational applications related to heavy rainfall and flood monitoring, precipitation nowcasting, and also as input data for Numerical Weather Prediction, which all require spatially highly resolved, near real-time information, the latest RADOLAN data are undoubtedly a good choice. Still, a certain underestimation of precipitation quantity has to be taken into account when using recent RADOLAN data. However, RADOLAN is not suited for climatological applications and aggregated precipitation statistics, due to the very inconsistent time series and the extreme uncertainties in quantitative precipitation estimations in the first years of the time series.

RADKLIM has been developed in order to provide a longer and largely consistent time series next to the operational data, which can, in return, not profit to the same extent as RADOLAN from recent technological developments since the Dual-Pol information is not available for large portions of the time series. The most striking result concerning RADKLIM's data quality is the universal underestimation of precipitation, which is evident at all analyzed temporal scales. RADKLIM underestimates the mean annual precipitation sum by about 7.9% (9.1% for gauge-pixel pairs) compared to the gauges and shows fewer hourly intervals of high intensity than the gauge dataset. Only about 0.3 percentage points of the MAP underestimation can be attributed to the radar gaps due to the reduced radius, so that there is quite a systematic negative bias in the data. Most other studies on radar-based QPE evaluations also revealed underestimations of precipitation totals [9,55–58], but a few authors reported an overestimation [56,59]. However, such results are hard to compare due to large differences in radar hardware, correction algorithms and evaluation methods in the studies. Still, the observed underestimation is rather surprising since a lot emphasis was laid on the correction of attenuation and spokes during the development of RADKLIM, which should, in theory, reduce underestimation and increase precipitation sums. Regarding attenuation, spokes and orographic precipitation, our analyses showed significant improvements, which should indicate an increase in precipitation depth. Nevertheless, the RADKLIM MAP is considerably lower than the RADOLAN MAP throughout the entire study period and the RADKLIM/RADOLAN ratio (see Figure 6) revealed that RADKLIM suffers from an almost ubiquitous negative bias, which is particularly pronounced at close range from the radar. Supported by the very low number of RADKLIM intervals between 0.1 and 1 mm/h (see Figure 10), these findings suggest that low reflectivity signals might be overcorrected and, hence, light rainfall is likely to be suppressed by the RADKLIM routines. In addition, high intensity rainfall is also underestimated, most likely due to the averaging of the pixel area and path-integrated rainfall-induced attenuation. The latter effect is very hard to account for sufficiently during reanalysis because it varies strongly in space and time. As a consequence, the RADKLIM data show many improvements concerning typical radar-related errors, but in return, new errors were induced that offset the positive developments at least to some degree. Regarding the degree of underestimation, however, it has to be noted that, especially with a higher prevalence of snow, the weighing gauge type used by DWD also tends to underestimate precipitation sums due to wind drift [60,61]. Taking this into account,

the underestimation of the actual precipitation by the radar products is most likely to be even higher than shown in the analyses.

Depending on the application the radar data is intended to be used for, the underestimation may need to be corrected. For erosion modelling, Fischer et al. [33] already suggested correction factors to account for different methods and spatiotemporal scales. More research on this topic and evaluation studies will be needed in order to further increase the usability of radar data and the reliability and transferability of such correction approaches.

An additional distortion and challenge for the usage of the German radar products arises from the custom polar-stereographic projection, which is used for the datasets. This custom projection is equal of angle while focusing on the North Pole, which is quite unusual for the spatial representation of Germany. Problems occur, when radar composite data are combined with geodata in official projections in GIS such as Digital Elevation Models (DEM) or land use data. Official coordinate systems, like ETRS89, UTM or Gauss–Krüger, are based on a transverse Mercator projection with a Cartesian coordinate grid. Transformations of polar stereographic radar data into Cartesian grids lead to rectangular cells with raster widths of e.g., 944 m horizontally and 955 m vertically. Blending such outcomes with quadratic raster data, e.g., DEM, leads to unavoidable three-dimensional distortions and loss of information. Comprehensive reprojection of the RADKLIM cells on a vector basis at high spatial resolution, including subsequent assignment of the radar data by zonal statistics, is then required to minimize the loss of value and spatial offset.

Despite the shortcomings and uncertainties discussed above, the high spatiotemporal resolution and nationwide coverage of RADKLIM and RADOLAN are major advantages over the point-scale resolution of gauges, which have a disputable spatial representativity especially for capturing local small-scale precipitation events. On the one hand, this high resolution of the radar datasets comes along with large data volumes and challenges in efficient processing of the proprietary binary data files used by DWD. On the other hand, the uniform, centralized dataset derivation of the radar climatology implies a high spatial and temporal consistency, completeness, reliability and documentation, whereas documentation on the gauge data is very insufficient and metadata are distributed over many different files. Consequently, a proper data quality check to account for erroneous entries in the gauge data becomes a very time-consuming task, which is unspecified in most studies using rain gauge data. Moreover, emerging open source software projects help to overcome the challenge of processing and visualizing the radar composite data [48].

Finally, it has to be noted that the direct comparison of radar and gauge data inevitably leads to discrepancies because of the different measurement methods and scales explained above. Moreover, both radar datasets and the gauge data are not entirely independent since some of the gauges are used for adjustment. Both limitations were accepted by the authors due to a lack of representative alternative data for evaluation. Further, more independent approaches for data evaluation and the impacts of the identified errors could include hydrological rainfall-runoff modelling and validation using discharge measurements. However, modelling also inevitably introduces new uncertainties related to model parameterization and input data resolution and quality [62].

5. Conclusions

In this study, the German radar-based QPE products RADOLAN and RADKLIM were compared and evaluated against rain gauge data in order to assess their inherent bias and errors and to assess their recent developments, differences and potentials. With regard to the research questions posed for this study, the key outcomes can be summarized as follows:

1. The modifications in the radar hardware network as well as changes in the RADOLAN processing routines are clearly visible in the RADOLAN time series and lead to a successive increase in data reliability. Clutter and extreme high outliers could be reduced significantly especially since 2010, whereas the quantification of orographic precipitation and range-dependent attenuation remain

major error sources. All in all, this causes a decrease in precipitation totals throughout the rather inconsistent RADOLAN time series.

2. The additional correction algorithms implemented for RADKLIM lead to a much more plausible spatial distribution of precipitation totals compared to RADOLAN. RADKLIM shows much fewer typical radar artefacts, an improved representation of orography with the greatest changes during the winter half-year and an efficient correction of range-dependent path-integrated attenuation at longer time scales. However, the latter improvement comes along with a reduced radar radius, which causes several temporary gaps during hardware updates in the otherwise consistent dataset. Moreover, despite the very positive developments in mapping the spatial precipitation distribution, there is an overall negative bias in the RADKLIM precipitation totals, which might be caused by overcorrection of low reflectivities and an underestimation of high intensity rainfall due to spatial averaging and rainfall-induced attenuation of the radar beam.

3. The high spatiotemporal resolution of the radar QPEs is a crucial advantage over the point-scale rain gauge data. Certainly, the higher resolution and spatial coverage require a more automated and efficient data processing approach, but first software solutions for this have already been developed by the radar user community. Moreover, the good documentation of the radar data and, in the case of RADKLIM also the high degree of consistency regarding hardware and data processing, increase their reliability compared to the sparsely documented gauge data, which require a thorough treatment of data gaps and erroneous values. In order to combine RADKLIM data more easily with official geodata, a projection should be sought that can be transformed into official projection systems, e.g., ETRS89, free of distortion and loss of value. This should be done in the framework of future reanalysis runs by DWD.

Certainly, users need to be aware of the outlined weaknesses of the radar-based QPEs in order to interpret their results properly. However, radar QPE products are the precipitation data with the highest spatiotemporal resolution for Germany. In addition to the high degree of consistency and the time series reaching a length that starts to become eligible for climatological analyses, this makes the radar climatology a very promising dataset for various applications.

References

1. Global Climate Observing System (GCOS). *The Global Observing System for Climate: Implementation Needs*; WMO-Pub GCOS-200; GCOS: Geneva, Switzerland, 2016; Available online: https://unfccc.int/sites/default/files/gcos_ip_10oct2016.pdf (accessed on 14 February 2019).

2. Kidd, C.; Becker, A.; Huffman, G.J.; Muller, C.L.; Joe, P.; Skofronick-Jackson, G.; Kirschbaum, D.B. So, how much of the Earth's surface is covered by rain gauges? *Bull. Am. Meteorol. Soc.* **2017**, *98*, 69–78. [CrossRef] [PubMed]

3. Lochbihler, K.; Lenderink, G.; Siebesma, A.P. The spatial extent of rainfall events and its relation to precipitation scaling. *Geophys. Res. Lett.* **2017**, *44*, 8629–8636. [CrossRef]

4.   Sun, X.; Mein, R.G.; Keenan, T.D.; Elliott, J.F. Flood estimation using radar and raingauge data. *J. Hydrol.* **2000**, *239*, 4–18. [CrossRef]

5.   Thorndahl, S.; Einfalt, T.; Willems, P.; Nielsen, J.E.; ten Veldhuis, M.-C.; Arnbjerg-Nielsen, K.; Rasmussen, M.R.; Molnar, P. Weather radar rainfall data in urban hydrology. *Hydrol. Earth Syst. Sci.* **2017**, *21*, 1359–1380. [CrossRef]

6.   Villarini, G.; Mandapaka, P.V.; Krajewski, W.F.; Moore, R.J. Rainfall and sampling uncertainties: A rain gauge perspective. *J. Geophys. Res.* **2008**, *113*. [CrossRef]

7.   Abon, C.C.; Kneis, D.; Crisologo, I.; Bronstert, A.; David, C.P.C.; Heistermann, M. Evaluating the potential of radar-based rainfall estimates for streamflow and flood simulations in the Philippines. *Geomat. Nat. Hazards Risk* **2015**, *7*, 1390–1405. [CrossRef]

8.   Cole, S.J.; Moore, R.J. Hydrological modelling using raingauge- and radar-based estimators of areal rainfall. *J. Hydrol.* **2008**, *358*, 159–181. [CrossRef]

9.   Hazenberg, P.; Leijnse, H.; Uijlenhoet, R. Radar rainfall estimation of stratiform winter precipitation in the Belgian Ardennes. *Water Resour. Res.* **2011**, *47*, 257. [CrossRef]

10. Jessen, M.; Einfalt, T.; Stoffer, A.; Mehlig, B. Analysis of heavy rainfall events in North Rhine–Westphalia with radar and raingauge data. *Atmos. Res.* **2005**, *77*, 337–346. [CrossRef]

11. Kitchen, M.; Blackall, R.M. Representativeness errors in comparisons between radar and gauge measurements of rainfall. *J. Hydrol.* **1992**, *134*, 13–33. [CrossRef]

12. Meißner, D.; Gebauer, S.; Schumann, A.H.; Pahlow, M.; Rademacher, S. Analyse radarbasierter Niederschlagsprodukte als Eingangsdaten verkehrsbezogener Wasserstandsvorhersagen am Rhein. *Hydrol. Und Wasserbewirtsch. Hywa* **2012**, *56*, 16–28.

13. Seo, B.-C.; Krajewski, W.F. Scale Dependence of Radar Rainfall Uncertainty: Initial Evaluation of NEXRAD's New Super-Resolution Data for Hydrologic Applications. *J. Hydrometeor* **2010**, *11*, 1191–1198. [CrossRef]

14. Satgé, F.; Ruelland, D.; Bonnet, M.-P.; Molina, J.; Pillco, R. Consistency of satellite-based precipitation products in space and over time compared with gauge observations and snow- hydrological modelling in the Lake Titicaca region. *Hydrol. Earth Syst. Sci.* **2019**, *23*, 595–619. [CrossRef]

15. Crisologo, I.; Warren, R.; Mühlbauer, K.; Heistermann, M. Enhancing the consistency of spaceborne and ground-based radar comparisons by using quality filters. *Atmos. Meas. Tech. Discuss.* **2018**, 1–20. [CrossRef]

16. Ramsauer, T.; Weiß, T.; Marzahn, P. Comparison of the GPM IMERG Final Precipitation Product to RADOLAN Weather Radar Data over the Topographically and Climatically Diverse Germany. *Remote Sens.* **2018**, *10*, 2029. [CrossRef]

17. Pejcic, V.; Tromel, S.; Muhlbauer, K.; Saavedra, P.; Beer, J.; Simmer, C. Synergy of GPM and ground-based radar observations for precipitation estimation and detection of microphysical processes. *Int. Radar Symp.* **2018**, 1–8.

18. Pejcic, V.; Saavedra Garfias, P.; Mühlbauer, K.; Troemel, S.; Simmer, C. *Evaluation of Germany's network radar Composite Rain Producs with GPM Near Surface Precipitation Estimations*; Earth and Space Science Open Archive: San Francisco, CA, USA, 2019.

19. Gilewski, P.; Nawalany, M. Inter-Comparison of Rain-Gauge, Radar, and Satellite (IMERG GPM) Precipitation Estimates Performance for Rainfall-Runoff Modeling in a Mountainous Catchment in Poland. *Water* **2018**, *10*, 1665. [CrossRef]

20. Kidd, C.; Bauer, P.; Turk, J.; Huffman, G.J.; Joyce, R.; Hsu, K.-L.; Braithwaite, D. Intercomparison of High-Resolution Precipitation Products over Northwest Europe. *J. Hydrometeor* **2012**, *13*, 67–83. [CrossRef]

21. Berne, A.; Krajewski, W.F. Radar for hydrology: Unfulfilled promise or unrecognized potential? *Adv. Water Resour.* **2013**, *51*, 357–366. [CrossRef]

22. Kidd, C.; Levizzani, V. Status of satellite precipitation retrievals. *Hydrol. Earth Syst. Sci.* **2011**, *15*, 1109–1116. [CrossRef]

23. Keupp, L.; Winterrath, T.; Hollmann, R. *Use of Weather Radar Data for Climate Data Records in WMO Regions IV and VI*; WMO: Geneva, Switzerland, 2017.

24. Overeem, A.; Holleman, I.; Buishand, A. Derivation of a 10-Year Radar-Based Climatology of Rainfall. *J. Appl. Meteor. Climatol.* **2009**, *48*, 1448–1463. [CrossRef]

25. Bartels, H.; Weigl, E.; Reich, T.; Lang, W.; Wagner, A.; Kohler, O.; Gerlach, N. *MeteoSolutions GmbH: Projekt RADOLAN—Routineverfahren zur Online-Aneichung der Radarniederschlagsdaten Mit Hilfe Von Automatischen Bodenniederschlagsstationen (Ombrometer)*; Zusammenfassender Abschlussbericht für die Projektlaufzeit von 1997 bis 2004; DWD: Offenbach, Germany, 2004.
26. Hänsel, P.; Kaiser, A.; Buchholz, A.; Böttcher, F.; Langel, S.; Schmidt, J.; Schindewolf, M. Mud Flow Reconstruction by Means of Physical Erosion Modeling, High-Resolution Radar-Based Precipitation Data, and UAV Monitoring. *Geosciences* **2018**, *8*, 427. [CrossRef]
27. Bronstert, A.; Agarwal, A.; Boessenkool, B.; Crisologo, I.; Fischer, M.; Heistermann, M.; Köhn-Reich, L.; López-Tarazón, J.A.; Moran, T.; Ozturk, U.; et al. Forensic hydro-meteorological analysis of an extreme flash flood: The 2016-05-29 event in Braunsbach, SW Germany. *Sci. Total Environ.* **2018**, 977–991. [CrossRef] [PubMed]
28. Johann, G.; Ott, B.; Treis, A. Einfluss von terrestrisch gemessenen und radarbasierten Niederschlagsdaten auf die Qualität der Hochwasservorhersage. *Korresp. Wasserwirtsch.* **2009**, *9*, 487–493.
29. Fischer, F.; Hauck, J.; Brandhuber, R.; Weigl, E.; Maier, H.; Auerswald, K. Spatio-temporal variability of erosivity estimated from highly resolved and adjusted radar rain data (RADOLAN). *Agric. For. Meteorol.* **2016**, *223*, 72–80. [CrossRef]
30. Fischer, F.K.; Kistler, M.; Brandhuber, R.; Maier, H.; Treisch, M.; Auerswald, K. Validation of official erosion modelling based on high-resolution radar rain data by aerial photo erosion classification. *Earth Surf. Process. Landf.* **2018**, *43*, 187–194. [CrossRef]
31. Winterrath, T.; Brendel, C.; Junghänel, T.; Klameth, A.; Lengfeld, K.; Walawender, E.; Weigl, E.; Hafer, M.; Becker, A. An overview of the new radar-based precipitation climatology of the Deutscher Wetterdienst—Data, methods, products. In Proceedings of the UrbanRain18, 11th International Workshop on Precipitation in Urban Areas, Urban Areas, Zürich, Switzerland, 5–7 December 2018.
32. Lengfeld, K.; Winterrath, T.; Junghänel, T.; Becker, A. Characteristic spatial extent of rain events in Germany from a radar-based precipitation climatology. In Proceedings of the UrbanRain18, 11th International Workshop on Precipitation in Urban Areas, Urban Areas, Zürich, Switzerland, 5–7 December 2018.
33. Fischer, F.K.; Winterrath, T.; Auerswald, K. Temporal- and spatial-scale and positional effects on rain erosivity derived from point-scale and contiguous rain data. *Hydrol. Earth Syst. Sci.* **2018**, *22*, 6505–6518. [CrossRef]
34. Auerswald, K.; Fischer, F.K.; Winterrath, T.; Brandhuber, R. Rain erosivity map for Germany derived from contiguous radar rain data. *Hydrol. Earth Syst. Sci.* **2019**, *23*, 1819–1832. [CrossRef]
35. Deutscher Wetterdienst Open Data Portal. Historische Stündliche RADOLAN-Raster der Niederschlagshöhe (Binär). Available online: https://opendata.dwd.de/climate_environment/CDC/grids_germany/hourly/radolan/historical/bin/ (accessed on 7 October 2019).
36. Weigl, E. RADOLAN Information Nr. 13. Available online: https://www.dwd.de/DE/leistungen/radolan/radolan_info/radolan_info_nr_13.pdf?__blob=publicationFile&v=3 (accessed on 8 October 2019).
37. Weigl, E. RADOLAN Information Nr. 15. Available online: https://www.dwd.de/DE/leistungen/radolan/radolan_info/radolan_info_nr_15.pdf?__blob=publicationFile&v=3 (accessed on 8 October 2019).
38. Weigl, E.; Winterrath, T. Radargestützte Niederschlagsanalyse und—Vorhersage (RADOLAN, RADVOR-OP). *Promet* **2009**, *35*, 78–86.
39. Weigl, E. RADOLAN-Information Nr. 17. Available online: https://www.dwd.de/DE/leistungen/radolan/radolan_info/radolan_info_nr_17.pdf?__blob=publicationFile&v=3 (accessed on 17 June 2019).
40. Stephan, K. Erfahrungsbericht zur Verwendung des PULL-Kompositverfahrens zur Erstellung des Radolan-Komposits (RZ-Komposit). 2007; Unpublished work.
41. Weigl, E. RADOLAN-Information Nr. 41. Available online: https://www.dwd.de/DE/leistungen/radolan/radolan_info/radolan_info_nr_41.pdf;jsessionid=65C71E4F45253E6B3CE3F24F443D3E2B.live11044?__blob=publicationFile&v=2 (accessed on 17 December 2019).
42. Weigl, E. RADOLAN-Information Nr. 45. Available online: https://www.dwd.de/DE/leistungen/radolan/radolan_info/radolan_info_nr_45.pdf;jsessionid=65C71E4F45253E6B3CE3F24F443D3E2B.live11044?__blob=publicationFile&v=3 (accessed on 17 December 2019).
43. Winterrath, T.; Brendel, C.; Hafer, M.; Junghänel, T.; Klameth, A.; Lengfeld, K.; Walawender, E.; Weigl, E.; Becker, A. Radar Climatology (RADKLIM) Version 2017.002 (RW). Gridded Precipitation Data for Germany; Available online: https://opendata.dwd.de/climate_environment/CDC/grids_germany/hourly/radolan/reproc/2017_002/bin (accessed on 25 June 2019).

44. Winterrath, T.; Brendel, C.; Hafer, M.; Junghänel, T.; Klameth, A.; Lengfeld, K.; Walawender, E.; Weigl, E.; Becker, A. Radar Climatology (RADKLIM) Version 2017.002 (YW). Gridded Precipitation Data for Germany; Available online: https://opendata.dwd.de/climate_environment/CDC/grids_germany/5_minutes/radolan/reproc/2017_002/bin/ (accessed on 25 June 2019).

45. Winterrath, T.; Brendel, C.; Hafer, M.; Junghänel, T.; Klameth, A.; Walawender, E.; Weigl, E.; Becker, A. Erstellung Einer Radargestützten Niederschlagsklimatologie. Berichte des Deutschen Wetterdienstes No. 251; 2017; Available online: https://www.dwd.de/DE/leistungen/pbfb_verlag_berichte/pdf_einzelbaende/251_pdf.pdf?__blob=publicationFile&v=2 (accessed on 29 March 2019).

46. Deutscher Wetterdienst Open Data Portal. Rain Gauge Precipitation Observations in 1-Minute Resolution. Available online: https://opendata.dwd.de/climate_environment/CDC/observations_germany/climate/1_minute/precipitation/ (accessed on 10 January 2019).

47. Kreklow, J.; Tetzlaff, B.; Kuhnt, G.; Burkhard, B. A Rainfall Data Intercomparison Dataset of RADKLIM, RADOLAN, and Rain Gauge Data for Germany. *Data* **2019**, *4*, 118. [CrossRef]

48. Kreklow, J. Facilitating radar precipitation data processing, assessment and analysis: A GIS-compatible python approach. *J. Hydroinformatics* **2019**, *21*, 652–670. [CrossRef]

49. Kreklow, J. *Radproc—A Gis-Compatible Python-Package for Automated Radolan Composite Processing and Analysis*; Zenodo: Geneva, Switzerland, 2018; Available online: https://zenodo.org/record/2539441 (accessed on 25 June 2019).

50. Kreklow, J.; Tetzlaff, B.; Kuhnt, G.; Burkhard, B. *A Rainfall Data Inter-Comparison Dataset for Germany: Version 1.0*; Zenodo: Geneva, Switzerland, 2019; Available online: https://zenodo.org/record/3262172 (accessed on 29 June 2019).

51. Tukey, J. *Exploratory Data Analysis*; Addison-Wesley: Boston, MA, USA, 1977.

52. Deutscher Wetterdienst. *Jahresrückblick 2007 des Deutschen Wetterdienstes. Gefährliche Wetterereignisse Und Wetterschäden in Deutschland*; Offenbach am Main: Offenbach, Germany, 2007.

53. Deutscher Wetterdienst. Jahresbericht 2016. 2017. Available online: https://www.dwd.de/DE/leistungen/jahresberichte_dwd/jahresberichte_pdf/jahresbericht_2016.pdf?__blob=publicationFile&v=3 (accessed on 18 December 2019).

54. Grazioli, J.; Tuia, D.; Berne, A. Hydrometeor classification from polarimetric radar measurements: A clustering approach. *Atmos. Meas. Tech.* **2015**, *8*, 149–170. [CrossRef]

55. Goudenhoofdt, E.; Delobbe, L. Generation and Verification of Rainfall Estimates from 10-Yr Volumetric Weather Radar Measurements. *J. Hydrometeor* **2016**, *17*, 1223–1242. [CrossRef]

56. Fairman, J.G.; Schultz, D.M.; Kirshbaum, D.J.; Gray, S.L.; Barrett, A.I. A radar-based rainfall climatology of Great Britain and Ireland. *Weather* **2015**, *70*, 153–158. [CrossRef]

57. Smith, J.A.; Baeck, M.L.; Villarini, G.; Welty, C.; Miller, A.J.; Krajewski, W.F. Analyses of a long-term, high-resolution radar rainfall data set for the Baltimore metropolitan region. *Water Resour. Res.* **2012**, *48*, 616. [CrossRef]

58. Schleiss, M.; Olsson, J.; Berg, P.; Niemi, T.; Kokkonen, T.; Thorndahl, S.; Nielsen, R.; Nielsen, J.E.; Bozhinova, D.; Pulkkinen, S. The Accuracy of Weather Radar in Heavy Rain: A Comparative study for Denmark, the Netherlands, Finland and Sweden. *Hydrol. Earth Syst. Sci. Discuss.* **2019**, 1–42. [CrossRef]

59. Marra, F.; Morin, E. Use of radar QPE for the derivation of Intensity–Duration–Frequency curves in a range of climatic regimes. *J. Hydrol.* **2015**, *531*, 427–440. [CrossRef]

60. Boudala, F.S.; Isaac, G.A.; Filman, P.; Crawford, R.; Hudak, D.; Anderson, M. Performance of Emerging Technologies for Measuring Solid and Liquid Precipitation in Cold Climate as Compared to the Traditional Manual Gauges. *J. Atmos. Ocean. Technol.* **2017**, *34*, 167–185. [CrossRef]

61. Kochendorfer, J.; Rasmussen, R.; Wolff, M.; Baker, B.; Hall, M.E.; Meyers, T.; Landolt, S.; Jachcik, A.; Isaksen, K.; Brækkan, R.; et al. The quantification and correction of wind-induced precipitation measurement errors. *Hydrol. Earth Syst. Sci.* **2017**, *21*, 1973–1989. [CrossRef]

62. Heistermann, M.; Kneis, D. Benchmarking quantitative precipitation estimation by conceptual rainfall-runoff modeling. *Water Resour. Res.* **2011**, *47*, 301. [CrossRef]

5

Comparing Rainfall Erosivity Estimation Methods Using Weather Radar Data for the State of Hesse (Germany)

J. Kreklow, B. Steinhoff-Knopp, K. Friedrich, B. Tetzlaff

water

MDPI

Article

Comparing Rainfall Erosivity Estimation Methods Using Weather Radar Data for the State of Hesse (Germany)

Jennifer Kreklow [1,*] **, Bastian Steinhoff-Knopp** [1] **, Klaus Friedrich** [2] **and Björn Tetzlaff** [3]

[1]   Institute of Physical Geography and Landscape Ecology, Leibniz Universität Hannover, Schneiderberg 50, 30167 Hannover, Germany; steinhoff-knopp@phygeo.uni-hannover.de

[2]   Hessian Agency for Nature Conservation, Environment and Geology, 65203 Wiesbaden, Germany; klaus.friedrich@hlnug.hessen.de

[3]   Institute of Bio- and Geosciences IBG-3, Forschungszentrum Jülich GmbH, 52425 Jülich, Germany; b.tetzlaff@fz-juelich.de

*   Correspondence: kreklow@phygeo.uni-hannover.de; Tel.: +49-511-762-19798

check for
updates

Abstract: Rainfall erosivity exhibits a high spatiotemporal variability. Rain gauges are not capable of detecting small-scale erosive rainfall events comprehensively. Nonetheless, many operational instruments for assessing soil erosion risk, such as the erosion atlas used in the state of Hesse in Germany, are still based on spatially interpolated rain gauge data and regression equations derived in the 1980s to estimate rainfall erosivity. Radar-based quantitative precipitation estimates with high spatiotemporal resolution are capable of mapping erosive rainfall comprehensively. In this study, radar climatology data with a spatiotemporal resolution of 1 km^2 and 5 min are used alongside rain gauge data to compare erosivity estimation methods used in erosion control practice. The aim is to assess the impacts of methodology, climate change and input data resolution, quality and spatial extent on the R-factor of the Universal Soil Loss Equation (USLE). Our results clearly show that R-factors have increased significantly due to climate change and that current R-factor maps need to be updated by using more recent and spatially distributed rainfall data. Radar climatology data show a high potential to improve rainfall erosivity estimations, but uncertainties regarding data quality and a need for further research on data correction approaches are becoming evident.

1. Introduction

The R-factor is a measure of rainfall erosivity and an important input variable for estimating soil losses by water using the Universal Soil Loss Equation (USLE) and its many variations [1]. Based on the documented relationship between the amount of soil erosion and the kinetic energy of precipitation, the rainfall erosivity can be derived directly from temporally highly resolved precipitation time series [1–3]. The R-factor of one event is defined as the product of the kinetic energy and the maximum 30-min intensity of an erosive rainfall event. The R-factors of all events throughout a year are added to obtain the annual R-factor, which is usually averaged over a period of at least ten years as an input to the USLE.

In the past, measurement data from rain gauges or, more recently, from automated rain gauges were used for estimating rainfall erosivity. Still today, the R-factors calculated from these point-scale data for every station are spatially interpolated to derive maps of rainfall erosivity. This approach has also been recently applied to generate a European erosivity map [4]. However, due to the small spatial

extent of convective precipitation cells and a high variability of precipitation intensity within these cells, which contributes significantly to rainfall erosivity, the spatial recording of the rainfall erosivity is incomplete and patchy [5]. Rain gauges are not capable of detecting the spatial distribution of local heavy rainfall hot spots or individual heavy rainfall events, which are highly relevant for erosion modelling. Interpolating R-factors calculated from point measurements therefore results in a smoothing and an underestimation of erosivity [6]. In order to capture the highly variable spatiotemporal distribution of rainfall intensity during erosive rainfall events, highly resolved precipitation data, both spatial and temporal, are needed. Weather radars are capable of providing such data, but the number of studies deriving erosivity directly from such highly resolved datasets is still rather low [4].

In practice, R-factor maps are frequently derived by regression equations from spatially interpolated summer precipitation sums or annual precipitation sums in order to obtain comprehensive erosivity information. This methodology is much easier to apply than the direct event-based derivation of the R-factor from gauge data, but it suffers from representativity issues. Again, data smoothing by spatial interpolation and regression equations lead to smoothed R-factors. High R-factors often remain limited to mountain tops, while the actual occurrence of heavy rainfall as a consequence of convective events in the lowlands is not taken into account [7].

In Germany, for instance, the R-factor is derived by regional authorities for each federal state according to the technical standard DIN 19708 [8], whereby most federal states use regional adjusted regression equations. The derived erosivity maps serve inter alia as an input for soil erosion modelling in order to evaluate the fulfilment of EU Cross-Compliance soil protection regulations. Based on these evaluation outcomes, income support for farmers is calculated and requirements for erosion control are imposed. However, the applied regression equations were usually derived based on data from a few rain gauge recorders (usually < 20) integrating rainfall data from the 1960s to the 1980s [9]. The regression equations are only rarely updated (e.g., in North-Rhine Westfalia [10]) or, in many federal states, not at all. However, several studies indicate spatial and temporal changes in precipitation distribution and quantities as well as an increase and intensification of heavy rainfall and thus an increase in precipitation erosivity due to climate change [6,11,12]. Consequently, the validity of the currently applied regression equations, which were determined based on precipitation data of the last climate period or even older data, must also be questioned, especially in regard to the current atmospheric conditions.

In the German federal state of Hesse, a lot of information on soil quality and degradation, including the R-factor, is collected in the technical information system "Erosion Atlas Hesse" [13,14]. The erosion atlas is an important instrument for precautionary soil protection in Hesse since it shows areas with a high risk of erosion and helps farmers to plan erosion control measures. Furthermore, it supports urban land-use planning through the identification of sites that require additional protection measures. The estimation of the R-factor for the erosion atlas is currently based on a regression equation derived in 1981 from data of 18 rain gauges in Bavaria, which comprise time series of up to 14 years throughout the period of 1958–1977 [9,15]. The precipitation data used for calculating the R-factor are spatially interpolated mean summer precipitation sums (May to October) for the period of 1971–2000 on a 1 km^2 grid [16]. There is evidence that rainfall distribution and intensity has changed since this time period [12,17], emphasising the need for updated precipitation datasets and methods that estimate rainfall erosivity.

The radar climatology dataset RADKLIM ("RADarKLIMatologie") [18] addresses the need for updating precipitation data. RADKLIM is a radar-based quantitative precipitation estimation dataset provided by the German Weather Service (Deutscher Wetterdienst, DWD). It is available for the whole of Germany starting from 2001 with a high spatial (1 km^2) and temporal (up to 5 min) resolution [19]. The largely comprehensive nationwide detection of all precipitation events indicates a high potential for the derivation of spatial information to calculate the R-factor. The high temporal resolution of the data as well as recent advances in computer hardware enable the direct event-based calculation of the R-factor. However, the differences in measurement method and scale between radar and rain

gauges, especially in detecting heavy rainfall, must be taken into account when interpreting the results. The precipitation totals in radar climatology tend to be slightly lower than the precipitation amounts measured by rain gauges and this underestimation by radar climatology is particularly pronounced for high precipitation intensities [20]. This is due to the averaging of precipitation over the area of the radar pixels and path-integrated rainfall-induced attenuation of the radar beam [21].

For the direct event-based calculation of the R-factor based on radar data, Fischer et al. [22] found similar effects and derived correction factors to compensate for the underestimation of the R-factor calculated with radar climatology data. The proposed factors include a spatial scaling factor, which reflects the attenuation of intensity peaks by averaging the precipitation over the radar pixel area, and a method factor, which should compensate for the systematic underestimation of erosion by the radar data compared to rain gauge measurements.

In addition, several studies have recently investigated the influence of the temporal resolution of precipitation data on the calculation of the R-factor [22,23]. In principle, the authors agree that the level of the R-factor decreases with decreasing temporal resolution. The intensity peaks, which are decisive for determining the kinetic energy of the precipitation, are detected less accurately with decreasing temporal resolution and are thus attenuated. However, authors disagree about the correction of this effect, since the level of any correction factor depends on the temporal resolution of the rainfall data that is used as a reference. Based on rain gauge and RADKLIM data for Germany, Fischer et al. [22] use one minute as the highest possible resolution for a factor value of 1. Panagos et al. [23], on the other hand, use a reference of 30 min as factor value of 1 in their European-wide study based on rain gauge data. For the RADKLIM product with a 5-min resolution, this results in a temporal correction factor of 1.05 [22] or 0.7984 [23], and for the RADKLIM product with hourly resolution, the temporal correction factors are 1.9 and 1.5597, respectively.

The goal of this study was to compare the performance of different calculation methods for the R-factor using rain gauge and radar rainfall data. The impacts, advantages, disadvantages and correction approaches for several input datasets were analysed; additionally, updated regression equations were derived. Taking the improvement in monitoring systems through a higher coverage by measurements and discrepancies concerning methodology, input data quality and resolution, observation period and correction approaches into account, the paper proposed these hypotheses for the derivation of R-factors from radar climatology and rain gauge data for the period 2001–2016:

1. The newly calculated R-factors from both datasets are higher than the R-factors from earlier calculations due to changes in climate, interannual rainfall distribution and rainfall intensity.
2. Since radar data include small-scale convective cells without gaps, the R-factors derived from the radar climatology should be higher on average than those calculated from rain gauge measurements. At the same time, the radar measurements underestimate the maximum precipitation intensities. The latter can be compensated by the correction factors according to Fischer et al. [22].
3. The spatial distribution of the R-factors derived from the radar climatology deviates from the patterns of the R-factors calculated and interpolated by means of the regression equation due to the comprehensive coverage of all heavy rainfall events.

2. Materials and Methods

2.1. Study Area

For this study, the federal state of Hesse was selected as the investigation area due to its central location within Germany and its complex terrain, which allow for a good transferability of the outcomes. The federal state of Hesse has a total area of approximately 21,115 km^2. The area is characterised by a diverse topography with several low mountain ranges and highlands crossed by depressions and river valleys (see Figure 1). The highest elevation is 950 m.a.s.l., whereas the lowest elevation is about 73 m.a.s.l. A large portion of the intensively used agricultural areas in the lowlands are

oriented in Rhenish direction (SSW-NNO) [24]. The study area is located in the humid midlatitudes in a transition zone between a maritime climate in north-western Germany and a more continental climate in the south and east of Germany. Westerly winds influence the distribution of precipitation and, thus, many of the intensively used agricultural areas are located in the rain shadow on the lee side east of the mountain ranges.
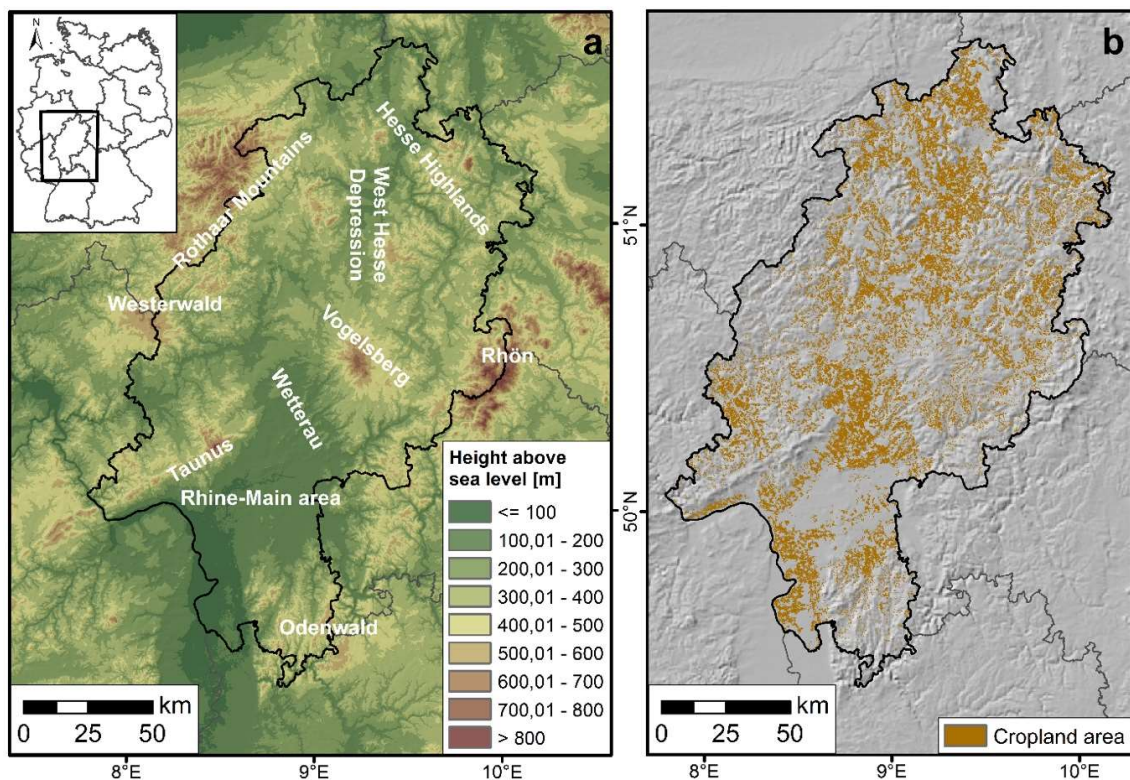
Figure 1. (**a**) Location, height above sea level [m] and selected landscape units of the federal state of Hesse, (**b**) spatial distribution of cropland areas in the study area.

2.2. Data Basis

2.2.1. Radar Climatology Data

The DWD currently operates 17 ground-based C-band weather radars. The nationwide coverage was established in 2001. In 2018, the DWD published the radar climatology dataset RADKLIM, which consists of gridded nationwide quantitative precipitation estimate composites with a spatial resolution of 1 km^2 and a temporal resolution of up to 5 min starting from 2001. For this study, we used the YW product in 5-min resolution [18] and the RW product [25] in hourly resolution for the period 2001–2016. Their derivation procedure comprises various correction algorithms to compensate for typical radar-related errors and artefacts such as clutter, spokes, signal attenuation and bright band effects. Ground clutter can be caused by non-meteorological objects such as mountains, buildings, wind energy plants or trees that disturb the radar signal and cause non-precipitation echoes. If the radar beam is blocked in whole or in part by such objects, the sector behind these obstacles is shielded, which causes a linear artefact, the so-called negative spoke. Signal attenuation may cause significant underestimation of rainfall rates. It can be caused by a wet radome, by heavy precipitation events that shield the sector behind or by range degradation at far range from the radar. Bright Band effects occur in the melting layer where the comparatively large surface of melting snowflakes is covered by a film of water, which may cause very strong radar signals.

For the derivation of the radar climatology, the reflectivity is converted to rain rates, and the local radar station data are merged and transformed to a cartesian grid. Aggregated hourly rain rates

are adjusted to ground-truth automated rain gauge measurements, which yields the RW product. Finally, the hourly rain rates are disaggregated to the original 5-min intervals in order to obtain the quasi-adjusted YW product [19]. For disaggregation, the hourly precipitation sum of the adjusted RW product is distributed to the twelve 5-min intervals based on the temporal rainfall distribution throughout the respective hour. The data processing was conducted by DWD. In the state of Hesse, only the stations operated by DWD are used for radar data adjustments.

2.2.2. Rain Gauge Data

For this study, we combined two different rain gauge datasets in 1-min resolution. We used data from 76 automated rain gauges throughout Hesse operated by DWD, which are freely available in the DWD Open Data Portal [26], as well as from 52 rain gauges of the Hessian monitoring network operated by HLNUG, which are not publicly available. Both datasets were carefully checked for plausibility and a cleaning procedure was implemented to remove erroneous values. For a detailed description of the data processing and cleaning procedure please refer to [27].

In general, the DWD rain gauge data are available for the period 2001–2016, whereas those of the HLNUG stations only cover the period 2001–2015. However, the time series of the combined rain gauge dataset varies strongly between stations. In this study, 21 stations with time series shorter than nine years were excluded. The final dataset used for analysis consisted of 110 rain gauge stations. Finally, the 1-min rain gauge data were aggregated to a temporal resolution of 5 min in order to match the temporal resolution of the radar climatology data.

2.3. Methodology

2.3.1. R-factor Calculation According to DIN 19708

The R-factors were calculated according to the specifications of DIN 19708 [8] for the RADKLIM YW product and the rain gauge data, both in 5-min resolution. According to DIN 19708 [8], which is based on the results of Schwertmann et al. [2], erosive precipitation events have a precipitation sum of at least 10 mm or a precipitation intensity exceeding 10 mm/h within a time window of 30 min (i.e., an actual precipitation quantity of 5 mm in 30 min). The maximum precipitation sum occurring within a 30-min window of a rainfall event is identified by applying a moving window of six 5-min intervals and is related to one hour by doubling it. This value is referred to as maximum 30-min intensity I_{30}. As defined by DIN 19708 [8], the total amount of precipitation is doubled and assigned to I_{30} if an event lasts less than 30 min. Rainfall events are separated by a precipitation pause of at least 6 h.

The R-factor of a specific precipitation event results from the product of the maximum 30-min intensity I_{30} [mm/h] and the kinetic energy E [kJ/m^2] of the total rainfall during the event.

$$R_{event} = E \cdot I_{30} \tag{1}$$

The kinetic energy E of an erosive rainfall event was calculated with the following equation from DIN 19708:

$$E = \sum_{i=1,n}^{i=n} E_i \tag{2}$$

with

$$E_i = (11.89 + 8.73 \cdot log_{10}(I_i)) \cdot N_i \cdot 10^{-3} \, for \, 0.05 \leq I_i \leq 76.2$$

$$E_i = 0 \, for \, I_i < 0.05$$

$$E_i = 28.33 \cdot N_i \cdot 10^{-3} \, for \, I_i > 76.2$$

Thereby is

i 5-min interval of the rainfall event

E_i kinetic energy of the rainfall in period i [kJ/m^2]

N_i rainfall depth in period i, [mm]

I_i rainfall intensity in period i, [mm/h], that is $I_i = N_i \cdot \frac{60 \text{ Min}}{5 \text{ Min}}$

Finally, the R-factor per year for a given location is the sum of the R_{event} products [kJ/m^2 mm/h = N/(ha a)] of all erosive rainfall events in a year. Due to the great interannual variability of erosivity, it is recommended to average the annual R-factors over a period of at least ten years [8]. For the calculations based on the radar climatology this criterion was fulfilled everywhere, whereas the time series of five rain gauges was limited to nine years.

For the calculation of the R-factor from both data sets, the development of new routines was necessary. One difficulty is the large data volume of the YW product for the whole of Hesse, which required a balancing of memory requirements and computing efficiency. The developed Python routines are based on the HDF5 file format [28] with monthly pandas [29] DataFrames introduced by Kreklow [30]. This enables a continuous calculation of the R-factor over all days of a month. However, for reasons of efficiency, no smooth transitions between months were implemented. The routine assumes an end of the precipitation event at the end of each month and carries out the calculation for the amount of precipitation that has fallen up to that point. Thus, long lasting nightly precipitation events may be divided into two events or one event can be classified as non-erosive due to the interruption. However, since erosivity shows a clearly pronounced maximum in the late afternoon [5], when convection is usually strongest, the inaccuracy in the calculation due to the interruption at the turn of the month was regarded as negligible.

2.3.2. R-factor Calculation Using Regression

For the erosion atlas Hesse [13], the R-factor was derived using the following regression equation from the mean long-term precipitation of the summer months May–October N_{su}:

$$R_{EA} = 0.141 \cdot N_{Su} - 1.48 \tag{3}$$

For comparison of methodologies and effects of precipitation changes, additional R-factors were calculated using this regression equation based on the hourly RW product of the radar climatology and the condensed rain gauge dataset. In conjunction with the R-factors calculated according to DIN 19708 (see Section 2.3.1) and the erosion atlas Hesse, these additional R-factor estimates based on regression allow to compare different combinations of input data and derivation methods.

All calculated R-factor derivatives are summarised in Table 1.

Since the R-factor is only important for estimating soil loss from agricultural land and not in forests or urban areas, we conducted an additional analysis of all of the abovementioned R-factor derivatives that only considered cropland areas. For this, all data pairs for which the respective RADKLIM pixel contained less than ten hectares of cropland were removed. The resulting datasets are marked by the appendix "*Agri*" in the R-factor index, e.g., $R_{YW,DIN,Agri}$.

Consequently, the analyses of this study cover three different spatial extents for which data pairs of all available datasets were created in order to enable meaningful comparisons for similar spatial scales:

(a)   all 1 km^2 pixels within Hesse (n = 23,320)

(b)   all pixels containing at least ten hectares of cropland (n = 11,555)

(c)   all rain gauge stations (n = 110)

In addition, the summer precipitation sums of RADKLIM and the rain gauges and their respective R-factor derivatives $R_{YW,DIN}$ and $R_{G,DIN}$ were used to determine two new regression equations. These serve to assess the following: the changes in the correlation between rainfall erosivity and precipitation sums, changes in comparison to the existing regression equation used for the erosion atlas, and the impact of sample size.

Table 1. Overview of all R-factor derivatives analysed in this study.

Name	Derivation Method	Input Dataset	Spatial Extent	n
$R_{YW,DIN}$	DIN 19708	RADKLIM YW (5 min)	All radar pixels in Hesse (1×1 km)	23,320
$R_{YW,DIN,\,Agri}$	DIN 19708	RADKLIM YW (5 min)	Radar pixels containing $\geq$ 10 ha of cropland	11,555
$R_{G,DIN}$	DIN 19708	Rain gauge data (5 min)	All rain gauges	110
$R_{YWG,DIN}$	DIN 19708	RADKLIM YW (5 min)	Pixels containing a rain gauge	110
R_{EA}	$0.141 \cdot N_{Su} - 1.48$	Interpolated rain gauge data (1971–2000)	1×1 km grid for Hesse	23,320
$R_{EA,Agri}$	$0.141 \cdot N_{Su} - 1.48$	Interpolated rain gauge data (1971–2000)	Grid cells containing $\geq$ 10 ha of cropland	11,555
$R_{RW,Reg}$	$0.141 \cdot N_{Su} - 1.48$	RADKLIM RW (1 h)	All radar pixels in Hesse	23,320
$R_{RW,Reg,Agri}$	$0.141 \cdot N_{Su} - 1.48$	RADKLIM RW (1 h)	Radar pixels containing $\geq$ 10 ha of cropland	11,555
$R_{G,Reg}$	$0.141 \cdot N_{Su} - 1.48$	Rain gauge data	All rain gauges in Hesse	110
$R_{RWG,Reg}$	$0.141 \cdot N_{Su} - 1.48$	RADKLIM RW (1 h)	Pixels containing a rain gauge	110
R_{EAG}	$0.141 \cdot N_{Su} - 1.48$	Interpolated rain gauge data (1971–2000)	Grid cells containing a rain gauge	110
$R_{YW,F}$	$R_{DIN} \cdot ((1.13 + 0.35) \cdot 1.05)$	RADKLIM YW (5 min)	All radar pixels in Hesse	23,320
$R_{YW,F,Agri}$	$R_{DIN} \cdot ((1.13 + 0.35) \cdot 1.05)$	RADKLIM YW (5 min)	Radar pixels containing $\geq$ 10 ha of cropland	11,555
$R_{G,F}$	$R_{DIN} \cdot 1.05$	Rain gauge data	All rain gauges	110
$R_{YWG,F}$	$R_{DIN} \cdot ((1.13 + 0.35) \cdot 1.05)$	RADKLIM YW (5 min)	Pixels containing a rain gauge	110
$R_{G,P}$	$R_{DIN} \cdot 0.7984$	Rain gauge data	All rain gauges	110

2.3.3. Application of Scaling Factors

Recent studies propose various scaling/correction factors to compensate for the temporal resolution of the input data and the differences between rain gauge and radar data. In order to be able to estimate the influence of the correction factors and to compensate for the presumed underestimation of the R-factor by the radar climatology, these factors were applied to the R-factors that were calculated according to DIN 19708.

The scaling according to [22] for the R-factors calculated from radar climatology results from

$$R_{YW,\ F} = R_{YW,DIN} \cdot ((spatial\ scaling + method\ factor) \cdot temporal\ scaling) \tag{4}$$

with

$$spatial\ scaling\ factor = 1.13;\ for\ a\ spatial\ resolution\ of\ 1\ km^2$$

$$method\ factor = 0.35$$

$$temporal\ scaling\ factor = 1.05;\ for\ a\ temporal\ resolution\ of\ 5\ min$$

For the rain gauge data, the scaling reduces to

$$R_{G,F} = R_{G,DIN} \cdot temporal\ scaling\ factor \tag{5}$$

with

$$temporal\ scaling\ factor = 1.05;\ for\ a\ temporal\ resolution\ of\ 5\ min$$

In order to include the strongly deviating temporal correction factor proposed by Panagos et al. [23], a further calculation was performed for $R_{G,DIN}$:

$$R_{G,P} = R_{G,DIN} \cdot temporal\ scaling\ factor \tag{6}$$

with

$$temporal\ scaling\ factor = 0.7984;\ for\ a\ temporal\ resolution\ of\ 5\ min$$

3. Results

3.1. Statistical Comparison of the Calculated R-Factors

The R-factor $R_{YW,DIN}$ calculated from the original unscaled RADKLIM YW product according to DIN 19708 ranges between 28.8 and 173.2 kJ/m^2 mm/h with an average value of 58.0 kJ/m^2 mm/h (see Table 2 and Figure 2). It is thus 6.4% higher on average than the values of the erosion atlas R_{EA}, whereas its range is 263.7% higher and its standard deviation is 122.7% higher. $R_{YW,DIN}$ shows thus a much higher variability than the strongly smoothed R_{EA} which was derived from spatially interpolated rainfall data using a regression equation (Equation (3)).

The R-factor calculated from the gauge dataset $R_{G,DIN}$ has an average of 80.6 kJ/m^2 mm/h, which is 47.8% higher than the average value of R_{EA} and 39% higher than the average of $R_{YW,DIN}$. At 107 of 110 stations the rain gauges show higher R-factors than the corresponding pixels of the radar climatology. The average R-factor difference for all point-pixel pairs amounts to 20.5 kJ/m^2 mm/h between $R_{YWG,DIN}$ and $R_{G,DIN}$. For the 72 stations operated by DWD, which were used for radar data adjustments, the average difference between $R_{YWG,DIN}$ and $R_{G,DIN}$ amounts to 19.1 kJ/m^2 mm/h, whereas the average difference at the 38 stations operated by HLNUG is slightly higher with 23.1 kJ/m^2 mm/h. Compared to the erosion atlas, all 110 rain gauge stations show higher R values with an average difference of 24.7 kJ/m^2 mm/h.

**Table 2.** Statistical summary of all R-factor derivatives.

R-factor	n	Method	Data Source	Mean	Standard Deviation	Min	Median	Max
$R_{YW,DIN}$	23,320	DIN 19708	RADKLIM	58.0	14.7	28.8	54.6	173.2
$R_{YW,DIN,Agri}$	11,555	DIN 19708	RADKLIM	54.2	12.0	28.8	52.3	146.1
$R_{G,DIN}$	110	DIN 19708	Gauges	80.6	20.6	53.4	75.3	157.2
$R_{YWG,DIN}$	110	DIN 19708	RADKLIM	60.1	15.8	31.0	57.8	104.7
R_{EA}	23,320	Regression	Erosion atlas	54.5	6.6	42.1	52.8	81.8
$R_{EA,Agri}$	11,555	Regression	Erosion atlas	52.8	5.3	42.1	51.7	81.0
$R_{RW,Reg}$	23,320	Regression	RADKLIM	53.2	6.8	32.8	53.0	77.0
$R_{RW,Reg,Agri}$	11,555	Regression	RADKLIM	51.9	6.4	32.8	52.1	71.4
$R_{G,Reg}$	110	Regression	Gauges	57.0	8.8	44.7	55.0	84.7
$R_{RWG,Reg}$	110	Regression	RADKLIM	53.1	7.8	35.9	52.4	73.0
R_{EAG}	110	Regression	Erosion atlas	55.9	8.1	45.2	53.7	81.8
$R_{YW,F}$	23,320	DIN scaled	RADKLIM	90.1	22.8	44.5	84.8	269.1
$R_{YW,F,Agri}$	11,555	DIN scaled	RADKLIM	84.2	18.6	44.5	81.3	227.0
$R_{G,F}$	110	DIN scaled	Gauges	84.6	21.6	56.1	79.1	165.1
$R_{YWG,F}$	110	DIN scaled	RADKLIM	93.4	24.6	48.0	89.8	162.7
$R_{G,P}$	110	DIN scaled	Gauges	64.4	16.4	42.6	60.1	125.5
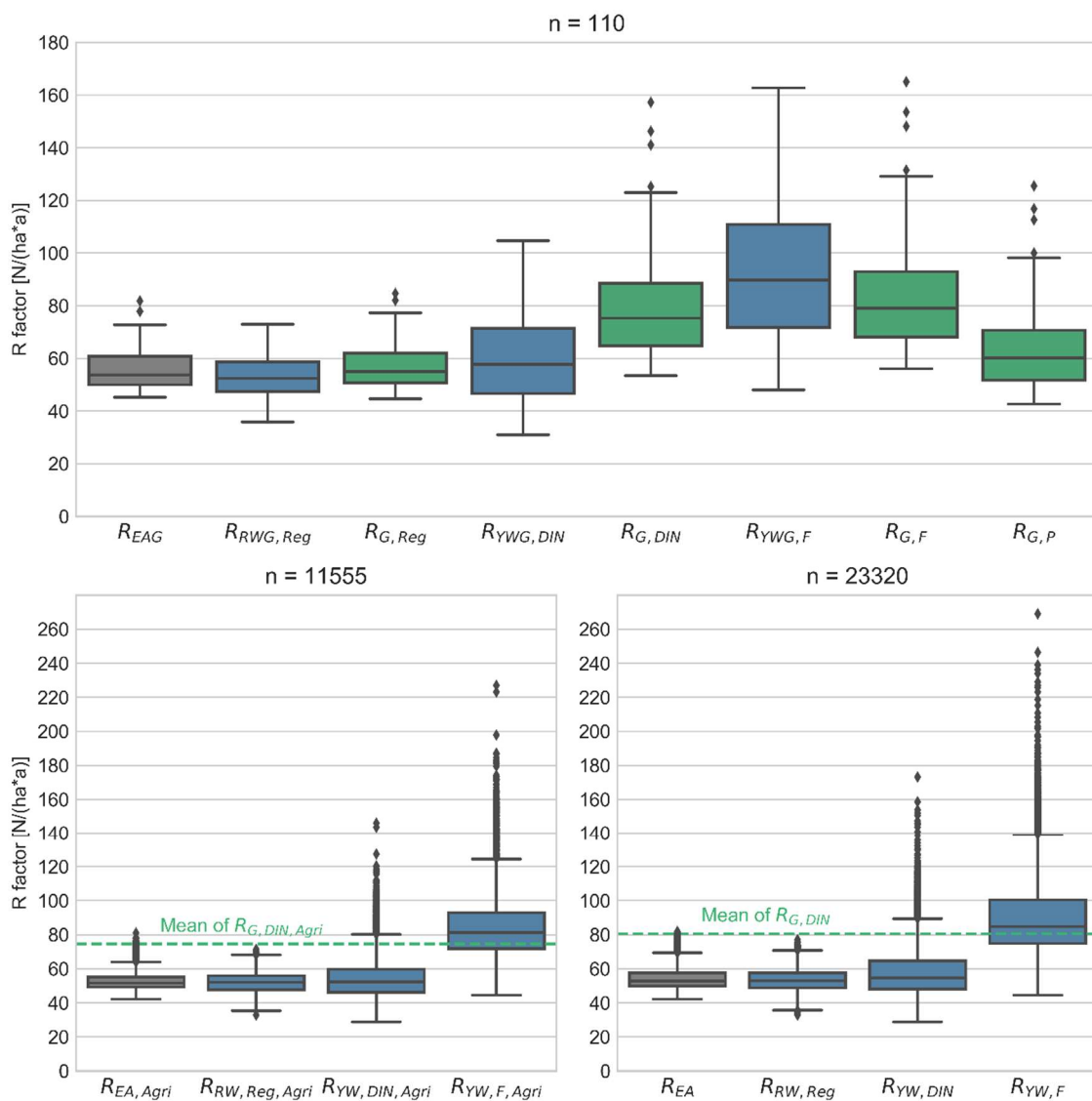
Figure 2. Boxplots of all R-factor derivatives grouped by spatial extent. In the lower subplots, the average of the rain gauges ($R_{G,DIN}$) and the rain gauges in pixels with cropland ($R_{G,DIN,Agri}$) have been added as a ground-truth reference. See Table 1 for explanation of the used abbreviations.

Using the regression equation from the erosion atlas (Equation (3)) and the RADKLIM RW product to derive $R_{RW,Reg}$ yielded comparable values as R_{EA} with a slightly lower mean and maximum, significantly lower minimum, but a slightly higher median and standard deviation. For $R_{G,Reg}$, all statistical values were slightly higher than for R_{EA} and $R_{RW,Reg}$. Consequently, before scaling, the rain gauge dataset consistently produces the highest R-factors, but the magnitude of the differences is governed by the derivation method. The input dataset has little influence on the statistical characteristics of the outcome when using a regression equation and the major differences between these regression-based derivatives are the spatial resolutions and spatial distributions (see Section 3.2). When grouping all R-factor derivatives by the calculation method—irrespective of input data and spatial extent—the mean of those R-factors derived according to DIN 19708 (without scaling) is 9.1 kJ/m^2 mm/h higher than the mean of all R-factors derived using the regression equation. Furthermore, with 15.8 kJ/m^2 mm/h, the DIN method group showed on average a 122.2% higher standard deviation than the regression method group (7.1 kJ/m^2 mm/h), which underlines the smoothing effect that can be obtained by using a regression equation instead of the event-based method according to DIN 19708. The difference between both methods is particularly well illustrated by the very steep empirical cumulative distribution functions (ECDF) of all regression-based derivatives (see Figure 3).
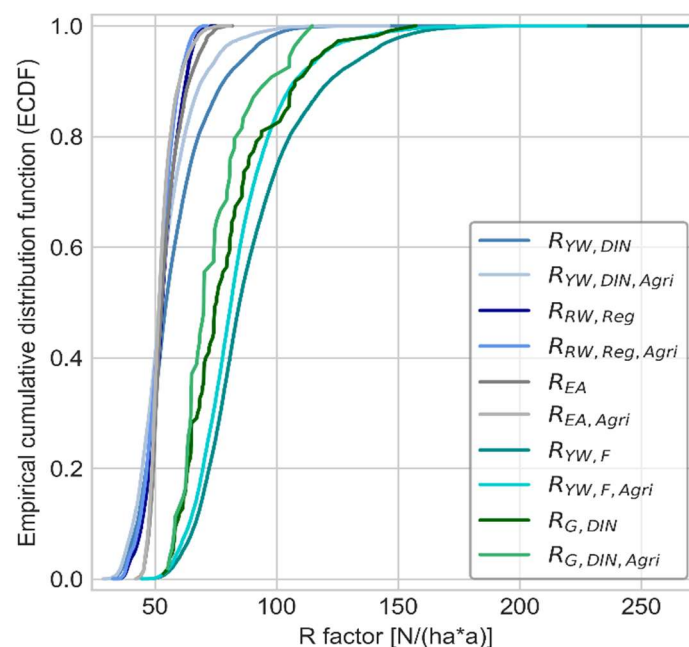
Figure 3. Empirical cumulative distribution functions (ECDF) for all spatially highly resolved R-factor derivatives. The ECDFs for the rain gauges ($R_{G,DIN}$) and the rain gauges in pixels with cropland ($R_{G,DIN,Agri}$) have been added as a ground-truth reference.

Selecting pixels with cropland leads to an average decrease of $R_{YW,DIN}$ by 3.8 kJ/m^2 mm/h (−6.6%). The minimum did not change, while the maximum decreased by 27.1 to 146.1 kJ/m^2 mm/h (see Figures 2 and 3). Taking into account only the pixels with cropland and rain gauges, the count was reduced to 54 (a total of 54 rain gauges are located in radar pixels with cropland), the average R-factor ($R_{YWG,DIN,Agri}$) decreased also by 3.8 to 56.3 kJ/m^2 mm/h and the maximum decreased by 12.5 to 92.2 kJ/m^2 mm/h. For $R_{G,DIN}$, the impact of the data selection on the statistical distribution is considerably higher due to the smaller sample size. Its average decreased by 6.1 to 74.5 kJ/m^2 mm/h, whereby the maximum decreased by 42.5 to 114 kJ/m^2 mm/h when selecting only pixels with cropland. Consequently, the removal of many high erosivity values in the mountainous regions (see Figure A1), for which the uncertainty and underestimation of the radar data is particularly high, leads to a slightly better agreement of the R-factors calculated according to DIN 19708 from RADKLIM and rain gauge

data. Grouping the nine R-factor derivatives based on $R_{YW,DIN}$, $R_{RW,Reg}$ and R_{EA} by spatial extent resulted in a mean of 55.2 kJ/m^2 mm/h for all pixels of the study area, 52.9 kJ/m^2 mm/h for pixels with cropland and 56.3 kJ/m^2 mm/h for pixels with a rain gauge.

In regard to the data source, the results showing an underestimation of rainfall erosivity by the radar climatology compared to rain gauge data are in line with the outcomes of Fischer et al. (2018), thus the application of the proposed correction factors was considered to be useful and necessary. After scaling, the R-factors of the radar climatology and rain gauges correspond much better (see Figures 2 and 3). The difference between the two datasets shifts in favour of the radar climatology, since on average $R_{YW,F}$ is 8.8 kJ/m^2 mm/h higher than R$_{G,F}$ (see Table 2). In comparison to R_{EA}, both R-factors were significantly higher after scaling. On average, $R_{YW,F}$ was 65.3% higher and $R_{G,F}$ was 58.5% higher than the R-factor R_{EA} of the erosion atlas. Although the correction factor proposed by Panagos et al. [23] reduces the R-factor to a level close to $R_{YW,DIN}$, $R_{G,P}$ still showed an 18.2% higher mean than R_{EA}. Irrespective of the dataset used for derivation and the application of correction procedures, an increase of the R-factor compared to R_{EA} can thus be determined without doubt.

3.2. Spatial Distribution

For erosion control applications at a federal state scale which aim to identify regions with a particularly high risk of erosion, the spatial distribution of rainfall erosivity is actually more relevant than the absolute erosivity values. The lowest values of $R_{YW,DIN}$ occur in the north of Hesse, around the West Hesse Depression, in an area for which no radar measurements were available during some months of the years 2007 and 2014 due to radar hardware upgrades. The average value of the annual R-factor without these two years shows that the minimum is nevertheless located in this area. This is therefore in accordance with the R-factor R_{EA} (calculation based on regression), which also shows a minimum in this area (see Figure 4). The areas of relatively low R-factors northwest of Fulda and in the Upper Rhine Plain correspond well in both datasets, too. In the north-east of Hesse, however, the newly calculated R-factor $R_{YW,DIN}$ showed slightly lower erosivity over a large area with a similar spatial distribution. Both datasets showed an increase of the R-factor with increasing terrain height, whereby $R_{YW,DIN}$ showed significantly higher values over a large area, especially in the Odenwald, Taunus, Westerwald and at Vogelsberg. However, at Vogelsberg, a weakness of the radar climatology to correctly quantify precipitation at higher altitudes was evident as the increase of the R-factor in the lower slope areas was considerably higher than in the summit area. In the area of Wetterau, a negative spoke of the Frankfurt Radar was clearly visible in $R_{YW,DIN}$ and all other R-factors derived from RADKLIM. Still, in this area an increase of the R-factor compared to the erosion atlas can be seen in most of the grid cells, in some places even up to 45% (see Figure 5a).

The scaling is able to compensate for the underestimation of the R-factor by the radar climatology, which becomes particularly obvious in the northern parts of Hesse where the difference to the erosion atlas shows mostly positive values except for a few single pixels (see Figure 5c). Moreover, Figure 5b shows much better conformity with $R_{G,DIN}$ in the entire study area, which has already been indicated in the previous section.
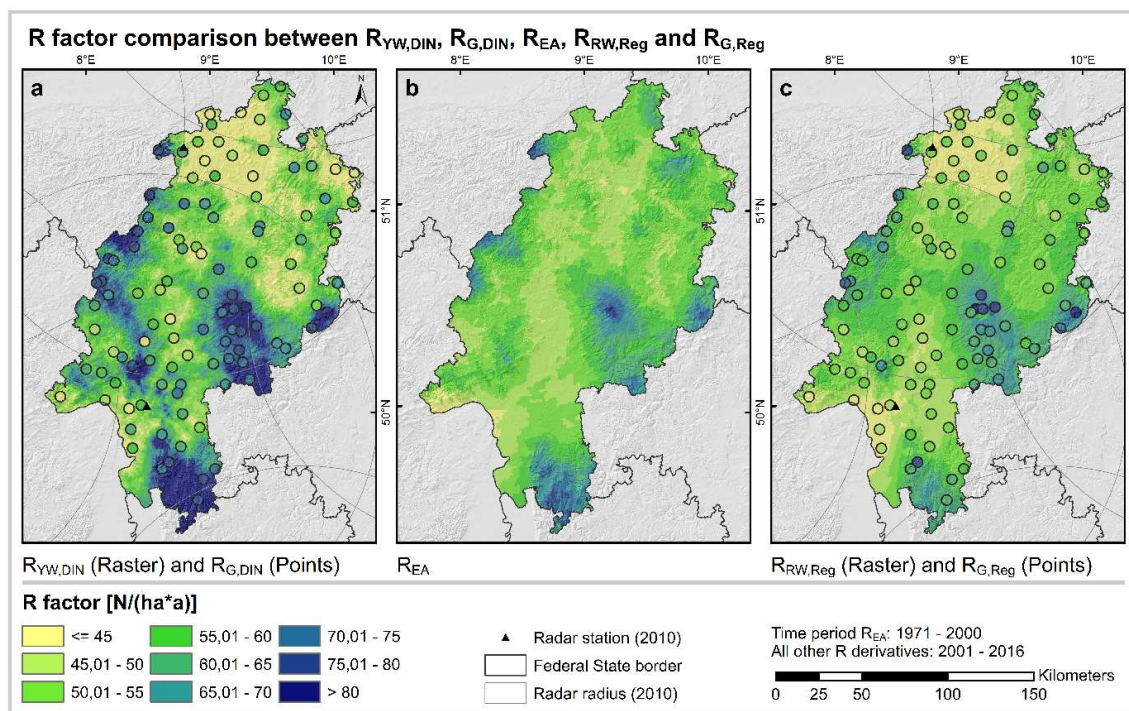
Figure 4. R-factor comparison between $R_{YW,DIN}$, $R_{G,DIN}$ (**a**), R_{EA} (**b**), $R_{RW,Reg}$ and $R_{G,Reg}$ (**c**).
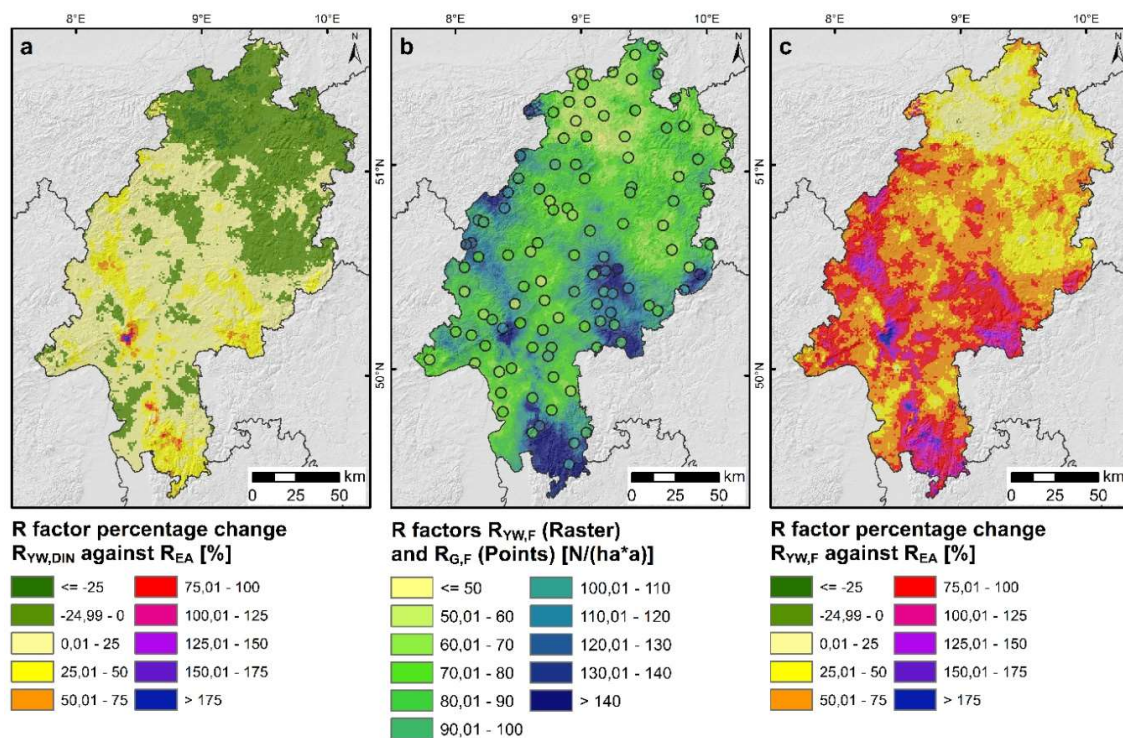

Figure 5. R-factor percentage change of $R_{YW,DIN}$ against R_{EA} (**a**), scaled R-factors $R_{YW,F}$ and $R_{G,F}$ (**b**) and percentage change of $R_{YW,F}$ against R_{EA} (**c**).

3.3. Derivation of Updated Regression Equations

The statistical comparisons in Section 3.1 show consistently lower values for all R-factors derived by means of regression. Besides the method itself and the input data source, the observation time

period of the data used for the derivation of the regression equation might play a role due to climate change, which is why we derived an updated regression equation for comparison.

The new regression equations derived from the rain gauge data and the radar climatology both show a strong correlation between summer precipitation and R-factor. The fitted regression line has a considerably higher slope than the original one used for the erosion atlas (Equation (3)) (see Figure 6). Some data points of $R_{YW,DIN}$, which are mainly located in the area of the radar gap in northern Hesse, are still below the regression line from the erosion atlas. For $R_{G,DIN}$, however, all data points are above. Consequently, for the period 2001–2016, the regression equation used in the erosion atlas provides a value deviating from the R-factor according to DIN 19708 for all of the rain gauges.
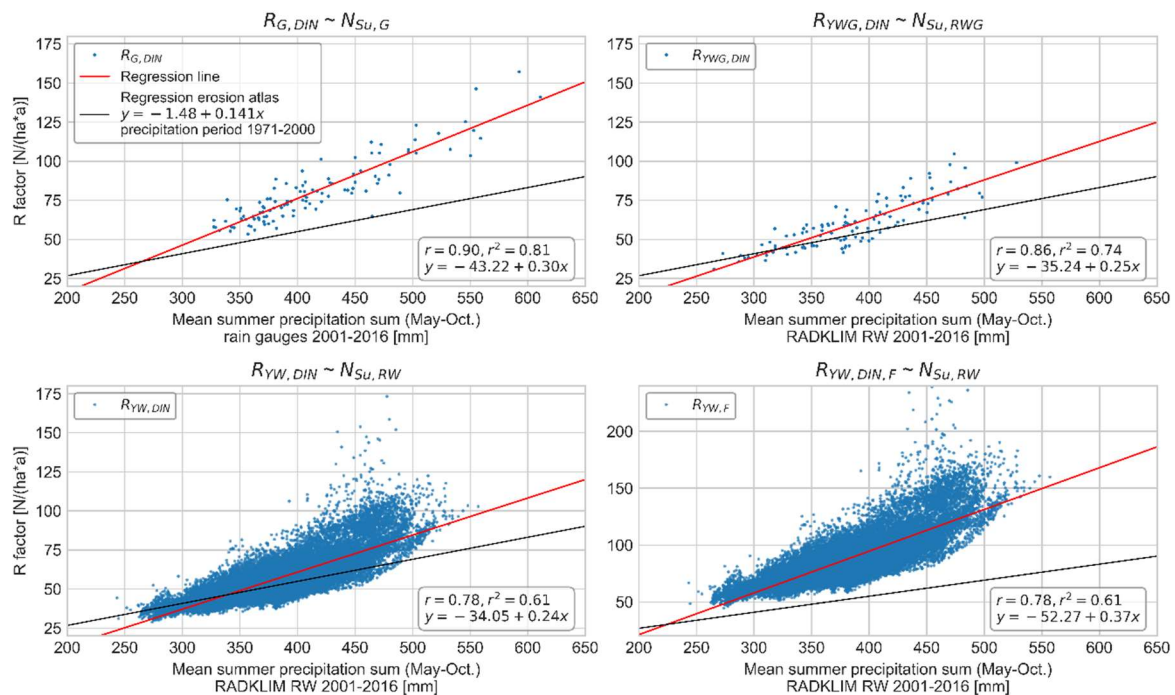
Figure 6. Comparison of regression models between different R-factors and the respective mean summer precipitation sums.

When considering the newly derived regression equations from the radar climatology, it is striking that the equations for the entire data set and the pixels at the rain gauge locations are almost identical (see Figure 6). Consequently, the spatial distribution of the rain gauge locations can be regarded as very representative for mapping the overall distribution of rainfall erosivity in Hesse.

Another striking difference with regard to the sample size, however, is a series of several very high values of $R_{YW,DIN}$ in the range between 400 and 500 mm summer precipitation. These are only included in the R-factor of the entire radar climatology dataset, but are not significantly reflected in the regression due to their relatively small number. Therefore, it can be assumed that extraordinarily intensive individual events have a strong impact due to the comparatively short time series. These events could only be detected by the high spatial resolution of the radar climatology and are not included in the rain gauge dataset.

Using the new regression equation derived from the rain gauges ($R = -43.22 + 0.3\ N_{Su}$) with the summer precipitation sums of the RADKLIM RW product for the federal state of Hesse leads to a R-factor value range between 29.7 and 123.9 kJ/m^2 mm/h with an average of 73.2 kJ/m^2 mm/h. It has thus a significantly lower maximum than all event-based R-factor derivatives. Its mean value is slightly lower than that of $R_{G,DIN}$ (80.6 kJ/m^2 mm/h) due to the slight overall underestimation of precipitation by the radar climatology, and lies approximately in the centre between the averages of $R_{YW,DIN}$ (58 kJ/m^2 mm/h) and the corrected $R_{YW,F}$ (90.1 kJ/m^2 mm/h).

4. Discussion

An evaluation of the radar climatology dataset revealed that it slightly underestimates precipitation quantities. This underestimation is particularly pronounced at higher altitudes and at high rainfall intensities [31]. In particular, the latter plays a decisive role for rainfall erosivity since rainfall intensity is directly linked to the kinetic energy of rainfall and, thus, its ability to detach soil particles. The assumption that the R-factor calculated from the radar climatology according to DIN 19708 without input data correction is too low could be confirmed by comparing it with the R-factor derived from the rain gauge dataset. However, irrespective of the dataset used for derivation, the spatial scale and the application of correction procedures, an increase of the R-factor compared to R_{EA} which is currently used in the technical information system erosion atlas Hesse [13] can be determined without doubt. This result highlights the need of updated R-factor methods for consultation and planning in Hesse.

The R-factors calculated by the regression equation from the erosion atlas, the summer precipitation sums of radar climatology, and rain gauges showed only slightly higher average values than the erosion atlas. Considering the significant differences to the R-factor derivations according to DIN 19708, this indicates that the regression equation used for the erosion atlas, which was derived from precipitation data of the 1960s, 70s and 80s, is no longer representative of the current climate conditions. Apparently, although there has only been a small increase in summer precipitation, there is a change in the heavy rainfall characteristics and/or in the relationship between erosive rainfall and total precipitation amount. This observation is in line with the projected changes in precipitation characteristics with regard to climate change. For most of Europe, it is expected that precipitation will increase during winter and decrease during summer [32,33]. Furthermore, the number of wet days is expected to decrease, whereas the intensity and the return levels of daily precipitation events will increase [12,32,34,35]. The combination of increasingly intense heavy rainfall and the reduced water infiltration capacity of dry soils is expected to amplify the risk of floods [36] and is also very likely to increase soil erosion. These observations indicate that the validity of regression equations for R-factor calculation might decrease, particularly if mean summer precipitation sums are used instead of mean annual sums. An additional influencing factor for higher R-factors calculated from rain gauge data could be the better recording of intensity peaks by more accurate modern rain gauges as opposed to the less accurate rain gauges used to collect the data for the 1971–2000 dataset [37].

Despite the discussed limitations, the regression-based approach has the advantage that it is much easier to apply in practice than the method according to DIN 19708, which is computationally much more expensive, especially when using it on spatially highly resolved data such as the radar climatology. Moreover, the use of a regression equation with precipitation sums always leads to a certain smoothing and is thus more robust against outliers than the event-based method when only comparatively short precipitation time series are available. However, as our results have clearly shown, the regression approach also requires frequent updates of the equations and hence a certain maintenance of the methodology. Obviously, updates to the equations rely on the availability of rain gauge data. For Germany, this is not a major issue anymore since temporally highly resolved rain gauge data are freely available at the DWD Open Data Portal. In other countries, however, this may be a greater obstacle.

With regard to the scaling of the R-factors which was proposed in recent studies [22,23], it should be noted that a correction that increases the RADKLIM R-factor is undoubtedly necessary to compensate for the systematic underestimation of precipitation data obtained from radar climatology. However, the degree of correction is difficult to estimate due to a lack of reference. If the scaled R-factor of the rain gauge dataset $R_{G,F}$ is regarded as a correct reference for validation, the correction applied for $R_{YW,F}$ and $R_{YWG,F}$ appears somewhat too high, especially when looking at Figure 2. When considering the identical sample size and the largely consistent location of the point-pixel data pairs of $R_{YWG,F}$, the advantage of the radar and the fact that more events tend to be recorded hardly matters. However, the median of $R_{YWG,F}$ almost corresponds to the third quartile of $R_{G,F}$. Here, a direct transferability of the correction factors, which were derived from a four-year series of measurements of 12 rain gauges

within one square kilometre in Bavaria [22], may be limited. Further research efforts and measurements to extend these time series and derive correction factors of higher spatial representativity from more than one single raster cell would have the potential to significantly reduce the uncertainty when using radar climatology data—not only for rainfall erosivity estimation but for applications related to heavy rainfall in general.

In contrast, the scaling according to Panagos et al. [23] to compensate for the temporal resolution of the input data provides very questionable results. Taking into account the conducted plausibility check of the radar climatology and the comparisons with the rain gauge data by Kreklow et al. [31], an underestimation of the R-factor by the radar data is clearly demonstrated. Since the correction factor proposed by Panagos et al. [23] reduces the R-factor of the rain gauges to a level almost identical to that of the radar climatology, a correction factor that is too low must be assumed. The correction factor does not appear to be representative for Hesse, due to the fact that its derivation is based on a rain gauge dataset for the whole of Europe and equally includes data from maritime, continental, temperate, subpolar and Mediterranean climates. Already for the two neighbouring countries Austria and Italy, Fiener et al. [38] found significant differences in the magnitude and monthly distribution of the R-factor, which indicates a lack of spatial representativity of the temporal scaling factor proposed by Panagos et al. [23]. Such representativity issues have been subject to discussion between the authors [4,38,39]. In addition, the original methodology for the calculation of the R-factor is based on continuous precipitation recordings, which were aggregated to intervals of constant intensity [1]. Consequently, a temporal resolution of 1 min as a lowest reference chosen by Fischer et al. [22] is much closer to the original method than the reference resolution of 30 min used by Panagos et al. [23]. The much lower reference resolution used by Panagos et al. [23] thus explains the significantly lower temporal correction factor compared to the factor proposed by Fischer et al. [22].

With regard to practical application, it is recommended that the R-factor map currently used in the erosion atlas should be updated. Our results show that the first and most important step is to use more recent precipitation data for derivation, which are more representative under current climate conditions. Obviously, using the event-based method according to DIN 19708 with radar climatology, which was proposed by Auerswald et al. [6], provides the R-factor with the highest spatial detail, but it may be locally biased by some extreme rainfall events or radar artefacts which are not balanced out in the comparatively short radar time series. Moreover, a correction of R-factors derived from radar climatology according to DIN 19708 is necessary to compensate for underestimation, but the level of correction required is still subject to discussion. However, the radar climatology time series is still considerably longer than the time series used for deriving the original regression equations by Sauerborn [9], of which one was also used in the erosion atlas Hesse. Consequently, during a transition period, the most robust and easy-to-use approach to obtain updated R-factors is by using an updated regression equation derived from recent rain gauge data with summer precipitation sums calculated from radar climatology data. On the one hand, this approach accounts for climate change by increasing the R-factors according to reliable rain gauge observations. On the other hand, it makes use of the high spatial resolution of radar data and comprises a certain smoothing, since precipitation sums are less biased by local extreme events and by the underestimation of high rainfall intensities by weather radar in comparison to the event-based R-factors derived according to DIN 19708. Moreover, due to less snowfall and thus fewer uncertainties in the radar climatology data during the summer half-year, the use of radar-based summer precipitation sums increases the robustness of the recommended method compared to the use of radar-based annual precipitation sums.

Due to the central location of Hesse within Germany, the recommended updated regression equation based on rain gauge data for Hesse ($R = -43.22 + 0.3\ N_{Su}$) has a high transferability for most of Germany. However, for federal states in northern and eastern Germany which have a more maritime or continental climate, regional regression equations should be calculated from recent local rain gauge data.

5. Conclusions

In this study, we compared several derivation approaches for the R-factor of the USLE and evaluated the performance of radar climatology and rain gauge data for different methods and three spatial extents. Moreover, two correction factors proposed in other studies were tested and updated regression equations were derived for the German federal state of Hesse.

Regarding the three hypotheses put forward at the beginning of this study, our results can be summarised as follows:

1. The newly derived R-factors from rain gauge and radar climatology data are indeed higher than the R-factors from existing calculations due to climate and weather changes. For the study period of 2001–2016, the regression equation used in the erosion atlas provides a lower R-factor than DIN 19708 for all of the rain gauges.

2. The contradiction between the theoretically higher R-factor of the radar climatology due to the more complete recording of all erosive rainfall events on the one hand and the underestimation of the R-factor due to the attenuation of intensity peaks, on the other hand, could be established. In the spatial average as well as when looking at the point-pixel data pairs, which largely eliminates the influence of the higher spatial resolution of the radar climatology data, the R-factors of the rain gauges are significantly higher. However, when looking at the entire radar data set, some strikingly high R-factor values, which were not captured by the rain gauges, become apparent. Due to their comparatively small number, however, they have no significant influence on the spatial mean value. In addition, these extraordinary high R-factors can also be a result of very intensive rainfall events in the comparatively short observation period that might be smoothed by prolonging the radar climatology dataset. The correction of the R-factors according to Fischer et al. [22] provides an improvement of the results for the radar climatology, although a possible overcorrection cannot be excluded.

3. The spatial distribution of the newly calculated R-factor according to DIN 19708 and that from the erosion atlas show a relatively good conformity with minima and maxima in similar regions as well as a consistent mapping of a relief dependency. In the northeast of Hesse, the R-factor calculated from the uncorrected radar climatology according to DIN 19708 shows comparatively lower values than the erosion atlas. In contrast, it also shows large areas of higher R-factor values than the erosion atlas, especially in the ridges of the low mountain ranges and in the central lowland areas of Hesse, for example, the Wetterau. The updated regression equations, which are almost identical for all radar pixels and the point-pixel data pairs, indicate that the rain gauge locations are very representative for mapping the overall spatial distribution of rainfall erosivity in the study area.

The results of this study clearly indicate that the R-factor map currently used in the erosion atlas should be updated. For a transition period until the radar climatology time series is long enough to compensate for bias from extraordinarily intensive rainfall events, it is recommended to apply a new regression equation derived from recent rain gauge measurements with summer precipitation sums calculated from radar climatology data.

With the progressive improvement of the data basis (time series, quality and correction), however, radar climatology data will be further incorporated into operational applications such as risk management and erosion consulting.
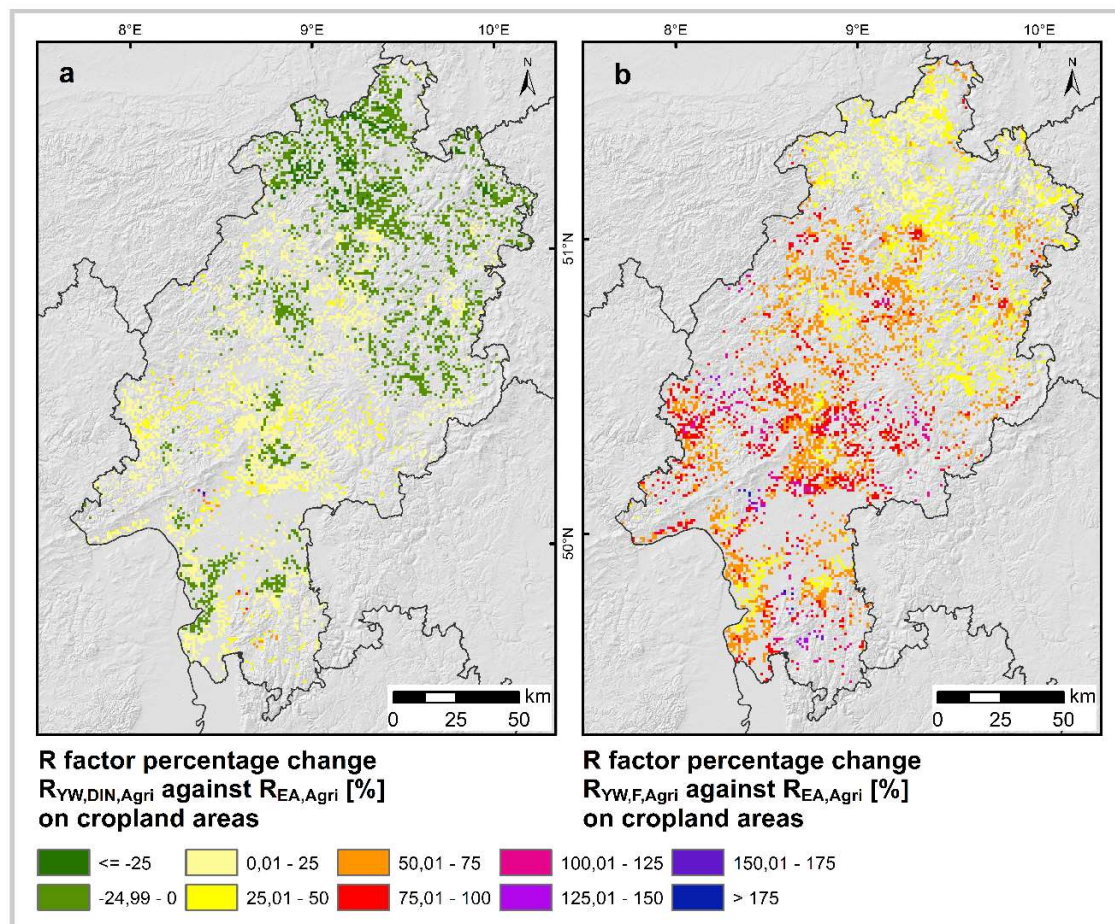
Conflicts of Interest: The authors declare no conflict of interest. The funders had no role in the design of the study; in the collection, analyses, or interpretation of data; in the writing of the manuscript, or in the decision to publish the results.

Appendix A

Figure A1. R-factor percentage change of $R_{YW,DIN,Agri}$ against $R_{EA,Agri}$ (**a**), and percentage change of $R_{YW,F,Agri}$ against $R_{EA,Agri}$ (**b**).

References

1. Wischmeier, W.H.; Smith, D.D. *Predicting Rainfall Erosion Losses. A Guide to Conservation Planning*; Agriculture handbook number 537; U.S. Department of Agriculture: Washington, DC, USA, 1978.

2. Schwertmann, U.; Vogl, W.; Kainz, M. *Bodenerosion durch Wasser. Vorhersage des Abtrags und Bewertung von Gegenmaßnahmen, 2. Aufl.*; Ulmer: Stuttgart, Germany, 1990; ISBN 3800130882.

3. Deutsches Institut für Normung. *DIN 19708. Bodenbeschaffenheit—Ermittlung der Erosionsgefährdung von Böden durch Wasser mithilfe der ABAG*; Normenausschuss Wasserwesen im DIN: Berlin, Germany, 2005; (19708).

4. Panagos, P.; Ballabio, C.; Borrelli, P.; Meusburger, K.; Klik, A.; Rousseva, S.; Tadic, M.P.; Michaelides, S.; Hrabalikova, M.; Olsen, P.; et al. Rainfall erosivity in Europe. *Sci. Total Environ.* **2015**, *511*, 801–814. [CrossRef] [PubMed]

5. Fischer, F.; Hauck, J.; Brandhuber, R.; Weigl, E.; Maier, H.; Auerswald, K. Spatio-temporal variability of erosivity estimated from highly resolved and adjusted radar rain data (RADOLAN). *Agric. For. Meteorol.* **2016**, *223*, 72–80. [CrossRef]

6. Auerswald, K.; Fischer, F.K.; Winterrath, T.; Brandhuber, R. Rain erosivity map for Germany derived from contiguous radar rain data. *Hydrol. Earth Syst. Sci.* **2019**, *23*, 1819–1832. [CrossRef]

7. Tetzlaff, B.; Friedrich, K.; Vorderbrügge, T.; Vereecken, H.; Wendland, F. Distributed modelling of mean annual soil erosion and sediment delivery rates to surface waters. *CATENA* **2013**, 13–20. [CrossRef]

8. Deutsches Institut für Normung. *DIN 19708. Bodenbeschaffenheit—Ermittlung der Erosionsgefährdung von Böden durch Wasser mit Hilfe der ABAG, 2017–08*; Beuth Verlag GmbH: Berlin, Germany, 2017.

9. Sauerborn, P. Die Erosivität der Niederschläge in Deutschland. Ein Beitrag zur quantitativen Prognose der Bodenerosion durch Wasser in Mitteleuropa. Ph.D. Thesis, Inst. für Bodenkunde, Bonn, Germany, 1994.

10. Elhaus, D. Erosionsgefährdung. Informationen zu den Auswertungen der Erosionsgefährdung durch Wasser, Germany. 2015. Available online: https://www.gd.nrw.de/zip/erosionsgefaehrdung.pdf (accessed on 11 March 2020).

11. Burt, T.; Boardman, J.; Foster, I.; Howden, N. More rain, less soil: Long-term changes in rainfall intensity with climate change. *Earth Surface Process. Landf.* **2016**, *41*, 563–566. [CrossRef]

12. Fiener, P.; Neuhaus, P.; Botschek, J. Long-term trends in rainfall erosivity–analysis of high resolution precipitation time series (1937–2007) from Western Germany. *Agric. For. Meteorol.* **2013**, *171-172*, 115–123. [CrossRef]

13. Friedrich, K.; Schmanke, M.; Tetzlaff, B.; Vorderbrügge, T. Erosionsatlas Hessen. In Proceedings of the Tagungsband d. Jahrestagung der DBG/BGS, Kommission VI, "Erd-Reich und Boden-Landschaft", Bern, Switzerland, 24–27 August 2019. DBG/BGS, Ed..

14. Hessisches Landesamt für Naturschutz, Umwelt und Geologie (HLNUG). BodenViewer Hessen. Available online: http://bodenviewer.hessen.de/mapapps/resources/apps/bodenviewer/index.html?lang=de (accessed on 21 January 2020).

15. Rogler, H.; Schwertmann, U. Erosivität der Niederschläge und Isoerodentkarte Bayerns. *Z. für Kult. und Flurberein.* **1981**, *22*, 99–112.

16. Hessisches Landesamt für Naturschutz, Umwelt und Geologie (HLNUG). R-Faktor. Available online: https://www.hlnug.de/themen/boden/auswertung/bodenerosionsbewertung/bodenerosionsatlas/r-faktor (accessed on 16 January 2020).

17. Donat, M.G.; Alexander, L.V.; Yang, H.; Durre, I.; Vose, R.; Dunn, R.J.H.; Willett, K.M.; Aguilar, E.; Brunet, M.; Caesar, J.; et al. Updated analyses of temperature and precipitation extreme indices since the beginning of the twentieth century: The HadEX2 dataset. *J. Geophys. Res. Atmos.* **2013**, *118*, 2098–2118. [CrossRef]

18. Winterrath, T.; Brendel, C.; Hafer, M.; Junghänel, T.; Klameth, A.; Lengfeld, K.; Walawender, E.; Weigl, E.; Becker, A. Radar climatology (RADKLIM) version 2017.002 (YW); gridded precipitation data for Germany. Available online: https://search.datacite.org/works/10.5676/dwd/radklim_yw_v2017.002 (accessed on 25 June 2019).

19. Winterrath, T.; Brendel, C.; Hafer, M.; Junghänel, T.; Klameth, A.; Walawender, E.; Weigl, E.; Becker, A. *Erstellung einer radargestützten Niederschlagsklimatologie*; Berichte des Deutschen Wetterdienstes No. 251; 2017; Available online: https://www.dwd.de/DE/leistungen/pbfb_verlag_berichte/pdf_einzelbaende/251_pdf.pdf?__blob=publicationFile&v=2 (accessed on 29 March 2019).

20. Kreklow, J.; Tetzlaff, B.; Burkhard, B.; Kuhnt, G. Radar-Based Precipitation Climatology in Germany—Developments, Uncertainties and Potentials. *Atmosphere* **2020**, *11*. [CrossRef]

21. Bronstert, A.; Agarwal, A.; Boessenkool, B.; Crisologo, I.; Fischer, M.; Heistermann, M.; Köhn-Reich, L.; López-Tarazón, J.A.; Moran, T.; Ozturk, U.; et al. Forensic hydro-meteorological analysis of an extreme flash flood: The 2016-05-29 event in Braunsbach, SW Germany. *Sci. Total Environ.* **2018**, 977–991. [CrossRef]

22. Fischer, F.K.; Winterrath, T.; Auerswald, K. Temporal- and spatial-scale and positional effects on rain erosivity derived from point-scale and contiguous rain data. *Hydrol. Earth Syst. Sci.* **2018**, *22*, 6505–6518. [CrossRef]

23. Panagos, P.; Borrelli, P.; Spinoni, J.; Ballabio, C.; Meusburger, K.; Beguería, S.; Klik, A.; Michaelides, S.; Petan, S.; Hrabalíková, M.; et al. Monthly Rainfall Erosivity: Conversion Factors for Different Time Resolutions and Regional Assessments. *Water* **2016**, *8*, 119. [CrossRef]

24. Semmel, A. Hessisches Bergland. In *Physische Geographie Deutschlands*, 2nd ed.; Liedtke, H., Marcinek, J., Eds.; Justus Perthes Verlag: Gotha, Germany, 1995; pp. 340–352. ISBN 3-623-00840-0.

25. Winterrath, T.; Brendel, C.; Hafer, M.; Junghänel, T.; Klameth, A.; Lengfeld, K.; Walawender, E.; Weigl, E.; Becker, A. Radar climatology (RADKLIM) version 2017.002 (RW); gridded precipitation data for Germany. Available online: https://search.datacite.org/works/10.5676/dwd/radklim_rw_v2017.002 (accessed on 25 June 2019).

26. Deutscher Wetterdienst Open Data Portal. Rain Gauge Precipitation Observations in 1-Minute Resolution. Available online: https://opendata.dwd.de/climate_environment/CDC/observations_germany/climate/1_minute/precipitation/ (accessed on 20 February 2020).

27. Kreklow, J.; Tetzlaff, B.; Kuhnt, G.; Burkhard, B. A Rainfall Data Intercomparison Dataset of RADKLIM, RADOLAN, and Rain Gauge Data for Germany. *Data* **2019**, *4*. [CrossRef]

28. The HDF Group. Hierarchical Data Format. Available online: https://portal.hdfgroup.org (accessed on 18 December 2018).

29. Mckinney, W. pandas: A Foundational Python Library for Data Analysis and Statistics. *Python High-Perform. Sci. Comput.* **2011**, *14*.

30. Kreklow, J. Facilitating radar precipitation data processing, assessment and analysis: A GIS-compatible python approach. *J. Hydroinformatics* **2019**, *21*, 652–670. [CrossRef]

31. Kreklow, J.; Tetzlaff, B.; Burkhard, B.; Kuhnt, G. Radar-Based Precipitation Climatology in Germany - Developments, Uncertainties and Potentials. Available online: https://www.preprints.org/manuscript/202002.0044/v1 (accessed on 10 February 2020).

32. Field, C.B.; Barros, V.R.; Dokken, D.J.; Mach, K.J.; Mastrandrea, M.D. *Climate Change 2014 – Impacts, Adaptation and Vulnerability: Part A: Global and Sectoral Aspects*; Working Group II Contribution to the IPCC Fifth Assessment Report; IPCC: Geneva, Switzerland, 2015. Available online: https://www.cambridge.org/core/books/climate-change-2014-impacts-adaptation-and-vulnerability-part-a-global-and-sectoral-aspects/1BE4ED76F97CF3A75C64487E6274783A (accessed on 7 February 2018).

33. Giorgi, F.; Bi, X.; Pal, J. Mean, interannual variability and trends in a regional climate change experiment over Europe. II: climate change scenarios (2071–2100). *Clim. Dyn.* **2004**, *23*, 839–858. [CrossRef]

34. Semmler, T.; Jacob, D. Modeling extreme precipitation events—A climate change simulation for Europe. *Glob. Planet. Chang.* **2004**, *44*, 119–127. [CrossRef]

35. Frei, C.; Schöll, R.; Fukutome, S.; Schmidli, J.; Vidale, P.L. Future change of precipitation extremes in Europe: Intercomparison of scenarios from regional climate models. *J. Geophys. Res.* **2006**, *111*, 224. [CrossRef]

36. Kyselý, J.; Beranová, R. Climate-change effects on extreme precipitation in central Europe: Uncertainties of scenarios based on regional climate models. *Theor. Appl. Clim.* **2009**, *95*, 361–374. [CrossRef]

37. Quirmbach, M.; Einfalt, T.; Langstädtler, G.; Janßen, C.; Reinhardt, C.; Mehlig, B. Extremwertstatistische Untersuchung von Starkniederschlägen in NRW (ExUS). *Korresp. Abwasser und Abfall* **2013**, *60*, 591–599.

38. Fiener, P.; Auerswald, K. Comment on "The new assessment of soil loss by water erosion in Europe" by Panagos et al. (Environmental Science & Policy 54 (2015) 438–447). *Environ. Sci. Policy* **2016**, *57*, 140–142. [CrossRef]

39. Panagos, P.; Meusburger, K.; Ballabio, C.; Borrelli, P.; Beguería, S.; Klik, A.; Rymszewicz, A.; Michaelides, S.; Olsen, P.; Tadić, M.P.; et al. Reply to the comment on "Rainfall erosivity in Europe" by Auerswald et al. *Sci. Total Environ.* **2015**, *532*, 853–857. [CrossRef] [PubMed]

6

Conclusions and Recommendations

6 Conclusions and Recommendations

This Chapter summarises the main outcomes and discussions, which have been described in more detail in the previous Chapters. It answers the research questions posed at the beginning of the thesis and thus illustrates the linkages between the different Chapters and highlights the main results. Finally, practical recommendations are provided based on the results and an outlook on future research goals is given.

6.1 Conclusions

This thesis aimed to improve the usability of weather radar data for environmental sciences. Due to the high spatiotemporal variability of precipitation, spatially and temporally highly resolved weather radar data undisputedly have a huge potential to improve rainfall-related modelling, monitoring and analyses in many environmental disciplines. In particular, applications dealing with the characteristics and impacts of heavy and extreme rainfall events benefit from comprehensive spatially distributed rainfall information. However, several challenges remain which hamper a more extensive use of these data. From a user's perspective, challenges include the processing of large volumes of data, which may comprise millions of files that are often provided in uncommon proprietary data formats, but also QPE uncertainties and inherent systematic or random bias, which have to be evaluated and taken into account or corrected when interpreting the results. Taking the German operational and reanalysed weather radar composite products RADOLAN and RADKLIM as practical application examples, this study tackled the outlined challenges by providing methodological and scientific contributions that help to facilitate radar data usage and answer the following research questions:

- How can the barrier to weather radar data usage be reduced and what role can open source software and open data have in this case?

- Which developments, potentials and uncertainties have to be considered when using operational radar-based QPEs and reanalysed radar climatology QPEs in comparison to rain gauge data?

- How do the German reanalysed radar climatology QPEs perform in a case study on rainfall erosivity and to what extent can correction factors compensate for systematic radar errors?

Based on the obtained results, the following conclusions can be highlighted.

6.1.1 Approaches to lower the barrier to weather radar data usage and the role of open science

Some of the main barriers to weather radar data usage are caused by the challenging processing of the large volumes of data, which are often provided in uncommon data formats, and by a scarcity of dedicated software tools that automate data processing and reduce the necessity of programming skills for users. The German weather radar composite products are provided in two different data formats. The original format is a proprietary binary data format, which requires dedicated software for reading, but allows for efficient data storage and processing. By now, all freely available RADOLAN and RADKLIM products are also provided as ASCII files. These are easy to read in and to visualise with any Geographic Information System (GIS), but they are not suited for climatological applications since the processing of large volumes of these text files is very inefficient.

The software review presented in **Chapter 2** showed that, at the time of the review in 2018, there were very few software tools available that allowed for importing the binary radar data format. Moreover, there were even fewer tools that comprised an automation of radar data processing and aggregation for longer time periods, whereby none of these was an Open Source Software (OSS). Most of the tools that were capable of processing RADOLAN data and that provided functionality beyond simple

visualisation and conversion tasks for single files were commercial software products. However, the first software to provide routines capable of importing the RADKLIM data format, which was slightly modified compared to RADOLAN, was the open source Python package *wradlib*. In contrast, a support for RADKLIM was not explicitly indicated on the websites of the reviewed commercial tool companies. Upon request, two of the engineering offices that develop commercial software admitted that they were not aware of the fact that there was a new dataset available. These findings indicate that community-driven OSS development and an increased sharing of code developed for data processing and analysis could accelerate the implementation of new developments into software and thus, into practice. Accordingly, the Python library *radproc*, which was developed as part of this thesis, could be built on the data import routines published in *wradlib* and these routines could be modified where needed. As a result, *radproc* was the first OSS to provide support for long-term 5-minute RADOLAN and RADKLIM data processing and analysis. In conjunction with *wradlib*, it comprised a broader and more extensible functionality than most commercial software products. Moreover, OSS potentially addresses a broader user base, since, on the one hand, commercial software products are hardly affordable for many users and, on the other hand, especially researchers put emphasis on being able to access and modify source code in order to develop new algorithms and workflows. *Radproc* has already been applied successfully by several scientific working groups conducting heavy rainfall analysis and data aggregation tasks and it has enabled several students to use weather radar data for Bachelor, Master and doctoral theses. However, it must to be mentioned that *radproc* does not entirely support the open source approach since it is only compatible with the commercial ArcGIS software. Thus, an additional module implementing compatibility with QGIS to *radproc*, which was out of the scope of this thesis, would be desirable in order to achieve a full-featured open source application.

As outlined in **Chapter 1** and analysed in **Chapter 4**, radar-based QPEs come along with several potential uncertainties, which may vary considerably in space and time. Consequently, the quality and suitability of a QPE dataset have to be evaluated for each study area and time period individually. This data quality assessment, which is more complex compared to rain gauge data, may already be a time-consuming task that requires lots of data processing. The rainfall data inter-comparison geodataset that is described in and published alongside **Chapter 3** aims to facilitate this step of data selection and workflow processing. It allows for a straightforward comparison of various precipitation statistics for all RADOLAN and RADKLIM pixels within Germany and all freely available automated rain gauges operated by DWD that provide temporally highly resolved precipitation data. Moreover, the dataset includes several additional parameters that may influence radar data quality such as the distance from the next radar, the elevation or the number and height of wind energy plants in the raster cell. For each radar pixel, a total of up to 95 attributes were collected. Since the information is provided as open data in shapefile format, each user can import the data directly into any GIS and clip them to the extent of the respective study area to assess data quality without any raw data processing. Moreover, for many applications that only require temporally aggregated rainfall information instead of highly resolved raw data, the published inter-comparison dataset already contains some of the required statistics such as rainfall sums or the number of wet days.

Furthermore, **Chapter 3** described the data processing workflow in detail and can serve as a guideline for individual data processing tasks and as a case study for the application of the *radproc* library. In particular, Chapter 3 also showed the necessity for thorough data quality checks when using rain gauge data. The rain gauge data files provided by DWD contained several inconsistencies and implausible values, which had to be cleaned carefully. This evidently showed the importance of dataset documentation. Such data inconsistencies were much easier to trace back for the radar datasets, for which an extensive, central documentation is available. In contrast, for the gauge data, there was no

overarching dataset description available, which explains the measuring devices and the correction algorithms applied to the data.

6.1.2 Potentials and uncertainties of using radar-based QPEs compared to rain gauge data

The most important advantages of radar-based QPEs compared to any other currently available precipitation dataset are the high spatiotemporal resolution and the contiguous spatial coverage. Thus, in contrast to rain gauges, these datasets allow to map the high spatial and temporal variability of precipitation without missing local small-scale convective cells. Many of the typical traditional applications for radar-based QPEs build on these capabilities, for example operational rainfall monitoring and forecasting, storm tracking, numerical weather modeling and hydrological modeling. For these applications, the operational RADOLAN QPE products have become a very good choice.

Chapter 4 described the development of the hourly RADOLAN product RW and showed the significant improvements that could be achieved in radar data correction and precipitation quantification. Particularly since the year 2010, the amount of high outliers and radar artefacts was reduced significantly and the RADOLAN RW product now provides largely reliable information on spatial precipitation distribution. However, due to the continuous development of data processing routines, RADOLAN is an inhomogeneous dataset that is not suited for long-term time series analyses. Moreover, several radar-related systematic biases such as range-dependent attenuation and the underestimation of orographic precipitation and snowfall, are still very hard to identify and correct in operational applications.

For these errors, which cause a considerable underestimation of precipitation sums at far ranges from the radar, correction algorithms on a climatological time scale were developed by DWD and applied for the radar climatology (RADKLIM). The analyses described in Chapter 4 showed that the abovementioned radar errors could be largely corrected with the new algorithms. In particular, aggregated RADKLIM precipitation sums showed no statistically significant range-dependent attenuation, whereas the increase of precipitation amount with terrain height increased significantly compared to RADOLAN. However, the analyses also revealed that there is most likely a certain overcorrection since precipitation sums of many RADKLIM cells are lower than the respective values at RADOLAN cells or rain gauges. This effect is particularly pronounced at close range from the radar. Moreover, the underestimation of high rainfall intensities during heavy rainfall events, which is a common problem with radar measurements due to strongly varying rainfall-induced beam attenuation, was clearly detected in the radar climatology dataset and could thus not be corrected adequately. Consequently, for the quantification of rainfall at one specific location and point in time, rain gauges still provide more reliable measurements. However, chances are much higher that the radar actually detects the maximum of a heavy rainfall cell and radar is the only measurement device that is capable of providing reliable information on size, shape, spatiotemporal variability, trail and movement speed of rainfall cells, which are much more important than the precise rainfall amount for many applications. Besides, temporally aggregated precipitation amounts are mapped reliably in RADKLIM except for a few remaining local radar artefacts, which are mainly negative spokes.

Hence, particularly for the radar climatology, there are huge potentials for applications beyond the traditional ones listed above. Examples include research on rainfall erosivity, statistical heavy rainfall analyses, storm path and life cycle analysis, shifts in spatiotemporal precipitation distribution in a changing climate, more detailed modeling of ecosystem services related to water and an improved implementation of (flash) flood mitigation into environmental planning and disaster management, to name a few.

6.1.3 Performance of radar climatology QPEs and proposed correction factors for rainfall erosivity estimation

In **Chapter 5**, an application case study on the usability of the radar climatology QPEs was presented. First of all, the analyses showed a significant increase of the R-factor due to climate change. Compared to existing calculations based on regression equations from the 1980s, the new R-factors that were derived from RADKLIM and rain gauge data for the period 2001-2016 according to the German technical standard DIN 19708 showed higher values. The combination of different estimation methods and rainfall inputs revealed that the existing regression equation, which is still used in soil protection practice in Hesse, significantly underestimates rainfall erosivity and has to be updated using more recent precipitation data.

With regard to the performance of the radar climatology data for rainfall erosivity estimation compared to rain gauge data, the results are more diverse. On the one hand, the radar-based R-factor estimate contains a series of strikingly high R-factor values that were not captured by the rain gauges. However, due to their comparatively small number, their impact on the spatial average of the R-factor is negligible. With regard to the relatively short time series, the high values may also be the result of single extreme events that would be averaged out in a longer time series. On the other hand, the attenuation of intensity peaks by the radar, which was discussed in Chapter 4, leads to significantly lower radar-based R-factor values compared to the R-factor derived from rain gauge data. This is in line with the findings by Fischer et al. (2018), who proposed correction factors to compensate for the differences in measuring method, spatial scale and temporal resolution between radar and rain gauges. The analyses presented in Chapter 5 showed that the correction factors are able to compensate for the underestimation of the radar QPEs and that this correction even led to higher radar-based R-factors compared to the R-factors derived from rain gauges. Using the correction factors undoubtedly provides an improvement of the R-factors derived from radar climatology. However, a possible overcorrection cannot be excluded. The correction factors were derived from a four-year time series of measurements from 12 rain gauges located within one square kilometre in Bavaria. Due to the high spatiotemporal variability of rainfall, this time series may be too short and the area of one radar pixel may be too small to provide reliable results that are transferable to any other radar pixel.

For application in soil protection practice, the spatial distribution of rainfall erosivity is of higher importance than the absolute values since the goal of soil erosion modelling usually is the identification of erosion risk hot-spots. These are needed in order to assess the fulfilment of EU Cross-Compliance soil protection regulations and to support the planning of soil protection measures. For this purpose, radar-based R-factors provide valuable, spatially highly resolved information which cannot be provided by R-factor derivatives based on rain gauge data or spatially interpolated rainfall estimates. Chapter 5 showed that the overall spatial distribution of the new radar-based R-factor and the existing erosivity map from the erosion atlas Hesse show a relatively good conformity with minima and maxima in the same regions. However, the radar-based R-factor map adds more detail and shows a much more heterogeneous distribution with a higher variability and a much wider value range. In particular, more detail was added for example in the Wetterau region located in the centre of Hesse. This is an intensively used agricultural area in which strong erosion occurred several times within the last decade. However, the existing R-factor map from the erosion atlas indicates a very low erosivity in this region, which is why erosion modelling obviously tended to underestimate the erosion risk in this region. In contrast, the new radar-based R-factor map shows much higher values for this region and characterises the erosivity in this area in a much more credible way.

6.2 Recommendations

6.2.1 Practical Recommendations

The variety of potential applications for radar-based QPEs actually exceeds the point of giving generally applicable recommendations on how to account for or correct QPE uncertainties. Nevertheless, a **guideline on how to approach the assessment of QPE quality** in a specific study area and a selection of possible solutions is provided in this Chapter.

When using radar climatology data, users should first check if their study area contains strongly biased radar pixels due to radar artefacts that are visible in long-term precipitation sums. In particular, for RADKLIM, these artefacts include negative spokes, temporary gaps between radars during hardware upgrades and patches of low outliers close to radars, as discussed in detail in Chapter 4. A first rough check can be made using the maps provided in Chapter 4. For an exact identification of strongly biased radar pixels, the open rainfall data inter-comparison dataset described in Chapter 3 can be applied. Depending on the intended application, there are several approaches that can take the identified biased pixels into account. The most important aspect is to be aware of possible errors, locate biased pixels and to take the potential impact of, for example, underestimated rainfall in pixels within a negative spoke into account when interpreting results. Moreover, for small biased areas, affected pixels could be identified and excluded from analysis by masking them and setting their values to *NoData*. If the study area is located in one of the temporary radar gaps as discussed in Chapter 4, the data from the respective time period could be excluded from the analysis if possible. Another way to account for these gaps or spokes can be to calculate a correction factor to account for the underestimation of precipitation depth in the affected area compared to the rest of the study area. However, especially the quantification of rainfall intensity during heavy and extreme rainfall events remains a major source of uncertainty. The rainfall intensity of single events can hardly be corrected due to a lack of reference. Long-term analyses based on heavy rainfall events, such as rainfall erosivity estimation, however, may be corrected based on correction factors as shown by Fischer et al. (2018) and discussed in Chapters 5 and 6.1.3. Nonetheless, particularly such heavy rainfall analyses still suffer from the comparatively short radar QPE time series. Results are still likely to be biased by extraordinarily rare events that may skew statistical and spatial distributions to a certain extent.

Since radar QPEs can add much spatial detail to many applications, it is important that researchers and other users assess whether radar QPEs are already suitable for their application. If they decide that this is not yet the case, they should nevertheless already work towards **preparing models, workflows, and analyses for the use of spatially highly resolved rainfall inputs**, so that these can be used as soon as the time series are long enough to allow analyses at a proper climatological time scale. For a **transition period, hybrid solutions** could be developed that combine the more precise rainfall quantification of rain gauge measurements with the continuous rainfall information provided by radar QPEs, as is recommended for erosivity mapping in Chapter 5.

Besides the guidelines for users presented above, there are also several aspects to be considered from a **data provider's point of view** in order to facilitate the usage of the radar climatology and RADOLAN products. In order to utilise the full potential of open data, they should be structured, documented and distributed according to the FAIR principles, which means data should be **Findable, Accessible, Interoperable and Re-usable**. In Europe, the provision of more open datasets and the implementation of the FAIR principles for these are promoted and specified by the INSPIRE (Infrastructure for spatial information in Europe) Directive[1]. As discussed in Chapters 3 and 4, the radar QPE products are well documented and the radar climatology has also been registered with a DOI (Digital Object Identifier) as a persistent identifier to improve its findability. However, the datasets and the documentation,

---

[1] *https://inspire.ec.europa.eu/* (last access: 27.04.2020).

which primarily consists of the radar climatology project report (Winterrath, T. *et al.* 2017) and the composite format description (Deutscher Wetterdienst 2018), are found at different websites. The DWD Climate Data Center and Open Data Portal have been restructured in the last years and the datasets were moved from one server to another, whereby support documents for data visualisation in GIS and recommendations for data processing software that referred, amongst others, to *wradlib* and *radproc*, have unfortunately not yet been transferred to the new server. For the radar climatology, the lack of metadata on the download server needs to be addressed to enhance the accessibility of the provided data. The metadata files for RADOLAN[23] require maintenance through updating hyperlinks regularly. Consequently, the state-of-the-art open data approach of the RADKLIM and RADOLAN datasets can be improved through maintained reference to their documentation. In conjunction with the issue that the RADOLAN and particularly the RADKLIM datasets are rather hard to find on the Open Data Server and on the DWD website, the findability and accessibility of the datasets are still a major barrier to a wider usage of these data, but also a barrier that could be relatively easily lowered by the DWD. An additional leverage to improve the findability of the datasets will be available by adding the datasets to the European INSPIRE Geoportal[4] and by orderly metadata maintenance on the German geoportal website[5], which is operated by Geodateninfrastruktur Deutschland (GDI-DE) in order to implement the INSPIRE Directive in Germany.

With regard to the interoperability of the German radar QPE datasets, two major changes to the data format could improve the usability of the data significantly. First, the proprietary binary data format should be replaced by a more common **data format** to bring it in line with the INSPIRE Directive. With the weather radar information model provided by OPERA (Michelson *et al.* 2014), a potentially suitable data format has been defined and established in several countries. Its implementation for all European radar data products would reduce the need for customised national software developments for data processing. Instead, existing software could be used for all radar QPE products, which would increase the overall functionality for all users. Second, the **spatial reference** of the radar QPEs should be transformed from the DWD's custom polar stereographic coordinate system to a widely used coordinate system, for example UTM (Universal Transverse Mercator), which would allow for a better interoperability with other geodata and would constitute a major improvement of radar QPE usability in environmental sciences.

6.2.2 Future Research Developments

The results of this thesis showed that the radar community has achieved much progress in improving the quality of radar measurements and QPE derivation in the last decades. However, **several uncertainties still remain and need to be addressed in future research**. As radar techniques have improved and operational radar hardware was successively upgraded in the last years, additional data can be retrieved and integrated into QPE derivation procedures. For RADOLAN, the integration of **polarimetric radar data** since October 2017, which provides, amongst others, information on hydrometeor shape and type, was a promising step in order to improve rainfall and particularly snowfall quantification. Due to the short time series, the impacts of this change to the RADOLAN routine could not be analysed in this thesis, but future research on the effects could help to improve the algorithms for the implementation of these additional data and to assess the impacts on QPE quality and subsequent applications.

---

[2] *https://opendata.dwd.de/climate_environment/CDC/grids_germany/hourly/radolan/recent/asc/BESCHREIBUNG_gridsger many_hourly_radolan_recent_asc_de.pdf* (last access: 27.04.2020).

[3] *https://opendata.dwd.de/climate_environment/CDC/grids_germany/hourly/radolan/recent/bin/BESCHREIBUNG_gridsger many_hourly_radolan_recent_bin_de.pdf* (last access: 27.04.2020).

[4] *https://inspire-geoportal.ec.europa.eu/index.html* (last access: 27.04.2020).

[5] *https://www.geoportal.de/portal/main/* (last access: 27.04.2020).

A potential improvement for RADOLAN and particularly RADKLIM could be the integration of **more rain gauges for adjustment**. Up to now, mostly data from the rain gauges operated by DWD are used as an input, whereas the stations of the federal state networks are not included. An increased number of rain gauges would reduce the gaps between stations and thus reduce the smoothing through interpolation of adjustment factors. Within the research project "KLIMPRAX-Starkregen", the DWD tested the implementation of the German federal stations for the federal state of Hesse. However, our QPE plausibility check, that was conducted within the same project, showed a series of artefacts around the additional stations, which were hard to explain from a meteorological point of view (Kreklow *et al.* 2019). Instead, the artefacts seemed to result from differences in rain gauge data processing, resampling and time of measurement between the two measurement networks. Further research on these effects is required in order to enable an efficient use of the additional available rain gauge data and avoid the introduction of new uncertainties. This is also a good example for the **importance of open data and metadata in science**. If these federal rain gauge datasets were available alongside documented open datasets, they could be more easily applied for adjustment or other applications. The publication of research results as open datasets and associated data descriptor papers that explain the applied methodology in much more detail than any research article can help researchers to exchange knowledge and expertise. Moreover, propagation of inherent uncertainties and effects such as the above-mentioned artefacts could be traced back more efficiently and the interoperability of datasets could be enhanced.

Furthermore, with more and bigger datasets such as the available radar climatology, it gets harder and more time-consuming to cope with the different data formats and larger volumes of data. Consequently, **more sharing of code and details on methodologies is required** so that no researcher has to start from scratch, but has more time for the actual research. The requirement of data management plans for new research project proposals is a good starting point, but the scientific community generally needs to give **more credit to other types of publications other than research articles** in order to increase the incentive for researchers to publish their code, data and detailed methodologies. If datasets are not fully accessible, for example due to data protection regulations, the provision as view-only WMS (Web Map Service) servers or online viewers such as the Hessian erosion atlas could be an alternative to a standard open data approach. In addition, new ways of dedicated **funding for scientific open source software development and maintenance** could help to increase the quality and persistence of software and documentation and thus to deal with the increasing number of large datasets such as the radar climatology.

References

Abraham, J., Stark, J. R. and Minkowycz, W. J. 2015. Briefing: Extreme weather: observed precipitation changes in the USA. *Proceedings of the Institution of Civil Engineers - Forensic Engineering*, **168**(2), 68–70.

Asadieh, B. and Krakauer, N. Y. 2015. Global trends in extreme precipitation: Climate models versus observations. *Hydrology and earth system sciences : HESS*, **19**(2), 877–891.

Auerswald, K., Fischer, F. K., Winterrath, T. and Brandhuber, R. 2019. Rain erosivity map for Germany derived from contiguous radar rain data. *Hydrol. Earth Syst. Sci.*, **23**(4), 1819–1832.

Berg, P., Moseley, C. and Haerter, J. O. 2013. Strong increase in convective precipitation in response to higher temperatures. *Nature Geosci*, **6**(3), 181–185.

Berne, A. and Krajewski, W. F. 2013. Radar for hydrology: Unfulfilled promise or unrecognized potential? *Advances in Water Resources*, **51**, 357–366.

Biodiversity Information System for Europe (BISE) 2020. Mapping and Assessment of Ecosystems and their Services (MAES). https://biodiversity.europa.eu/maes (accessed 12 March 2020).

Bronstert, A., Agarwal, A., Boessenkool, B., Crisologo, I., Fischer, M., Heistermann, M., Köhn-Reich, L., López-Tarazón, J. A., Moran, T., Ozturk, U., Reinhardt-Imjela, C. and Wendi, D. 2018. Forensic hydro-meteorological analysis of an extreme flash flood: The 2016-05-29 event in Braunsbach, SW Germany. *Science of The Total Environment*(630), 977–991.

Burkhard, B. and Maes, J. (eds.) 2017. *Mapping Ecosystem Services.* Pensoft Publishers, Sofia.

Catto, J. L., Ackerley, D., Booth, J. F., Champion, A. J., Colle, B. A., Pfahl, S., Pinto, J. G., Quinting, J. F. and Seiler, C. 2019. The Future of Midlatitude Cyclones. *Curr Clim Change Rep*, **39**(10), n/a-n/a.

Cifelli, R. and Chandrasekar, V. 2010. Dual-Polarization Rainfall Estimation. In: *Rainfall – State of the Science*, F. Testik and M. Gebremichael (eds.). Geophysical Monograph Series 191, Washington, pp. 105–125.

Deutscher Wetterdienst 2018. *RADKLIM: Beschreibung des Kompositformats und der verschiedenen Reprozessierungsläufe*: *Version 1.0,* Deutscher Wetterdienst, Abteilung Hydrometeorologie, Offenbach am Main, 13 pp. https://www.dwd.de/DE/leistungen/radarklimatologie/radklim_kompositformat_1_0.pdf;jsessio nid=0889B3A8CB74341FAA652DB2A4FB7F63.live11041?__blob=publicationFile&v=1 (accessed 26 March 2019).

Deutsches Institut für Normung 2017. *DIN 19708*: *Bodenbeschaffenheit - Ermittlung der Erosionsgefährdung von Böden durch Wasser mit Hilfe der ABAG,* 2017th ed. Beuth Verlag GmbH, Berlin (accessed 31 January 2020), 28 pp.

Donat, M. G., Alexander, L. V., Yang, H., Durre, I., Vose, R., Dunn, R. J. H., Willett, K. M., Aguilar, E., Brunet, M., Caesar, J., Hewitson, B., Jack, C., Klein Tank, A. M. G., Kruger, A. C., Marengo, J., Peterson, T. C., Renom, M., Oria Rojas, C., Rusticucci, M., Salinger, J., Elrayah, A. S., Sekele, S. S., Srivastava, A. K., Trewin, B., Villarroel, C., Vincent, L. A., Zhai, P., Zhang, X. and Kitching, S. 2013. Updated analyses of temperature and precipitation extreme indices since the beginning of the twentieth century: The HadEX2 dataset. *J. Geophys. Res. Atmos.*, **118**(5), 2098–2118.

Einfalt, T., Arnbjerg-Nielsen, K., Golz, C., Jensen, N.-E., Quirmbach, M., Vaes, G. and Vieux, B. 2004. Towards a roadmap for use of radar rainfall data in urban drainage. *Journal of Hydrology*, **299**(3-4), 186–202.

Einfalt, T. and Michaelides, S. 2008. Quality Control of precipitation data. In: *Precipitation*. *Advances in measurement, estimation, and prediction*, S. Michaelides (ed.), Springer, Berlin, pp. 101–126.

Fairman, J. G., Schultz, D. M., Kirshbaum, D. J., Gray, S. L. and Barrett, A. I. 2015 A radar-based rainfall climatology of Great Britain and Ireland. *Weather*, **70**(5), 153–158.

Field, C. B., Barros, V. R., Dokken, D. J., Mach, K. J. and Mastrandrea, M. D. 2015. *Climate Change 2014 – Impacts, Adaptation and Vulnerability: Part A: Global and Sectoral Aspects*. Working Group II Contribution to the IPCC Fifth Assessment Report, IPCC, Cambridge, 696 pp.

Fiener, P., Neuhaus, P. and Botschek, J. 2013. Long-term trends in rainfall erosivity–analysis of high resolution precipitation time series (1937–2007) from Western Germany. *Agricultural and Forest Meteorology*, **171-172**, 115–123.

Fischer, F. K., Winterrath, T. and Auerswald, K. 2018. Temporal- and spatial-scale and positional effects on rain erosivity derived from point-scale and contiguous rain data. *Hydrology and Earth System Sciences*, **22**(12), 6505–6518.

Förster, K. and Thiele, L.-B. 2019. Variations in sub-daily precipitation at centennial scale. https://eartharxiv.org/2f54a/ (accessed 05 February 2020).

Frei, C., Schär, C., Lüthi, D. and Davies, H. C. 1998 Heavy precipitation processes in a warmer climate. *Geophys. Res. Lett.*, **25**(9), 1431–1434.

Frei, C., Schöll, R., Fukutome, S., Schmidli, J. and Vidale, P. L. 2006. Future change of precipitation extremes in Europe: Intercomparison of scenarios from regional climate models. *J. Geophys. Res.*, **111**(D6), 224.

Germann, U., Galli, G., Boscacci, M. and Bolliger, M. 2006. Radar precipitation measurement in a mountainous region. *Q. J. R. Meteorol. Soc.*, **132**(618), 1669–1692.

Giorgi, F., Bi, X. and Pal, J. 2004. Mean, interannual variability and trends in a regional climate change experiment over Europe. II: climate change scenarios (2071-2100). *Climate Dynamics*, **23**(7-8), 839–858.

Goudenhoofdt, E. and Delobbe, L. 2009. Evaluation of radar-gauge merging methods for quantitative precipitation estimates. *Hydrol. Earth Syst. Sci.*, **13**, 195–203.

Hänsel, P., Kaiser, A., Buchholz, A., Böttcher, F., Langel, S., Schmidt, J. and Schindewolf, M. 2018. Mud Flow Reconstruction by Means of Physical Erosion Modeling, High-Resolution Radar-Based Precipitation Data, and UAV Monitoring. *Geosciences*, **8**(11), 427.

Hazenberg, P., Leijnse, H. and Uijlenhoet, R. 2011. Radar rainfall estimation of stratiform winter precipitation in the Belgian Ardennes. *Water Resour. Res.*, **47**(2), 257.

Heistermann, M., Jacobi, S. and Pfaff, T. 2013. Technical Note: An open source library for processing weather radar data (*wradlib*). *Hydrology and earth system sciences : HESS*, **17**(2), 863–871.

Heistermann, M. and Kneis, D. 2011. Benchmarking quantitative precipitation estimation by conceptual rainfall-runoff modeling. *Water Resour. Res.*, **47**(6), 301.

Holleman, I., Michelson, D. B., Galli, G., Germann, U. and Peura, M. 2006. *Quality information for radars and radar data*: *Deliverable: OPERA 2005 19*. OPERA work package 1.2, 77 pp. http://opera.radar.tugraz.at/docum/opera_2/OPERA_2005_19_DataQuality.pdf (accessed 11 December 2019).

IPCC 2013. *Climate Change 2013*: *The Physical Science Basis*. Contribution of working group I to the fifth assessment report of the Intergovernmental Panel on Climate Change, Cambridge, 1552 pp. http://www.climatechange2013.org/images/report/WG1AR5_ALL_FINAL.pdf (accessed 16 April 2018).

Jessen, M., Einfalt, T., Stoffer, A. and Mehlig, B. 2005. Analysis of heavy rainfall events in North Rhine–Westphalia with radar and raingauge data. *Atmospheric Research*, **77**(1-4), 337–346.

Keeler, J. and Serafin, R. 2008. Meteorological Radar. In: *Radar handbook*, M. Skolnik (ed.), 3rd edn, McGraw-Hill Publishing Company, New York, USA, 19.1 - 19.49.

Keupp, L., Winterrath, T. and Hollmann, R. 2017. *Use of Weather Radar Data for Climate Data Records in WMO Regions IV and VI*, 16 pp.

Kidd, C., Becker, A., Huffman, G. J., Muller, C. L., Joe, P., Skofronick-Jackson, G. and Kirschbaum, D. B. 2017. So, how much of the Earth's surface is covered by rain gauges? *Bulletin of the American Meteorological Society*, **98**(1), 69–78.

Kidd, C. and Levizzani, V. 2011. Status of satellite precipitation retrievals. *Hydrol. Earth Syst. Sci.*, **15**(4), 1109–1116.

Krajewski, W. F., Kruger, A., Smith, J. A., Lawrence, R., Gunyon, C., Goska, R., Seo, B.-C., Domaszczynski, P., Baeck, M. L., Ramamurthy, M. K., Weber, J., Bradley, A. A., DelGreco, S. A. and Steiner, M. 2011. Towards better utilization of NEXRAD data in hydrology: an overview of Hydro-NEXRAD. *Journal of Hydroinformatics*, **13**(2), 255–266.

Krajewski, W. F. and Smith, J. A. 2002. Radar hydrology: rainfall estimation. *Advances in Water Resources*(25), 1387–1394.

Kreklow, J., Tetzlaff, B., Ta, P. and Kuhnt, G. 2019. *Ausweisung von starkregengefährdeten Gebieten in Hessen für Planungen zur Gefahrenabwehr auf Landes- und kommunaler Ebene*: *Abschlussbericht KLIMPRAX-Starkregen Arbeitspaket 1.4*, 108 pp. https://www.hlnug.de/fileadmin/dokumente/klima/klimprax/starkregen/Abschlussbericht_Starkregen-Hinweiskarte.pdf (accessed 08 May 2020).

Kyselý, J. and Beranová, R. 2009. Climate-change effects on extreme precipitation in central Europe: uncertainties of scenarios based on regional climate models. *Theor Appl Climatol*, **95**(3-4), 361–374.

Lenderink, G., Barbero, R., Loriaux, J. M. and Fowler, H. J. 2017. Super-Clausius–Clapeyron Scaling of Extreme Hourly Convective Precipitation and Its Relation to Large-Scale Atmospheric Conditions. *Journal of Climate*, **30**, 6037–6052.

Lenderink, G. and van Meijgaard, E. 2008. Increase in hourly precipitation extremes beyond expectations from temperature changes. *Nature Geosci*, **1**(8), 511–514.

Lengfeld, K., Winterrath, T., Junghänel, T. and Becker, A. 2018. Characteristic spatial extent of rain events in Germany from a radar-based precipitation climatology. In: *UrbanRain18*. *11th International Workshop on Precipitation in Urban Areas*, vol. 11.

Lorenz, D. J. and DeWeaver, E. T. 2007. Tropopause height and zonal wind response to global warming in the IPCC scenario integrations. *J. Geophys. Res.*, **112**(D10), 30,937.

Löwe, P. 2008. *Niederschlagserosivität – Eine Fallstudie aus Südafrika, basierend auf Wetterradar und Open Source GIS.* VDM-Verlag Dr. Müller, Saarbrücken.

Madsen, H., Lawrence, D., Lang, M., Martinkova, M. and Kjeldsen, T. R. 2014. Review of trend analysis and climate change projections of extreme precipitation and floods in Europe. *Journal of Hydrology*, **519**, 3634–3650.

Marra, F. and Morin, E. 2015. Use of radar QPE for the derivation of Intensity–Duration–Frequency curves in a range of climatic regimes. *Journal of Hydrology*, **531**, 427–440.

Michelson, D. B., Lewandowski, R., Szewczykowski, M. and Beekhuis, H. 2014. EUMETNET OPERA weather radar information model for implementation with the HDF5 file format: Version 2.2. http://eumetnet.eu/wp-content/uploads/2017/01/OPERA_hdf_description_2014.pdf (accessed 16 November 2018).

Min, S.-K., Zhang, X., Zwiers, F. W. and Hegerl, G. C. 2011. Human contribution to more-intense precipitation extremes. *Nature*, **470**(7334), 378–381.

Overeem, A., Holleman, I. and Buishand, A. 2009. Derivation of a 10-Year Radar-Based Climatology of Rainfall. *J. Appl. Meteor. Climatol.*, **48**(7), 1448–1463.

Peleg, N., Marra, F., Fatichi, S., Paschalis, A., Molnar, P. and Burlando, P. 2018. Spatial variability of extreme rainfall at radar subpixel scale. *Journal of Hydrology*, **556**, 922–933.

Ramsauer, T., Weiß, T. and Marzahn, P. 2018. Comparison of the GPM IMERG Final Precipitation Product to RADOLAN Weather Radar Data over the Topographically and Climatically Diverse Germany. *Remote Sensing*, **10**(12), 2029.

Reed, S., Koren, V., Smith, M., Zhang, Z., Moreda, F., Seo, D.-J. and DMIP Participants, 2004. Overall distributed model intercomparison project results. *Journal of Hydrology*, **298**(1-4), 27–60.

Sauerborn, P. 1994. *Die Erosivität der Niederschläge in Deutschland*: *Ein Beitrag zur quantitativen Prognose der Bodenerosion durch Wasser in Mitteleuropa*. Zugl.: Bonn, Univ., Diss., 1993, Bonner bodenkundliche Abhandlungen, **13.** Inst. für Bodenkunde, Bonn.

Schwertmann, U., Vogl, W. and Kainz, M. 1990. *Bodenerosion durch Wasser*: *Vorhersage des Abtrags und Bewertung von Gegenmaßnahmen,* 2. Aufl. Ulmer, Stuttgart.

Semmler, T. and Jacob, D. 2004. Modeling extreme precipitation events—a climate change simulation for Europe. *Global and Planetary Change*, **44**(1-4), 119–127.

Sene, K. 2010. *Hydrometeorology.* Springer Netherlands, Dordrecht.

Seo, B.-C. and Krajewski, W. F. 2010. Scale Dependence of Radar Rainfall Uncertainty: Initial Evaluation of NEXRAD's New Super-Resolution Data for Hydrologic Applications. *J. Hydrometeor*, **11**(5), 1191–1198.

Seo, B.-C., Seed, A. W. and Delrieu, G. 2010. Radar and Multisensor Rainfall Estimation for Hydrologic Applications. In: *Rainfall – State of the Science*, F. Testik and M. Gebremichael (eds.). Geophysical Monograph Series 191, Washington, pp. 79–104.

Sharp, R., Tallis, H. T., Ricketts, T., Guerry, A. D., Wood, S. A., Chaplin-Kramer, R., Nelson, E., Ennaanay, D., Wolny, S., Olwero, N., Vigerstol, K., Pennington, D., Mendoza, G., Aukema, J., Foster, J., Forrest, J., Cameron, D., Arkema, K., Lonsdorf, E., Kennedy, C., Verutes, G., Kim, C. K., Guannel, G., Papenfus, M., Toft, J., Marsik, M., Bernhardt, J., Griffin, R., Glowinski, K., Chaumont, N., Perelman, A., Lacayo, M., Mandle, L., Hamel, P., Vogl, A. L., Rogers, L., Bierbower, W., Denu, D. and Douglass, J. 2020. InVEST 3.8.0.post29+ug.g0215cb1 User's Guide, The Natural Capital Project, Stanford University, University of Minnesota, The Nature Conservancy, and World Wildlife Fund. http://releases.naturalcapitalproject.org/invest-userguide/latest/ (accessed 16 March 2020).

Shelton, M. 2008 *Hydroclimatology – Perspectives and Applications.* Cambridge University Press, Cambridge.

Skolnik, M. 2008. An Introduction and Overview of Radar. In: *Radar handbook*, M. Skolnik (ed.), 3rd edn, McGraw-Hill Publishing Company, New York, USA, 1.1 - 1.24.

Thorndahl, S., Einfalt, T., Willems, P., Nielsen, J. E., Veldhuis, M.-C. ten, Arnbjerg-Nielsen, K., Rasmussen, M. R. and Molnar, P. 2017. Weather radar rainfall data in urban hydrology. *Hydrology and Earth System Sciences*, **21**(3), 1359–1380.

Trenberth, K. E., Dai, A., Rasmussen, R. and Parsons, D. B. 2003. The changing character of precipitation. *Bulletin of the American Meteorological Society*, 1205–1218.

Villarini, G. and Krajewski, W. F. 2010. Review of the Different Sources of Uncertainty in Single Polarization Radar-Based Estimates of Rainfall. *Surv Geophys*, **31**(1), 107–129.

Villarini, G., Mandapaka, P. V., Krajewski, W. F. and Moore, R. J. 2008. Rainfall and sampling uncertainties: A rain gauge perspective. *J. Geophys. Res.*, **113**(D11).

Winterrath, T., Brendel, C., Hafer, M., Junghänel, T., Klameth, A., Walawender, E., Weigl, E. and Becker, A. 2017. *Erstellung einer radargestützten Niederschlagsklimatologie,* Berichte des Deutschen Wetterdienstes 251, Deutscher Wetterdienst, Offenbach am Main, 75 pp. https://www.dwd.de/DE/leistungen/pbfb_verlag_berichte/pdf_einzelbaende/251_pdf.pdf?__blob=publicationFile&v=2 (accessed 26 March 2019).

Winterrath, Tanja, Weigl, Elmar, Junghänel, Thomas, Brendel, Christoph and Becker, Andreas 2017. *Verfügbarkeit und Qualität von hochaufgelösten Radarniederschlagsdaten,* Natur.Umwelt.Technik - Radar Symposium, 21 April 2017, Wiesbaden.

Wischmeier, W. H. and Smith, D. D. 1978. *Predicting rainfall erosion losses*: *A guide to conservation planning,* Agriculture handbook number 537, 63 pp.

Wright, D. B., Smith, J. A., Villarini, G. and Baeck, M. L. 2014. Long-Term High-Resolution Radar Rainfall Fields for Urban Hydrology. *J Am Water Resour Assoc*, **50**(3), 713–734.

Acknowledgements

I would not have been able to finish this PhD without help and support of all the people that surrounded me in the last years.

Thanks to my promoters, Gerald Kuhnt and Benjamin Burkhard, for giving me the opportunity to do this great experience. Gerald, thanks for your trust, support and inspiration throughout the last years and for giving me much freedom to shape my work. I really enjoyed our joint excursions from which I've learned a lot (as a student and as a colleague) and particularly our "Tour de France" was a great experience and a welcome diversion from PhD life! Benjamin, thanks for always having an open door, for your steady support and for many lively discussions on science - and of course on the most important sideline of the world!

Special thanks to Björn Tetzlaff, for your encouragement to do the PhD, your support and all the good input that made this work possible. Without you, I would have definitively not pursued this path!

Some parts of this work are based on the project "KLIMPRAX – Starkregen", work package 1.4 (funded by the Hessian Agency for Nature Conservation, Environment and Geology (HLNUG), grant no. 4500859537). I want to express my thanks to Andreas Hoy, Heike Hübener and Klaus Friedrich from HLNUG as well as to Tanja Winterrath, Andreas Becker and Mario Hafer from DWD, for many inspiring discussions and inputs.

Thanks to Frank Beisiegel, for IT support and for having made every wish for better hardware and new software become true. Thanks to Bastian Steinhoff-Knopp for starting to discover the world of Python together and for many discussions and inputs on soil erosion, GIS and data processing. To Angie Faust, thanks for proofreading.

Thanks to all colleagues at PhyGeo, for your support, a great working atmosphere and of course lots of delicious cake. I enjoyed being part of the team and I will definitively miss you guys!

To my amazing "PhyGeo girls": Ina, Claudia, Anne and Sylvie. Thanks for all the nice chats, coffee breaks, after work beers and game evenings, but also thanks for listening to all my problems and for the always useful suggestions. You are great colleagues and friends!

To the "GIS is Sparta" group: Philipp, Jan, Fabian, Alex, Moritz, Eduard, Malte, Thea and Senta. Thanks for many discussions on GIS, programming and data and for many unforgettable nights at The Harp. May the Irish car bomb always be with you!

To Tim, Christian, Sean, Cristina, Georgi, Svenja, Sören, Tobias M., Robin, Anna, Sabine and Morgane: Thanks for many years of friendship, support and all the great time we spent together!

Special thanks go of course to my family: To my parents Marion and Karl-Heinz, my grandmothers Margrit and Hilla and my parents-in-law Axel and Sabine who always supported and motivated me. Most importantly, I am grateful to my husband Tobias for his love, motivation, patience, comfort and technical support. However, beside all professional success the last one and a half years were also a time of farewells. So last but not least, I want to express my gratitude to my grandfathers Karl and Uli, who awakened my interest in nature and geography with countless hours spent together in their gardens and many quiz games on the capitals, mountains and rivers of this world, and who have always been very proud of their "Frau Doktor" but did not live to see this become true.

Thank you!

Curriculum Vitae

Jennifer Kreklow (Geburtsname: Peußner)

28.03.1989   Geboren in Hameln, Deutschland

Ausbildung

2017 – 2020	**Promotionsstudium im Fach Geographie**
	Leibniz Universität Hannover, Deutschland

           Titel: „Improving Usability of Weather Radar Data in Environmental Sciences: Potentials, Challenges, Uncertainties and Applications"

           Referent: Prof. Dr. rer. nat. Gerald Kuhnt

           Korreferent: Prof. Dr. rer. nat. Benjamin Burkhard

2011 – 2014   **Masterstudium Landschaftswissenschaften**

Leibniz Universität Hannover, Abschluss: Master of Science

           Abschlussarbeit: „Untersuchung der Nutzbarkeit von zeitlich hoch aufgelösten Radardaten des Niederschlags zur verbesserten Simulation des Bodenabtrags durch Wasser"

2008 – 2011   **Bachelorstudium der physischen Geographie**

Leibniz Universität Hannover, Abschluss: Bachelor of Science

           Abschlussarbeit: „Auswirkung unterschiedlicher Rasterweiten auf die Modellierung ausgewählter geomorphometrischer Reliefparameter"

2008   Abitur, Albert-Einstein Gymnasium in Hameln

Berufserfahrung & Praktika

Seit 06/2020   **Data Scientist im Bereich Stadtforschung** (Stadt Wolfsburg, Referat Strategische Planung, Stadtentwicklung, Statistik)

Seit 04/2020   **Lehrbeauftragte** (Institut für Physische Geographie und Landschaftsökologie, Leibniz Universität Hannover)

04/2014 – 03/2020   **Wissenschaftliche Mitarbeiterin** (Institut für Physische Geographie und Landschaftsökologie, Leibniz Universität Hannover)

01/2014 – 2/2016   **Nebentätigkeit als GIS-Sachbearbeiterin** (Planungsgruppe Umwelt, Hannover)

04/2013 – 09/2013   **Studentische Hilfskraft** (Forschungszentrum Jülich, Institut für Bio- und Geowissenschaften – Agrosphäre (IBG-3))

09/2012   **4-wöchiges Praktikum** (Forschungszentrum Jülich, Institut für Bio- und Geowissenschaften – Agrosphäre (IBG-3))

02/2012 & 03/2013	**Werkverträge** für GIS-Tätigkeiten (Stadt Wolfsburg, Abteilungen Statistik & Straßen- und Verkehrsplanung)
10/2011 – 03/2013	**Studentische Hilfskraft** (Planungsgruppe Umwelt, Hannover)
09/2011 – 10/2011	**5-wöchiges Praktikum** (Planungsgruppe Umwelt, Hannover)
08/2011 & 08/2012	**Reisebegleiterin** (SR Travel Gießen)
07/2010 – 08/2010	**6-wöchiges Praktikum** (Alfred-Wegener-Institut für Meeres- und Polarforschung, Arbeitsgruppe Meereisphysik, Bremerhaven)
10/2009 – 12/2011	**Wochenendaushilfe** (Hameln Marketing und Tourismus GmbH)
08/2009 – 09/2009	**8-wöchiges Praktikum** (Hameln Marketing und Tourismus GmbH)
02/2006	**3-wöchiges Praktikum** (CW Niemeyer Buchverlage, Hameln)

Hannover, Oktober 2020

List of Publications

Peer reviewed scientific articles

Kreklow, J. 2019. Facilitating radar precipitation data processing, assessment and analysis: A GIS-compatible Python approach. *Journal of Hydroinformatics* 21(4), 652–670.
DOI: 10.2166/hydro.2019.048

Kreklow, J., Tetzlaff, B., Kuhnt, G. and Burkhard, B. 2019. A Rainfall Data Intercomparison Dataset of RADKLIM, RADOLAN, and Rain Gauge Data for Germany. *Data* 4(3), 118.
DOI: 10.3390/data4030118

Kreklow, J., Tetzlaff, B., Burkhard, B. and Kuhnt, G. 2020. Radar-Based Precipitation Climatology in Germany – Developments, Uncertainties and Potentials. *Atmosphere* 11(2), 217.
DOI: 10.3390/atmos11020217

Kreklow, J., Steinhoff-Knopp, B., Friedrich, K. and Tetzlaff, B. 2020. Comparing Rainfall Erosivity Estimation Methods Using Weather Radar Data for the State of Hesse (Germany). *Water* 12(5), 1424.
DOI:10.3390/w12051424

Software and data publications

Kreklow, J. 2018. Radproc - A GIS-compatible Python-Package for automated RADOLAN Composite Processing and Analysis. *Software Publication*. *Zenodo.*
DOI: 10.5281/zenodo.1313702

Kreklow, J., Tetzlaff, B., Kuhnt, G. and Burkhard, B. 2019. A rainfall data inter-comparison dataset for Germany (Version 1.0). *Data Publication*. *Zenodo.*
DOI: 10.5281/zenodo.3262172.

Other publications

Kreklow, J., Tetzlaff, B., Ta, P. and Kuhnt, G. 2019. Ausweisung von starkregengefährdeten Gebieten in Hessen für Planungen zur Gefahrenabwehr auf Landes- und kommunaler Ebene: Abschlussbericht KLIMPRAX-Starkregen Arbeitspaket 1.4, 108 pp.

Oral Presentations

Kreklow, J. 2018. Radproc – ein GIS-kompatibles Tool zur Verarbeitung und Analyse von RADOLAN-Daten. Workshop „Starkregen und Sturzfluten" 07.06.2018, TU München.

Kreklow, J. 2018. Erstellung von Starkregen-Hinweiskarten für das Bundesland Hessen. Workshop „Starkregen und Sturzfluten" 08.06.2018, TU München.

Kreklow, J. 2018. Radproc: Eine GIS-kompatible Python-Bibliothek zur Auswertung von Radarniederschlagsdaten. IALE-D Jahrestagung 06.09.2018, Univ. Hannover.
DOI: 10.5281/zenodo.1419141.

Kreklow, J. 2019. Die Potenziale des Python-Ökosystems für die Geographische Datenwissenschaft am Beispiel des Radardaten-Analysetools radproc. Deutscher Kongress für Geographie 27.09.2019, Univ. Kiel.